Atmospheric Dispersion Modelling Liaison Committee

Annual Report 2005/2006

INCLUDING

Review of atmospheric dispersion in complex terrain

Health Protection Agency
Chilton
Didcot
Oxon OX11 0RQ

ISBN 0 85951 587 7

PREFACE

In 1977 a meeting of representatives of government departments, utilities and research organisations was held to discuss methods of calculation of atmospheric dispersion for radioactive releases. Those present agreed on the need for a review of recent developments in atmospheric dispersion modelling, and a Working Group was formed. Those present at the meeting formed an informal Steering Committee, that subsequently became the UK Atmospheric Dispersion Modelling Liaison Committee. That Committee operated for a number of years. Members of the Working Group worked voluntarily and produced a series of reports. A workshop on dispersion at low wind speeds was also held, but its proceedings were never published.

The Committee has been reorganised and has adopted terms of reference. The organisations represented on the Committee, and the terms of reference adopted, are given in this report. The organisations represented on the Committee pay a small annual subscription. The money thus raised is used to fund reviews on topics agreed by the Committee, and to support in part its secretariat, provided by Health Protection Agency (HPA). The new arrangements came into place for the start of the 1995/96 financial year. This report describes the eleventh year in which the Committee has operated under the new arrangements, and during which it placed one contract. This covered a review of atmospheric dispersion in complex terrain. The technical specification for the contract is given in this report, and the contract report is attached as an annex to this report. The Committee funded 24 studies in previous years; they are described in its earlier annual reports.

The Committee intends to place further contracts in future years and would like to hear from those interested in tendering for such contracts. They should contact the Secretary:

Mr J G Smith
Health Protection Agency
Chilton
Didcot
Oxon OX11 0RQ

E-mail: ADMLC@hpa.org.uk

CONTENTS

1 ORGANISATIONS REPRESENTED ON THE COMMITTEE

The organisations on the committee during the year covered by this report were:

GE Healthcare

Atomic Weapons Establishment, Aldermaston

Defence Science and Technology Laboratory

Department for Environment Food and Rural Affairs (DEFRA)

Environment and Heritage Service, Northern Ireland

Environment Agency

Food Standards Agency

Health and Safety Executive

- Methodology and Standards Development Unit, Hazardous Installations Directorate
- Nuclear Installations Inspectorate

Health Protection Agency

Home Office

Meteorological Office

National Nuclear Corporation

Nuclear Department, HMS Sultan

Scottish Environment Protection Agency

Shell Global Solutions

Westlakes Research Institute

The Chairman and Secretary are provided by the radiation protection division of the HPA.

2 TERMS OF REFERENCE

The terms of reference of the committee are:

Areas of technical interest

1. ADMLC's main aim is to review current understanding of atmospheric dispersion and related phenomena for application primarily in authorisation or licensing of discharges to atmosphere resulting from industrial, commercial or institutional sites. ADMLC is primarily concerned with dispersion from a particular regulated site or from discrete sources, and will not normally consider work in the following areas: traffic pollution, acid rain and ozone.
2. ADMLC is concerned both with releases under controlled conditions occurring at a constant rate over long periods, and with releases over shorter periods such as accidents or controlled situations where the release rate varies.
3. ADMLC is concerned with modelling dispersion at all scales, including on-site and within buildings.

Organisations and outputs

4. The Committee shall consist of representatives of Government Departments, Government Agencies and organisations with an interest in modelling dispersion of material for the situations identified above. Each organisation represented on the Committee shall pay an annual membership fee.
5. ADMLC believes that it can be most effective by limiting its membership to about 25 organisations. New organisations will only be admitted to membership of ADMLC if the majority of existing members agree to their membership.
6. ADMLC aims to review, collate, interpret and encourage research into applied dispersion modelling problems. It does not endorse particular brands or suppliers of commercial models. However, it is concerned to ensure that users for industrial applications are aware of what is available, how it can be applied to particular problems and of the uncertainties in the results.
7. The Committee will commission work on selected topics. These should be selected following discussion and provisional agreement at meetings of the Committee, followed by confirmation after the meeting. It will produce reports describing current knowledge on the topics. These may be reports from contractors chosen by the committee or may be based on the outcome of conferences or workshops organised on behalf of the committee. The money raised from membership fees will be used to fund contractors, organise workshops and report on their outcome, and any other matters which the Committee may decide.

3 WORK FUNDED DURING THE YEAR

3.1 Review of atmospheric dispersion in complex terrain

The Atmospheric Dispersion Modelling Liaison Committee is interested in reviewing methods of modelling dispersion in the types of complex terrain found in the vicinity of nuclear and other industrial sites in the UK. Although many UK nuclear sites are located in coastal regions this work is concerned primarily with orographic effects rather than coastal effects. However, the case where coastal and orographic effects combine to influence concentrations measured at a receptor is relevant.

The review should give general guidance on the types of terrain for which the standard Gaussian plume model could be applied, and comment on the likely effect of complex terrain on predicted air concentrations.

The review should identify a number of models, and comment on the types of terrain for which each model is appropriate and the extent to which the model is based on experimental data or generally accepted theoretical assumptions. The review should comment briefly on the extent to which predicted annual average and short term peak concentrations would change if calculated using a complex terrain model rather than a standard Gaussian plume model. The review should also comment on ways in which modelling of dispersion in complex terrain could be improved.

The review should comment on the quality of meteorological information needed for such studies, including the calculation of concentration on flat terrain with complex terrain in the vicinity.

The review should comment in particular on the model incorporated in ADMS.

The report on this work is published as ADMLC/2005/1.

A REVIEW OF ATMOSPHERIC DISPERSION IN COMPLEX TERRAIN

A report prepared for ADMLC by

Richard A. Hill, Emma R. Lutman and Alistair D. Arnott

Westlakes Scientific Consulting

This study was funded by the UK Atmospheric Dispersion Modelling Liaison Committee.

EXECUTIVE SUMMARY

This review was commissioned by the Atmospheric Dispersion Modelling Liaison Committee (ADMLC) to consider modelling the dispersion of material in the atmosphere in regions of complex terrain.

The methodologies for modelling flows in complex terrain were reviewed, including the dividing streamline approach; linear analytical solutions of the momentum and continuity equations; the use of diagnostic wind field models; the application of prognostic meteorological models and the use of full computational fluid dynamics flow-field solutions. Whilst it was concluded that CFD modelling remains limited by computational requirements, useful information on the applicability of other simpler models may still be obtained. Much like wind-tunnel modelling therefore, the best use of CFD may be in the evaluation of specific conditions where the applicability of the aforementioned models may not be assumed *a priori*.

Experimental datasets have been widely used to evaluate and develop models of dispersion over terrain. These datasets include numerous investigations of wind flows over complex terrain, with studies designed from a wind engineering perspective, and also studies of flow and dispersion over complex terrain that have been approached from the perspective of predicting environmental concentrations. The review focussed particularly on the latter though the large body of work conducted to evaluate wind flows was also discussed briefly.

The final section of this report evaluated two models (ADMS and AERMOD) that are widely used in the UK for addressing regulatory compliance issues, and have algorithms for determining the influences of terrain features. Substantial differences were found in the predictions of the effects of terrain on atmospheric dispersion between these models, with disparities being particularly marked where the prediction of dispersion within extremely complex terrain was concerned. In these regions, the lack of a detailed horizontal flow-field model within AERMOD lead to concentration contour plots that did not realistically represent the channelled flow that would be expected.

AERMOD did however predict similar patterns of near-field plume impaction on terrain features to those found using ADMS. Furthermore, predictions of maximum concentrations were within 20% when the two models were applied in a region of highly complex terrain. More significant differences were found for the case of the interaction of a plume on a downwind region of highly complex terrain where the predictions of AERMOD were a factor of 2.6 higher than those of ADMS.

The strength of interaction between a dispersing plume and the underlying terrain was shown to be a function of the release height, with stronger terrain interactions occurring where plumes were released at heights similar to those of the surrounding terrain. Terrain effects were not found to be significant when modelling elevated releases over relatively low lying terrain.

One of the key areas highlighted in this review is that, for the accurate assessment of dispersion in regions of complex terrain, it is of primary importance to be able to predict the wind-field accurately. For situations where locally-representative meteorological data are available and where the assessment of impacts to local receptors is required, then models, such as AERMOD (that only model the interaction of the dispersing plume with the underlying terrain) can be applied. However, for situations where input meteorological data do not represent the flows close to the source, or where longer-range dispersion is to be predicted, then more detailed modelling of the flow-field should be made.

It is noted that care should be taken when applying linear models to ensure that the model domain includes the terrain features that are likely to affect flow. However, domain sizes that are greater than the distance a plume is likely to be advected during a single hour should be avoided.

CONTENTS

1 INTRODUCTION

This review was commissioned by the Atmospheric Dispersion Modelling Liaison Committee (ADMLC) to consider modelling the dispersion of material in the atmosphere in regions of complex terrain. The definition of the term "complex terrain" is itself somewhat ambiguous, depending on the perception of the individual as to what "complex" may mean. In this review we define complex terrain as non-flat terrain that has the potential to affect the dispersion of material in the atmosphere. It should also be noted that this review focuses on dispersion from point sources over scales of relevance to the interpretation of local effects, *i.e.* of the order of several kilometres from the source.

The effects that terrain features may have on flows and dispersion were summarised in the American Meteorological Society workshop held in May 1983 (Egan and Schiermeier, 1986). It should be noted that regulation of air pollutants in the United States of America (USA) focuses on the maximum air concentration. Hence, the summary of Egan and Schiermeier (1986) was directed towards the near-field interaction of a dispersing plume with the immediately surrounding terrain features as such a situation would represent the worst case scenario of a poorly-dispersed plume being grounded. Their considerations of the interactions of a plume with the terrain features provide a useful summary of dispersion in complex terrain and are as follows:

- Plume interactions with windward-facing terrain features
  - Streamline interactions with terrain features whereby receptors on hills at a similar elevation to the stack experience elevated concentrations.
  - Streamline divergence and impaction on hill slopes in stable conditions.
  - Flow over moderately sloped hills in neutral conditions can experience decelerations on the upwind slope, causing reduced rates of dispersion and increase air concentrations.
  - Localised flow modifications due to thermal effects in convective and stable conditions.
  - Increased turbulence, stagnation areas, waves and recirculation effects can increase the interaction of a plume with the surface and thus elevate ground level air concentrations.
- Plume interactions with lee sides of terrain features
  - Regions of recirculation behind steep terrain features can rapidly advect pollutants towards the ground and furthermore plumes interacting with the turbulent lee wake of a hill can experience reduced advection speeds and increased rates of vertical dispersion both of which can cause localised peaks in air concentrations.
  - Releases into the lee of a hill in stable conditions can also be recirculated and lead to increased ground level air concentrations.

- Plume interaction within valleys
    - Shallow valleys (with heights below the mean plume height) can develop internal boundary layers in stable conditions, with the overlying plume dispersing as though released over flat terrain, though from a somewhat lower height.
    - Releases within deep draining valleys experience restricted lateral dispersion due to the valley sidewalls and during stable overnight conditions an inversion layer within the valley essentially traps pollutants. Following daybreak and the erosion of the inversion, elevated ground level concentrations can be attributed to fumigation from the trapped nocturnal plume.
    - Closed valleys with restricted outflows can trap pollutants during stable conditions, with lateral dispersion being limited by the valley sidewalls and vertical dispersion being limited by the inversion layer.
    - Convective circulations in complex terrain due to differential heating can lead to the impingement of pollutant plumes due to crossflow onto the valley side walls, subsidence of plume centrelines within the valley or the formation of downdrafts all serving to elevate ground level air concentrations.

The first section of the review focuses on the application of models currently used in the UK or overseas for determining the meteorological inputs into dispersion codes, and also includes a brief review of experiences in the field of Computational Fluid Dynamics (CFD).

An important factor in addressing the suitability of any model for a particular application is its performance in model validation studies. Some of the more widely used studies that have been applied to develop and evaluate models for dispersion in complex terrain are reviewed in Section 2. This section investigates how well the models compared with the field data and also how realistic these datasets may be to the situations that the models may be routinely applied in.

The final section of this review considers two "regulatory" dispersion models commonly used to address compliance issues within the UK. The predictions of these models (ADMS and AERMOD) are compared for a range of different terrain types to determine the extent to which air concentrations may increase due to topographic effects and to what extent the predictions of these models agree in terms of both the magnitude of any increase and the spatial variation.

It should be noted that a comprehensive review of the topics considered herein is beyond the scope of this work. This review is an overview of the subject matter with the aim of providing some useful insights into atmospheric dispersion in a complex environment.

2 REVIEW OF COMPLEX TERRAIN DISPERSION MODELS

This section considers a variety of different dispersion modelling methodologies that are applied world-wide to include the influences of complex terrain on dispersion from point sources. The methodologies included in the review include the dividing streamline approach; linear analytical solutions of the momentum and continuity equations; the use of diagnostic wind field models; the application of prognostic meteorological models and the use of full computational fluid dynamics flow-field solutions.

2.1 Simple streamline dividing approach: AERMOD

The methodology used to model complex terrain in the Gaussian Plume model AERMOD is described in detail in Cimorelli *et al.* (2002) and Venkatram *et al*. (2001). AERMOD applies a simplified version of the methodology that is included in the CTDMPLUS model (Perry, 1992). CTDMPLUS is designed to provide predictions of air concentrations in complex terrain at specific receptor locations for defined time periods. In order to achieve this, CTDMPLUS includes algorithms to determine the stream-line distortions, the effects of terrain on rates of vertical dispersion and applies the "dividing streamline" approach to determine whether the dispersing plume moves over or around terrain features. AERMOD applies the "dividing streamline" approach, though does not model the larger scale flow-field explicitly as AERMOD is not designed to provide estimates of the spatial pattern of concentrations or to predict concentrations for specific periods of time (Venkatram *et al*., 2001).

The meteorological preprocessor, AERMAP imports gridded terrain data and simplifies multiple hills by deriving an effective elevation of surrounding terrain, depending both on the height of the terrain and its distance from the receptor point. Having established an effective terrain, this allows the calculation of an height scale h_c for each receptor location, which is representative of the terrain surrounding that receptor point and its effect on the flow in the vicinity of the receptor. This methodology allows AERMOD to apply the "dividing streamline" simplification which is based on a single Gaussian hill (Venkatram *et al.*, 2001). The plume is modelled as a combination of two limiting cases: a horizontal plume (terrain impacting) and a terrain-following (terrain responding) plume (Figure 1). The flow is modelled as a two-layer flow, defined at a critical height, the dividing streamline height (H_c). The flow below H_c remains horizontal and will either flow around the hill or impinge on it, whereas the flow above H_c rises over the terrain. The dividing streamline theory is applied in all stability categories. In stable conditions, the contribution from the terrain-impacting plume prevails, while in neutral and convective conditions the contribution from the plume rising over the hill governs the flow.

The total air concentration (C_T) is calculated according to Equation 1 (from Cimorelli *et al*., 2002) and is illustrated in Figure 1.

$$C_T\{x_r, y_r, z_r\} = f.C_{cs}\{x_r, y_r, z_r\} + (1-f)C_{cs}\{x_r, y_r, z_p\} \qquad \text{Equation 1}$$

$C_{cs}\{x_r, y_r, z_r\}$ is the concentration at a receptor height (z_r) of a plume unaffected by terrain (*i.e.* a horizontal plume state, in stable and convective conditions), likewise the concentration in the plume travelling over the hill is denoted by $C_{cs}\{x_r, y_r, z_p\}$ (*i.e.* the terrain following plume state), where z_p is the height of the receptor above the terrain and f is the plume state weighting function.

The dividing stream-height (H_c) is taken as the height at which an air parcel has enough kinetic energy to ascend to the receptor height (assuming the wind speed increases with height). H_c is thus a function of the receptor height.

The weighting factor f is calculated from the fraction of the plume mass below the dividing stream height, termed f_p, according to Equation 2. This is shown graphically in Figure 2.

$$f_p = \frac{\int_0^{H_c} C_S\{x_r, y_r, z_r\}dz}{\int_0^{\infty} C_S\{x_r, y_r, z_r\}dz} \qquad \text{Equation 2}$$

The weighting factor is calculated as follows according to Venkatram *et al.* (2001):

$$f = \frac{1}{2}(1+f_p) \qquad \text{Equation 3}$$

The weighting of the two states in Equation 1 depends on the atmospheric stability, the wind speed (which affects the value of H_c) and the plume height relative to the terrain height. In flat terrain, or when the plume is entirely below H_c, f_p = 1.0 and the concentration is determined by the horizontal plume.

When the plume is entirely above H_c or when the atmosphere is either neutral or convective (*i.e.* H_c=0, f_p = 0) then the horizontal plume and the terrain-following plume concentrations contribute equally to the total air concentration. Since the plume will spread partially around the side of the hill, the model is constrained such that there is always a component of the plume from the horizontal state, even for plumes above H_c. Therefore, the plume is never allowed to approach the terrain-following state completely.

2.1.1 Limitations of AERMOD

AERMOD has been designed to predict the concentration frequency distributions observed under various release conditions. Unlike CTDMPLUS (Perry *et al*., 1992), AERMOD does not model the details of the flow field. Features of the flow such as acceleration and amplification of vertical turbulence caused by the

convergence of streamlines as the plume flows over a hill are not accounted for in AERMOD's treatment of the flow due to the computational expense. AERMOD requires detailed local meteorological data and the turbulence in the flow is assumed to be represented by meteorological measurements. The model therefore does not predict the location and temporal distribution of concentrations (Venkatram *et al*., 2001) since these are not generally required under legislation in the USA, unlike UK legislation where air concentrations at specific receptor points are required.

The application of a dividing streamline concept is based on an idealised three-dimensional hill and flow over multiple or irregular shaped hills may differ from the idealised case. Towing tank experiments (Snyder *et al.*, 1985) investigated the applicability of the dividing streamline approach to different shapes of hills and ridges, including the effects of the orientation of a ridge and the effect of wind shear in the approach flow. Their results indicated that for symmetric hills and for wind angles less than 45^{o} from the centreline, the estimated H_c was valid for the stable conditions under investigation. For truncated ridge-shaped hills it was found that the value of H_c should be considered a lower limit (*i.e.* streamlines above H_c would not necessarily rise over the hill).

CERC (2001a) and Carruthers *et al*. (2001) noted some deficiencies in AERMOD's treatment of terrain. Their results showed that AERMOD overestimates air concentrations for a stack located on top of a hill. According to US EPA (2003) this error has been corrected. In addition, a correction to the model has been added to fix the problem of high air concentrations being predicted at receptor points below the base of the stack (US EPA, 2003).

2.2 Analytical solutions to the governing equations of flow: FLOWSTAR (ADMS)

A version of the FLOWSTAR model (Carruthers *et al.*, 1991) is used by the Gaussian Plume model ADMS (Carruthers *et al.*, 1994) to simulate dispersion over complex terrain. This module treats both dispersion over hills and regions of changing surface roughness and applies linear analytical solutions to the equations governing airflow and turbulence in the boundary layer. The linear equations have the advantage of being computationally efficient (both in terms of calculation efficiency and memory requirements) and thus allow much faster run times than models based on computing the full equations of motion. Furthermore, as the equations can be solved analytically, they have an exact numerical solution and do not suffer from convergence problems that are encountered when non-linear equations are solved using iterative methods.

FLOWSTAR calculates the flow and turbulence fields over complex terrain and uses them to adjust the plume height and plume spread parameters calculated by the flat terrain model. The module takes account of all common cases where the mean wind dominates the flow. It is used to calculate the mean air flow and dispersion over hilly terrain of variable roughness and to allow for the effects of

stratification in the mean flow and turbulence (Carruthers *et al.,* 1994). The effects of horizontal temperature gradients on flow, such as the formation of anabatic or katabatic slope winds are not accounted for in FLOWSTAR. The "Complex Terrain Module" implementation of FLOWSTAR is described in the ADMS 3 Technical Specification (Carruthers *et al*., 2000), also in Carruthers and Hunt (1990) and Carruthers *et al.* (1991) and a summary is presented here.

2.2.1 FLOWSTAR

The FLOWSTAR model applies a mathematical solution for airflow and turbulence over complex terrain based on the theory that flow perturbations induced by terrain features are relatively small. The approximations applied in FLOWSTAR are that the flow is steady-state, the buoyancy forces are locally small, Coriolis effects are negligible and only vertical gradients of the shear stress term are important. By applying a small perturbation theory to the airflow, the Navier-Stokes equations can be linearised (Jackson and Hunt, 1975), whereby the non-linear terms are replaced either by constants or defined as simple functions of the mean flow. Flow velocities at a particular point can be determined from the upstream flow plus a perturbation (or change) term that accounts for the effects of the terrain. Small perturbation theory can only be applied to model flow over terrain when the topographical features are low and of moderate slope (often cited as being less than approximately 1:3).

The linear method allows the analytical solution of flow for a wide range of upwind conditions and shapes of hill. However, it cannot describe large (non-linear) perturbations to the flow such as the formation of flow separation areas or recirculation zones and assumes that the slope is small enough for the linear theory to be a reasonable approximation of two or more effects combined, such as roughness and topographic effects (Carruthers and Hunt, 1990).

The flow over the terrain is divided into two main regions, an inner region and an outer region, though it should be noted that the outer region is itself comprised of middle and upper layers and the solution for the inner region is only compatible with the surface boundary condition if a separate thin surface layer is included (Sykes, 1980, in Wood, 2000). In FLOWSTAR the inner region surface layer is not included, though the velocity perturbations are constrained to be zero at the surface. A diagram of the subdivision of the flowfield is shown in Figure 3.

The main features of these regions are as follows (Carruthers and Hunt, 1990):

1) The inner region, of height *l*, is adjacent to the ground and so the shear stresses have an important influence on the flow, but stratification is unimportant in this layer. Carruthers and Hunt (1990) note that stratification effects are only likely to have a significant effect on flow in the inner region when very strongly stable conditions occur or when flows are driven thermally. The height of this region (*l*) is derived by balancing the advection and shear stress terms and, for the situation of an isolated hill, can be determined from the characteristic length scale of

the terrain features (L) as $l \ln(l/z_0) = 2k^2 L$, where k is the von Karman constant (≈ 0.4) and L is defined as the length from the summit of the hill to a position where the elevation is half of that of the summit. For more complicated terrain (involving numerous hills), L and the heights of the inner and outer regions are determined from the Fourier transformed mean wave number.

2) The outer region middle layer occurs between heights of l and h_m above the ground and is a region of flow which is far enough from the ground that local shear stresses are not important but the effects of upwind shear are important. Stratification is unimportant in this layer. The height of the middle region (h_m) can be approximated from L and the roughness length (z_0) as $h_m^2 \ln(h_m / z_0) = L^2$.

3) The outer region upper layer contains the outer part of the turbulent boundary layer where wind shear and shear stress are unimportant. However, stratification is likely to be important hence the flow is affected by both pressure and buoyancy forces. The vertical scale of the outer region (including both layers) has been assumed by Jackson and Hunt (1975) to be approximated by the horizontal scale of the inner region (or the length of the hill, L) for the situation of an isolated hill.

The FLOWSTAR model calculates the perturbation terms in Fourier space then inverts the Fourier transformed perturbation terms to allow the determination of actual flow over the terrain. The use of Fourier analysis in the context of the FLOWSTAR model permits the horizontal variation (*i.e.* variation with along-wind and crosswind distance) of the perturbation terms to be parameterised fully by their respective wavenumbers. Consequently, the differential functions that are required to be solved to determine the horizontal variation of the perturbation terms can be solved from their algebraic dependence on wavenumber, (Homicz, 2002). It should be noted however that the application of Fourier transforms to terrain data requires that there is either constant or periodic terrain height at the domain boundaries.

The detailed solution using a linear three-dimensional theory is given in Hunt *et al*. (1988a) for the inner region and middle layer and in Carruthers and Hunt (1990) for the inner, middle and upper regions. The linear solutions for the stratified upper layer of the flow are provided in Hunt *et al*. (1988b). The equations and numerical methods of solution can be found in these texts or in Carruthers *et al*. (2000).

Boundary conditions to the model are defined such that at distances far from the terrain features (both in horizontal and vertical co-ordinates), the perturbation terms tend to zero and the wind field assumes the horizontally uniform and vertically logarithmic shape as defined in the undisturbed upstream flow. A lower boundary condition is also included in FLOWSTAR whereby the perturbation terms of the flow components tend to zero, replacing the requirement for a separate surface layer (Robinson, 1996).

To a first approximation the modelled vertical velocity throughout the inner layer follows the terrain contours. By assuming upper boundary conditions that: (1) the vertical velocity must tend to zero with height and distance from the hill; and (2) that horizontal velocity must tend to the value at the same height in the undisturbed upwind flow, then it is apparent that the upper boundary of the outer region cannot be deformed to compensate for the deformation of the interface between the inner and outer layers. Furthermore, as flow in the upper region is assumed to be irrotational and inviscid, this leads to the development of an in-homogenous pressure field. The coupling of the regions in the model ensures that this upper level "perturbation pressure" drives the perturbation velocities in the lower regions of the model. A closure method is required to resolve the Reynolds stresses in the inner layer and to meet this requirement a simple mixing length approximation is made, assuming that turbulence is in local equilibrium. As the flow in the outer region is advected over a hill with timescales significantly greater than those related to the transport of momentum, then the shear stresses have a negligible effect on flow in this region (Belcher and Hunt, 1998).

Stratification effects, that are of significance when modelling the flow and pressure perturbations in the outer region upper layer, are assumed in the ADMS implementation of FLOWSTAR to follow one of three cases. It should be noted that neutral stratification is assumed in the inner region and outer middle layer, though the coupling of the solutions between the layers of the model ensures that the influence of non-neutral stability is included implicitly in the lower level flows (Carruthers *et al*., 1991). The three stratification cases that are considered are:

- A neutral boundary layer uncapped by an inversion layer.
- A stratified boundary layer uncapped by an inversion.
- A neutral boundary layer capped by an inversion with the free troposphere above the inversion.

For neutral or constant stratification an upper radiative condition is applied in FLOWSTAR to ensure that energy is radiated upwards. The situation where an inversion layer is modelled can result in the development of lee waves downstream of terrain features and has also been shown to influence the flow speed close to the summit of the hill significantly. Upper layer stratification creates a more asymmetrical flow and higher velocities in the lee side of a hill (Carruthers and Hunt, 1990).

One of the theoretical constraints on the application of the FLOWSTAR model is that it is limited to the situation where air flows over a hill (Carruthers and Hunt, 1990). The dividing streamline theory (Section 2.1) illustrates that this constraint is unrealistic for strongly stable meteorological conditions where air above a critical height (H_c) flows over a hill whilst air below H_c flows around a hill.

In ADMS, the dividing streamline approach is implemented by defining a region of flow around the hill to exists if:

$$\frac{U_{h\max}}{N\left(h_{\max}-h_{mean}\right)}<1 \qquad \text{Equation 4}$$

where U_{hmax} is the wind speed at the maximum height of the hill, N is the buoyancy frequency, h_{max} is the maximum height of the hill and h_{mean} is the mean height of the hill.

As FLOWSTAR calculations are required to address flow over real terrain, the dividing streamline approach needs to be modified to include multiple hills. Defining the flow surface and combining the flow solutions for each hill would be computationally expensive, hence ADMS adopts the simpler solution of defining the dividing surface based on the height of the highest hill (Figure 4).

The flow field used in the dispersion calculations depends on the source conditions. The effective height of the plume is calculated, taking into account the discharge momentum and buoyancy. If the height is below the dividing surface, the stable flow field is used for the dispersion calculations. If it is above the dividing surface, the standard FLOWSTAR flow field is applied over the whole model domain.

To calculate the flow field, the terrain data is simplified to a single Gaussian-shaped hill of hemispherical shape. Its height is taken to be the height of the highest hill and the horizontal length scale is the characteristic length scale calculated by FLOWSTAR (discussed previously). A dividing surface is defined, which is Gaussian in shape and is based on the single idealised hill. Below the dividing surface, the flow field is approximated by assuming a horizontal potential flow around a cone of radius $r(z)$ (*i.e.* the radius of the hill at height z). Above the dividing surface, the flow field is assumed to be unperturbed by the terrain and can therefore be assumed to be the same as that at the undisturbed upwind boundary. The vertical velocity is smoothed to avoid discontinuities at the dividing surface (Carruthers *et al*., 2000) and a scaling factor is applied to the turbulence parameters.

The influence of variations in the roughness length on flow are also considered in FLOWSTAR using the methods detailed in Belcher *et al*. (1990). Assuming linear theory, the perturbations caused by non-uniform surface roughness can be simply added to perturbations caused by terrain (essentially a superposition of the two features), hence any non-linear links between terrain influences and roughness are ignored. The influences of non-uniform surface roughness are only considered in the inner region and outer region middle layer, the two layers closest to the surface where wind shear is considered important. The analysis of the effects of terrain roughness is included as a first order approximation, with roughness length changes having no effect on either the pressure gradient or the crosswind velocity perturbation. Hence roughness length variations are only considered to perturb the vertical and along-wind velocity components and so do

not cause any variation to the mean horizontal wind direction within the model domain.

So far the review of the FLOWSTAR model has only considered the effects of surface topography and roughness on the mean flow across the modelled area. When considering the effects of topography for inclusion in the framework of an atmospheric dispersion model it is also necessary to consider the influence that terrain features may have on the rates of dispersion in a plume. In order to consider these effects, FLOWSTAR includes algorithms for the calculation of turbulence velocities that are applied directly in the determination of the horizontal and vertical plume spread parameters (σ_y and σ_z). Turbulence in the inner region is estimated from the calculated shear stresses as eddies form a local equilibrium with the mean flow velocities before they can be advected (Belcher and Hunt, 1998). Turbulence in the outer region is modelled assuming rapid distortion theory, whereby the advection of eddies over the hill occurs much faster than the eddy turnover time. Consequently, the turbulence in this region depends largely on the distortion of the upstream turbulence by the mean strain (Belcher and Hunt, 1998). Of course these two approximations represent extremes of a continuum, consequently a blending term is applied in FLOWSTAR to prevent discontinuities in the vertical turbulence structure. The influence of convection on the turbulence velocities is modelled through adding the convective velocities determined over flat terrain to those calculated using the complex terrain equations.

FLOWSTAR requires gridded data on the terrain height and surface roughness and can be applied with horizontal resolutions of up to 64 $\times$ 64 grid nodes. As is discussed in Section 3, the choice of grid resolution affects the model speed, memory requirement and predicted air concentrations. Carruthers *et al*. (2000) recommend the use of a resolution of 32 $\times$ 32 grid nodes is acceptable for most practical applications, including gradients up to 1:3, if the domain size is no greater than 10 km $\times$ 10 km. The FLOWSTAR grid has 10 vertical levels ranging from 1.3 times the minimum surface roughness to 2 km (Carruthers *et al*., 2000). The calculation grid is aligned in the direction specified by the wind at the upstream boundary to enable the determination of the Fourier transforms of terrain height data to be used in the analytical solution for the perturbation terms. These perturbation terms are added to the initial flow to determine the perturbed flow.

The outputs of the model are:

- Local mean wind velocity components (U+u, v, w)
- Local root mean square velocity scales σ_u, σ_v, σ_w
- Vertical and transverse length scales L_v and L_w
- Lagrangian time scale T_L
- Energy dissipation rate ε

The software developers recommend that the model is used for moderate gradients (up to 1:3) only, however they state useful results can be obtained for

slopes as great as 1:2 (Hunt *et al.,* 1991). It should be noted that the original model developed by Jackson and Hunt (1975) was quoted as being suitable for hills where $h/L < 0.05$, hence caution should be applied when modelling extreme gradients. Carruthers *et al*. (2000) recommended that the model is not used for shallow slopes with gradients less than 1:10, based on the anticipation that terrain effects will be negligible for such areas.

2.2.2 Regions of reverse flow

A development to the FLOWSTAR model has been introduced to allow flows to be modelled in recirculation regions, such as the wake region downstream of a steeply sloped hill. However, these only apply to the situation where a source is located within a region of reverse flow and are not applied to the situation where a plume advected over a hill may be entrained in a wake region thus leading to elevated ground level concentrations downwind of the source. In ADMS 3, a plume released into a reverse flow region is assumed to be well-mixed within that region, and is represented downwind by dispersion from a virtual source (Carruthers *et al*., 2000).

2.2.3 Benefits and limitations of FLOWSTAR

The FLOWSTAR model provides a methodology to determine the flows and turbulence over moderately sloped terrain features based on meteorological data from a single upwind site. Furthermore, the computational intensity of the model makes it suitable for calculations on standard desktop personal computers (PCs) where regulatory compliance is addressed through the use of annual timeseries of meteorological data.

The performance of the code has been demonstrated through numerous comparisons between the underlying theoretical basis of the model with measured flows (*e.g.* Bradley, 1980; Hewer, 1998; Jenkins *et al*., 1981; Mason and Sykes, 1979; Mason and King., 1985; Walmsley *et al*., 1982, Taylor *et al*., 1983). Overall, linear models have been found to give good predictions of flows on upwind slopes and for summit wind speeds, though can over-predict flows in the lee of hill due to being unable to treat the recirculations that occur in such regions. It is useful to note that most comparisons between linear models and measurement data have focused on the windfield studies at Askervein and Blashaval hills (see Section 3) and in both these regions maximum terrain gradients of approximately 1:3 and 1:2 occur, which may be assumed to be strictly above the limit of linear theory.

Wood (1995) provided an approximate expression to determine the "critical gradient" at which flow separation was likely for two-dimensional hills from the heights of the inner and middle regions and the roughness length (Equation 5). Hewer (1998) noted that for three-dimensional terrain, values of the critical gradient would be approximately 20% higher than for two-dimensional hills.

$$q_{crit} \approx \frac{(\ln(l/z_0))^2}{(\ln(h_m/z_0))^2(1+4.2/\ln(l/z_0))}$$ Equation 5

The approximations for the heights of the inner and middle layers can be substituted into Equation 5 to enable this equation to be shown graphically for a range of possible terrain lengths and roughness (shown as Figure 5). This shows that flow separation occurs more readily over terrain with low half-lengths and high surface roughness (*e.g.* forested mountain regions). It should be noted that some dependence of the onset of non-linear flow on stability may occur as noted by Apsley and Castro (1996) and discussed in Section 3.2.1.

CERC (2001b) compared the predictions of FLOWSTAR with the wind speed-up ratios observed over Askervein Hill on South Uist (details of the experiments are discussed later), finding a good agreement between model predictions and measurements on the upwind side and summit of the hill, though poorer agreement downwind of the summit. It is interesting to note that the maximum gradients of Askervein Hill are around 1:3 and consequently flow separation in the lee side of the hill may be expected. Such re-circulatory conditions have been modelled using non-linear CFD codes (*e.g.* Stangroom, 2004; Chow and Street, 2004; Kim and Patel, 2000). Similarly, Hewer (1998) used Blashaval Hill data to compare the predictions of the FLOWSTAR model with those of a non-linear fluid dynamics code, finding a good agreement between the predictions of both models and the measurement dataset. However, in the lee of the hill FLOWSTAR tended to over-predict wind speeds, with the non-linear CFD model providing a better comparison with the measurements. Such recirculation areas could lead to peak concentrations occurring in the lee of a hill due to the rapid rates of vertical transport. An example of peak concentrations being measured in the lee of a hill is discussed in Dawson *et al*. (1991), though would not have been accurately modelled by a linear flow code.

Further assumptions that are implicit in the formulation of linear models, such as FLOWSTAR, should also be recognised to ensure the applicability of the model. These include the model neglecting slope winds caused by temperature differences that can result in localised nocturnal drainage flows. Moreover, the original algorithms developed by Jackson and Hunt (1975) are only applicable to the situation where moderate or strong winds occur. From an air pollution perspective, light winds often result in the highest air concentrations and are, in the UK, typically associated with high pressure systems bringing with them clear skies and significant positive or negative surface heat fluxes. During such conditions thermally-driven flows have been shown to be significant in regions of highly complex terrain (Weber and Kaufmann, 1998) or even moderate terrain (Robinson, 1996).

2.3 Diagnostic wind field models

Diagnostic wind field models apply a range of techniques to determine the wind field across an area from a set of often limited or scattered observations. These techniques include simple interpolation routines, semi-empirical expressions and the application of equation sets (more typically used by prognostic models) to interpolate between observational sites or to diagnose local features of the flow field, such as anabatic or katabatic winds. Such models are likely to be applied most successfully over large geographical areas and at relatively coarse resolutions, allowing the inclusion of numerous observational sites in the analysis. However, when considering dispersion from point sources in complex terrain, where locally high concentrations are of interest, it is useful to review the calculation routines applied by such models to determine the level of detail that they may provide. This section reviews three diagnostic wind field models that are applied for such situations. These are the Danard (1976) model used in the SMHI Airviro Air Quality Management System, the MINERVE model (included within the modelling package Aria Industry) and the CALMET model (included with the CALPUFF modelling system).

2.3.1 The Danard wind field model

A simple model for predicting the effects of topography on surface (anemometer level) winds was purported by Danard (1976) and has been applied as the wind field model in the Airviro Air Quality Management System (SMHI, 1997). The wind field from this model is determined from the consideration of (a) the first thermodynamic equation, (b) the pressure tendency equation and (c) the horizontal momentum equation. Based on the assumption that surface level winds can be determined from the adaptation of an undisturbed geostrophic wind by the influence of local terrain features. The model further assumes that this adaptation process is very fast (1.5 hours for a model resolution of 10 × 10 km and 4 minutes for a resolution of 250 m × 250 m) and that only horizontal processes are non-linear. Initial values of surface temperature (T_s) across the model domain are determined from the geostrophic temperature and the lapse rate (γ), whilst the surface pressure field is determined from Equations 6 and 7.

$$P_s = P_g \left(\frac{T_s}{T_g} \right)^{\frac{g}{Rg}} \quad \text{where } 0 < \gamma > 0 \qquad \text{Equation 6}$$

$$P_s = P_g \exp\left(\frac{g(Z_g - Z_s)}{RT_g} \right) \quad \text{where } \gamma = 0 \qquad \text{Equation 7}$$

Of course, the pressure differences calculated using Equations 6 and 7 are unaffected by local thermal influences that may be present, such as heating or cooling on hill slopes that give rise to anabatic or katabatic winds. To diagnose such cases, the model relies on surface temperature measurements, defining the difference in temperature ΔT as the difference between the "pseudo" initial

temperature and the measured values. The rate of temperature change (Q) can then be determined as Equation 8:

$$Q = \frac{q_s}{T_s}\frac{\Delta T}{t} \qquad \text{Equation 8}$$

where t is the time interval over which the heating is added.

The field of surface temperatures within the modelling domain is then determined using the first law of thermodynamics (Equation 9).

$$\frac{\partial q_s}{\partial t} = -V.\nabla q_s + K_t \nabla^2 q_s + Q \qquad \text{Equation 9}$$

The surface pressure field is calculated from the pressure tendency equation (Equation 10) where it should be noted that subscripts refer to surface values and that *H* is the boundary layer height.

$$\frac{\partial \ln(P_s)}{\partial t} = -\frac{g}{Rq_s T_s}\int_0^H \frac{dq}{dt}dz \qquad \text{Equation 10}$$

Following the determination of the surface pressure field the surface wind field is determined using Equation 11, where the second term (in parentheses) is the horizontal pressure gradient force at the Earth's surface in sigma co-ordinates (see Section 2.4 for more details). The last three terms on the right hand side of Equation 11 are the Coriolis force, surface friction and lateral mixing. Equations 9-11 are solved for each time step with the initial values being replaced by the calculated values.

$$\frac{\partial V}{\partial t} = -V.\nabla V - (g\nabla Z_s + RT_s \nabla \ln P_s) - fk\,V + F + K_m \nabla^2 V \qquad \text{Equation 11}$$

The friction force in Equation 11 is determined from Equation 12, where *c* is a constant of 2.8 for a stable or neutral atmosphere and decreases to 1.0 for extreme instability.

$$F = \frac{\sqrt{2}\,c\,C_d\,V^2}{h} \qquad \text{Equation 12}$$

Balancing the pressure gradient force, Coriolis force and frictional force for the initial wind yields the following expressions (Equation 13), which can be used to derive the surface wind direction from the angle between the surface and geostrophic winds (ε):

$$\sqrt{2}fV_g \sin e = F \quad \text{and} \quad \sqrt{2}fV_g \cos e = \sqrt{2}fV_s + F \qquad \text{Equation 13}$$

This model treats the channelling of flow within an area of complex topography, the effects of non-uniform surface roughness (through the drag co-efficient in Equation 12) and can treat the effects of thermal influences on wind flows provided that appropriate monitoring data are available. The model does not

account however for the vertical streamline deflection due to the interaction between a dispersing plume and the terrain and furthermore, the model does not treat any enhancement of turbulence caused by topographic effects. The predictions of the Danard model were compared successfully by Danard (1976) with measured wind data for the Juan De Fuca Strait and Georgia Strait at the western border between Canada and the USA. Wroblewski *et al.* (2001) compared the predictions of the AIRVIRO wind field model and the MINERVE model (a fully mass-consistent diagnostic wind model) with wind tunnel data. They concluded that overall the Danard model provided a good agreement with the measurements, though it was not able to predict the reversed flow in the lee of the steeper of the two hills they tested (aspect ratios, L/H, of 3 and 5). The equation set produced by Danard (1976) has the advantage of being extremely fast to solve (taking 40 timesteps to converge) and as only the surface (anemometer) level flow field is computed, the requirements in terms of computational memory are low.

2.3.2 MINERVE

The MINERVE model was developed by Electricité de France (Aria, 1995) to determine local (5 - 50 km from a point source) or regional (50 - 500 km from a point source) wind fields. This model (unlike the Danard model) is a three-dimensional code, explaining its improved performance in the model evaluation by Wroblewski *et al*. (2001) where vertical profiles of wind vectors were compared). The MINERVE code defines a three-dimensional grid using a terrain following co-ordinate system and determines the wind field from the following two-step process.

- Interpolation from the available meteorological observations.
- Adjustment to the topography.

The first of these steps applies a range of interpolation procedures (including inverse square of the distance and non-isotropic triangulation) to determine the initial wind field from the observational dataset. It should be noted that this stage is data intensive and used to determine the wind field at the boundaries of the model domain as well as the macro features of the flow field. The second step applies the equations for mass conservation in an incompressible fluid, with the constraint that the predicted field should be as close as possible to the interpolated field from the previous step. It should be noted however that the numerical equations applied by MINERVE do not account for the conservation of momentum or energy.

2.3.3 CALMET

A further diagnostic wind field model that is used widely (and is regarded as an approved model by the USEPA) is CALMET (Scire *et al*., 2000). This model is integrated within the CALPUFF modelling system, using a Lagrangian Gaussian Puff model to determine dispersion over scales of tens of metres to hundreds of kilometres and treats effects such as dispersion over complex terrain, dispersion

over water, coastal boundary layers, building downwash, deposition and simple air chemistry.

The diagnostic wind field model in CALMET calculates an "initial guess" wind field, which can be derived from one of three options:

- A mean wind field averaged across the domain, whereby the modeller specifies the vertical layer to be used and whether a single upper air station or all stations within the domain are interpolated.
- The vertical extrapolation of surface observations using similarity theory.
- The use of factors within each layer to determine the weighting between surface and upper air data.

The terrain within the model domain is then introduced to allow the "initial guess wind field" to be modified to include certain relatively localised flow features. These are:

- Kinematic effects.
- Slope flows.
- Blocking effects.

Kinematic effects (changes to the flow velocities) due to the terrain are modelled by calculating Cartesian vertical velocities (w) across the domain using Equation 13.

$$w = (V.\nabla h_t)\exp(-kz) \qquad \text{Equation 13}$$

Where V is the domain mean wind, h_t is the terrain height, k is a stability-dependant exponential decay coefficient and z is the vertical co-ordinate.

This is then used to determine the terrain following vertical wind W using Equation 14.

$$W = w - u\frac{\partial h_t}{\partial x} - v\frac{\partial h_t}{\partial y} \qquad \text{Equation 14}$$

A divergence minimisation scheme is used to iteratively adjust the u and v components of the wind until the overall differences meet a specified criteria.

Slope flows occur due to differential heating or cooling causing the formation of anabatic or katabatic winds. A semi-empirical scheme is employed in CALMET based on the "shooting flow" parameterisation by Mahrt (1982). This assumes that the flow is steady, of constant depth, and occurs parallel to terrain of constant slope. The slope speed (S) for down-slope flows is determined from Equations 15 and 16.

$$S = \left[\frac{Q_H \; g \; x \sin(a)}{r \; C_p \; T \; (C_D + k_{sf})} \right]^{1/3} 1 - \left[\exp(-x / L_e) \right]^{1/3}$$ Equation 15

Where:

$$L_e = \frac{h}{C_d + k}$$ Equation 16

L_e is the equilibrium length scale, x is the distance to the crest of the hill, Q_H is the surface heat flux, α is the angle of the terrain and k_{sf} is the entrainment coefficient at the top of the slope flow layer.

The slope speeds for up-slope flows are determined from Equation 17, where x in this case is the distance in height from the valley floor.

$$S = \left[\frac{Q_H \; g \; x \sin(a)}{r \; C_p \; T \; (C_D + k_{sf})} \right]^{1/3}$$ Equation 17

Blocking effects are determined by calculating the Froude number (*Fr*) at each of the grid points using Equation 18, where *N* is the Brunt-Väisälä frequency. Blocking effects are identified by this model in areas where the local Froude number is less than a critical Froude number of 1.0. At these locations wind vectors are re-aligned across the slope, though the magnitude of the wind speed is not modified. Where local Froude numbers are less than the critical values no changes to either wind direction or speed are made.

$$Fr = \frac{U}{N \; \Delta h_t}$$ Equation 18

Clearly, the aforementioned analysis makes some radical corrections to the simple wind field estimated initially. If left, these corrections could lead to significant and unrealistic discontinuities in the modelled flow field. The second phase of the analysis by CALMET introduces the measured wind data into the Phase 1 predictions of the flow field and utilises algorithms to combine and interpolate the datasets, weighing the observational data at locations close to the measurement stations. Following this, data are extrapolated vertically and boundary layer parameters (friction velocity, convective velocity scale, Monin-Obukhov length *etc*.) are determined using either an Energy Balance approach (applied for overland areas) or a Profile method (applied for overwater areas). In order to include regions where lakes or sea breezes may occur, options are provided to allow the specification of such areas manually, with a separate interpolation scheme being applied to interpolate winds based on distances from the coast. Discontinuities are reduced further by the application of a smoothing routine, followed by the calculation of vertical velocities using the incompressible mass conservation equation and the application of a divergence minimisation scheme to smooth the horizontal wind field.

The CALMET modelling system also can apply the results of prognostic wind field models, such as CCSUM and MM5, within the calculation routines. These predictions can be introduced as either the "initial guess wind field", the "Step 1 wind field", or as "observational data" interpolated into the "Step 2 windfield". The formulations of these models will be discussed in Section 2.4.

2.3.4 Benefits and limitations of diagnostic wind field models

Diagnostic wind field models provide a methodology for determining the flow field over a wide range of scales and terrain types and, according to Homicz (2002), do not represent a significant increase in computational requirements to methods based on linearlised solutions.

The main limitation of diagnostic models is the availability and quality of the observational data within a model domain (King and Bunker, 1984). Gross (1996) compared the predictions of a diagnostic wind field model with those of a prognostic model, using the latter model to simulate the input meteorological data for the diagnostic model. The results showed that for complex terrain, a network of some 50 – 100 sampling sites was required to capture the detailed flow field within the domain.

It is useful however to compare the idealised results of Gross (1996) with those derived from field data by Desiato *et al*. (1998) who found that, when modelling flow and dispersion in alpine terrain, the most accurate results were obtained when three surface measurements and a single vertical profile were used. The reason for this apparent discrepancy was due to the influence of very localised (sub-grid scale) topographical features at many of the sites in the measurement dataset of Desiato *et al*. (1998). This point was also made by Lamprecht and Berlowitz (1998) who noted that sensitivity tests should be conducted on measurement data prior to their inclusion in a diagnostic model to ensure that they are truly representative of the flow over the area they are interpolated to.

Further evidence of the applicability of diagnostic wind field models for evaluating dispersion using limited meteorological data may be found in the work of Davakis *et al*. (1998) and Gariazzo *et al*. (2004). Davakis *et al*. (1998) showed that a diagnostic wind field model coupled with a Lagrangian particle model could produce realistic predictions of dispersion in moderately complex terrain, even when run with very limited meteorological input data (in this case from a single meteorological site and from synoptic charts). Similarly, Gariazzo *et al*. (2004) simulated air concentrations of SO_2, NOx and CO in a 10×10 km domain near the Apennine mountains using the wind field from a diagnostic model determined from four surface stations and a SODAR to provide upper air data.

2.4 Prognostic Meteorological models

The application of prognostic (forecast) meteorological models to the field of modelling dispersion in complex terrain is becoming more widespread due to recent increases in computing power, though these are still mainly applied for mesoscale studies where grid resolutions of several kilometres are used. Numerous prognostic models have been applied when modelling air pollution transport, including the MM5 model developed by Pennsylvania State University and the National Centre for Atmospheric Research (Dudhia *et al*., 2005), TAPM developed by CSIRO in Australia (Hurley, 2005) and RAMS developed by Colorado State University (CSU, 1997). The wind fields generated by these models can be either used directly in Eulerian or Lagrangian dispersion models (*e.g.* Luhar and Hurley, 2003; Cox *et al*., 2003; Carvalho *et al*., 2002) or can be applied as the "observations" input to a diagnostic modelling system such as CALMET-CALPUFF (*e.g.* Chandrasekar *et al*., 2003).

These models are all based on the "Primitive Equation Set" which is a set of coupled equations for momentum (*x*, *y* and *z* components), continuity and thermodynamics derived from the Navier-Stokes equation. These models are therefore specialised Computational Fluid Dynamics (CFD) models, a discussion of other uses of CFD is presented in Section 2.5. Typically, the initialisation of these equations is determined from the output of a coarser resolution meteorological model, such as those run by National Weather Services. These models also include modules for predicting precipitation, the radiation balance, the surface energy balance and the vertical structure of the planetary boundary layer. A further common feature of these models is the use of 4-dimensional data assimilation. This allows the horizontal momentum equations to be "nudged" by real time observational data as a simulation progresses. Nudging is not used for the vertical components as there are often inadequate observational data and this can lead to divergences in the simulation (CSU, 1997).

One of the key considerations when applying these models is whether to model the atmosphere as being in hydrostatic balance or not. It is useful to note that hydrostatic balance is the state whereby the atmosphere settles, under gravity, to the point where the upward and downward pressure forces on a column of air exactly balance the column's weight (McIlveen, 1998). The advantage to using the hydrostatic assumption is that it simplifies the modelling of the vertical structure of the atmosphere considerably, enabling the effects of vertical acceleration on the pressure gradient to be neglected. A further simplification that is often applied is the Boussinesq Approximation, whereby density variations are neglected for the inertial terms (as discussed above) though are retained in the buoyancy (gravity) term.

The assumption that a hydrostatic balance occurs only holds where flow is predominantly in the horizontal direction. For many situations this is perfectly acceptable, as shown by the good agreement found between hydrostatic and non-hydrostatic models for predicting dispersion in the Rhine valley by Castelli *et al*. (2004). However, the hydrostatic approximation does not hold in regions of

extremely complex mountainous terrain when horizontal grid resolutions of less than 1 km would typically be required to resolve terrain features (Finardi *et al*., 1997).

All of the prognostic models listed above are optionally non-hydrostatic, enabling the modelling of complex terrain at fine horizontal resolutions. Of course the more comprehensive (and coupled) physics sets that are used in the non-hydrostatic solution methods applied by these models result in a significant increase in computational demand. It should also be noted that for highly complex terrain (where vertical slopes may be encountered), the ability of non-hydrostatic models to describe the flow features may be limited by the choice of vertical co-ordinate system. Some models analyse vertical data on pressure surfaces, often using a terrain-following sigma co-ordinate system determined from the reference-state pressure (P_0), the pressure at the top of the domain (P_t) and the reference-state pressure at the surface (P_{s0}) (Equation 19).

$$s = \frac{P_0 - P_t}{P_{s0} - P_t} \qquad \text{Equation 19}$$

The use of a sigma co-ordinate system in the vertical enables the model to map the undulations of the surface with progressive flattening towards the upper boundary (see Figure 6). Whilst this system is well suited to most terrain types it cannot be used to model vertical faces.

2.4.1 Benefits and limitations of prognostic wind field models

The main benefit from the use of prognostic meteorological models is that the equation sets that are applied describe a full range of the processes likely to be encountered in complex terrain (such as the channelling effects of hills, the presence of slope winds and the divergence of streamlines round hills). However, these equations are computationally intensive, with non-hydrostatic simulations at a moderate resolution (defined in this case as a coarse mesh with 90 km resolution and 25x28x23 cells and a fine mesh with 30 km resolution and 34x37x23 cells) taking around 10 minutes of processing time on a standard PC (Intel Pentium II running at 650MHz) to simulate 12 hours of real time[*]. This places practical limitations on the resolutions and domain sizes to which prognostic model can be applied. Furthermore, the grid resolution, smoothing and the assumptions required for modelling surface heat fluxes may result in the predictions of prognostic models missing some of the localised flow features that can be significant when modelling atmospheric dispersion (Carvalho *et al*., 2002; McQueen *et al*., 1995).

[*] Data from http://www.mmm.ucar.edu/mm5/mm5v2/mm5v2-timing.html

A recent study by Lee *et al*. (2004) found that mass inconsistency errors occurred when the prognostic model MM5 was coupled with the Community Multiscale Air Quality (CMAQ) model, with the errors being considerably larger for non-hydrostatic simulations. These errors were caused by differences in both the numerical schemes and time-stepping between the meteorological and air quality models and were found to result in errors of up to 242% in the concentration field.

2.5 Computational Fluid Dynamics (CFD)

The application of CFD to determining flow over areas of complex terrain attempts to bridge the gap between the models that can consider a limited range of local scale phenomena (such as the dividing streamline approach) and models that can consider a more comprehensive set of physical processes but are applied at resolutions whereby the fine scale features that are of interest to dispersion modellers are not resolved.

CFD is essentially an engineering toolbox, enabling a specific solution to a problem to be constructed. It is useful at this stage to recognise that the prognostic meteorological models discussed in the previous section are Computational Fluid Dynamics models, though their formulations have been tailored to allow the prediction of the development of atmospheric flows across a range of scales, with horizontal resolutions of typically 1 km or more.

One of the earliest proponents of CFD for determining dispersion over localised terrain features was Dawson *et al*. (1991). They used the TEMPEST-PEST CFD model to study the flow fields and dispersion around a 330 m high isolated axi-symmetric hill "Steptoe Butte". Gradients on the upper section of this hill were found to be of the order of 1:5. The model which was applied used a variable resolution Cartesian computational mesh ($40 \times 32 \times 32$ cells), with a higher resolution across the top of the hill where gradients were more severe. The use of a Cartesian mesh in the vertical resulted in the profile of the hill resembling that of a stepped pyramid, though despite the relatively shallow gradients a significant recirculation zone was modelled on the lee side of the hill. The model predictions of Dawson *et al*. (1991) were compared with field measurements from an SF_6 tracer release experiment by Ryan *et al*. (1984), showing that whilst the model was able to reproduce the concentrations in the lee of the hill quite accurately (where the peak measured concentration occurred), the model predictions of the concentrations on the windward side of the hill were significantly higher than the measured data. Dawson *et al*. (1991) attributed this artefact to the use of Cartesian co-ordinates and the corresponding increase in drag in the model simulations.

Over recent years the use of CFD for application within atmospheric dispersion studies has increased significantly, with operational models being available from a range of developers including Star CD, CFX, Fluent and Fluidyn. These models provide a range of tools applicable to evaluating dispersion in complex terrain.

These include the ability to use co-ordinate systems such as body-fitted co-ordinates (BFC), where the 3-dimensional mesh wraps around terrain features, ensuring that such features are well resolved. The mesh type itself can also be modified to enable the meshing of complex terrain features, with the current state-of-the-art being un-structured (typically tetrahedral) meshes allowing a better fit to more complex regions (Stangroom, 2004). A comparison of Cartesian, structured BFC and un-structured meshes is shown in Figure 7, illustrating the improved fitting to terrain that is achieved through the use of more modern mesh types, of course the computational demand for such simulations also would increase with the use higher resolution meshing.

Most CFD models that have been applied to study flow over complex terrain have used the Reynolds Averaged Navier-Stokes (RANS) equations (Bitsuamlak *et al*., 2004). This system of equations (similar to those applied in prognostic meteorological models) decomposes velocities into a mean component and a fluctuating component allowing equations originally developed for laminar flows to be applied to the turbulent atmosphere. Equation 20 shows the RANS equation, it should be noted that the subscripts (*i,j*) relate to horizontal directions and the last term on the right hand side details the Reynolds stresses.

$$\frac{\partial r U_i}{\partial t} + \frac{\partial}{\partial x_j} r (U_j + U_i) = \frac{\partial \overline{p}}{\partial x_i} + \frac{\partial}{\partial x_j} \left(m \left(\frac{\partial U_i}{\partial x_j} + \frac{\partial U_j}{\partial X_i} \right) - r \overline{u_i' u_j'} \right) \qquad \text{Equation 20}$$

The RANS equations have no explicit solution as the Reynolds stresses are an unknown, however these stresses can be related to mean rates of strain assuming linear and isotropic eddy viscosity (ν_t) (Kim and Patel, 2000).

The most commonly used methods to achieve turbulence closure are derivatives of the *k-e* model (*e.g.* Baklanov, 2000; Bitsuamlak *et al*., 2004; Castro and Apsley, 1997; Castro *et al*., 2003; Kim and Patel, 2000) originally developed by Hanjalic and Launder (1972). Alternative models for turbulence closure include the *k-l* model, though this model has been shown to be problematic when applied to modelling complex flows over terrain (Baklanov, 2004). Furthermore, intercomparison studies have shown improved results can be obtained using the *k-e* model (Hewer, 1998). The *k-e* model uses two equations, the first to characterise the turbulent kinetic energy (*k*) and the second to determine the dissipation rate (*e*) enabling the determination of the eddy viscosity, turbulent velocity and length scales at any point in space or time. This model is shown in Equations 21- 23.

$$u_t = \frac{C_m k^2}{e} \qquad \text{Equation 21}$$

$$\frac{\partial (U_i k)}{\partial x_i} = \frac{\partial}{\partial x_i} \left(\frac{\nu_t}{\partial k} + \frac{\partial k}{\partial x_i} \right) - \overline{u_i' u_j'} S_{ij} - e \qquad \text{Equation 22}$$

$$\frac{\partial(U_i e)}{\partial x_i} = \frac{\partial}{\partial x_i}\left(\frac{\nu_t}{\partial e} + \frac{\partial e}{\partial x_i}\right) - \frac{e}{k}(C_1 \overline{u_i' u_j'} S_{ij} + C_2 e) \qquad \text{Equation 23}$$

Different types of *k*-*e* turbulence model were evaluated by Kim and Patel (2000) for modelling flow over complex terrain, including the standard parameterisation for neutral conditions (Jones and Launder, 1972), a modified model that can account for stable stratification (Duynkerke, 1988), a Preferential Dissipation Modification model (PDM) that accounts for streamline curvature effects (Leschziner and Rodi, 1981) and a Renormalisation Group (RNG) model that allows e to change dynamically with respect to the local ratio of the turbulent time scale to the mean strain time-scale (Yakhot and Orszag, 1986). Kim and Patel (2000) compared CFD model predictions with field and wind tunnel measurements for a range of different terrain types including: a 2-dimensional triangular ridge; an area of south Wales (Sirhowy Valley) comprising almost 2-dimensional periodic ridges and valleys; an embankment; and Askervein Hill on South Uist. They found that the choice of turbulence model could significantly affect the accuracy of the flow-field predictions (in particular the location and depth of recirculation regions) with improved performance being found for the RNG model. Their tests of a non-linear non-isotropic turbulence model showed poor results that they attributed to the simplicity of the wall functions used in the model.

It is interesting to note that Kim and Patel (2000) found an improved agreement between their model and the field measurements in the lee of Askervein hill when they included adjacent hills that were immediately downstream. They hypothesised that this was due to blockage effects generated by the surrounding terrain and noted that the model only predicted flow separation when the other hills in the domain were included.

An alternative approach to the RANS models is to solve the Navier-Stokes equations directly to simulate the motion of large eddies which are dependent on the flow geometry, whilst the smaller (universal and self-similar) eddies in the flow are dissipated using a sub-filter closure scheme (Wood, 2000). This computational method (Large Eddy Simulation, LES) enables the time dependent properties of flow and turbulence to be modelled whilst removing the dependence of the model predictions on the choice of turbulence model.

Chow and Street (2004) applied an LES method to model flow over Askervein Hill. Their simulation initially required running the model with no terrain present to develop a realistic turbulent inflow database. The next step, with terrain present, involved the simulation "spinning-up" for 2700s to generate eddies and flow patterns. Following this period they allowed the model to run for a further 900s to simulate a realistic flow field and for 1800s to allow the collection of turbulence statistics. Chow and Street (2004) compared the results from their simulation with field data illustrating that the model provided a good agreement with the measured wind speed-up factors across the domain and also with measurements of Turbulent Kinetic Energy (TKE) and shear stresses. Observations of the intermittency of recirculation regions in the lee of the hill

were also featured in the model simulations, highlighting the difficulties of performing such a simulation by applying the, essentially steady state, RANS equations. The simulation results from Chow and Street (2004) for intermittent recirculation are shown in Figure 8. It should however be noted that their model results showed problems in the prediction of turbulence closure near to the edge of the computational domain which required further investigation. The computational demands for these simulations were high requiring the use of a $163 \times 163 \times 59$ point computational grid to resolve a domain 5.6 km in the horizontal directions and 700 m in the vertical.

Iizuka and Kondo (2004) performed LES for predicting flow over a 2-dimensional isolated hill with surface roughness set to simulate grass ("smooth conditions") or trees ("rough conditions"), focusing on the sensitivity of the predictions to the choice of model for resolving the sub-grid scale turbulence. Their comparison with wind tunnel data for these scenarios showed that for the forested hill, a large recirculation region developed behind the hill, the prediction of which was strongly dependent on the choice of sub-grid scale model. The simulations of dispersion over the grassed hill showed that a smaller recirculation zone developed than for the forested hill. However, the forested hill simulations showed less sensitivity to the selection of sub-grid scale model and were generally in poorer agreement with the measured data (especially TKE) than the simulations for a grassed hill. It is interesting to note that the influence of surface roughness on non-linear "re-circulation" areas is also predicted by Wood (1995).

2.5.1 Benefits and limitations of CFD models

The use of CFD for modelling flow and turbulence fields for dispersion modelling is likely to increase as the costs of the computational resources required continue to decrease. The main advantage to the use of CFD for modelling flow and dispersion in complex terrain is the level of control that can be exercised in tuning the simulations to specific features of the flow field. However, this requires a considerable level of expertise by the modellers and often the choices of parameters, such as the most appropriate mesh resolution or turbulence model, can only be established by conducting sensitivity or validation testing. The issue of domain size versus resolution is also a limiting factor for considering the use of CFD models. This issue is well illustrated by the experience of Kim and Patel (2000) who found that the inclusion of downstream hills was critical to the accurate simulation of recirculating flows using a RANS model. To increase the domain size whilst keeping the horizontal resolution constant would increase the computational demand of the calculation substantially, which is at present the primary limitation in the application of CFD techniques for such assessments.

2.6 Summary comments

This section has presented a review of the types of model that can be used to determine dispersion in complex terrain and their strengths and limitations. Of

the range of models that have been considered, it is clear that the selection of the most appropriate model depends on a range of factors including:

- Slope and extent of terrain
- Availability and spatial resolution of meteorological data
- Availability of computational resources and timescale for modelling

Guidance on the selection of appropriate models for determining dispersion in complex terrain is given in the review of Finardi *et al*. (1997) conducted under the auspices of the European Union COST Action 710. Their conclusions regarding the applicability of different model types are summarised below:

- Single low hill or hilly terrain with moderate slopes (linear flow model).
- Single simple large valley or non-homogeneous flat terrain with 3D circulations (diagnostic mass consistent model or hydrostatic prognostic model).
- Complex terrain including mountains or steep slopes (diagnostic mass consistent model, hydrostatic prognostic model or non-hydrostatic prognostic model).
- Very complex terrain such as canyons or alpine regions (diagnostic mass consistent model (with care) or non-hydrostatic prognostic model).

The use of CFD models has been discussed herein, though was not considered in Finardi *et al*. (1997), who were mainly concerned with operational models for predicting pollutant dispersion. It may be concluded from Section 2.5 that CFD modelling remains limited by computational requirements, however useful information on the applicability of the operational models may still be obtained. Much like wind-tunnel modelling therefore, the best use of CFD may be in the evaluation of specific conditions where the applicability of the aforementioned models may not be assumed *a priori*.

3 MODEL EVALUATION DATASETS

This section of the report reviews the datasets that have been used to validate the models for dispersion over complex terrain. These datasets include numerous investigations of wind flows over complex terrain with studies designed from a wind engineering perspective and also studies of flow and dispersion over complex terrain that have been approached from the perspective of predicting environmental concentrations. This review focuses on the latter, though the large body of work conducted to evaluate wind flows is also discussed briefly.

3.1 Studies of wind flow over complex terrain

A considerable body of work has been conducted evaluating flows over terrain. Such studies include measurements at Black Mountain (Bradley, 1980), Blashaval Hill (Mason and King, 1985), Askervein Hill (Taylor and Teunissen, 1987), Kettles Hill (Salmon *et al*., 1988) and Brent Knoll (Mason and Sykes, 1979) and the experimental details have been reviewed by Taylor *et al.* (1987). In order to address the level of complexity in the terrain considered in these studies and hence the range of complexity across which models had been evaluated, Taylor *et al.* (1987) determined the parameter space that each study related to. This was determined in terms of the ratios of hill height to half-length and half-length to roughness length, bearing in mind the correlation between these parameters and the onset of flow separation discussed in Section 2. Figure 9 shows a parameter space diagram from Taylor *et al*. (1987), illustrating the clustering of the studies in the region $L/z_0 = 7 \times 10^3 - 5 \times 10^4$ and $h/L = 0.1 - 0.6$. It is also interesting to compare the gradients from Taylor *et al.* (1987) with the estimation of the critical gradient for flow separation in Wood (1995). This suggests that for the majority of the studies considered some non-linear effects may be anticipated.

The detailed measurements made at Askervein Hill (South Uist) in the early 1980s provide the most widely used dataset for evaluating models of wind-flow over complex terrain; full details of this experiment are given in Taylor and Teunissen (1987). These data were collected as part of an International Energy Agency Programme for wind energy research[†] and involved the placement of fifty anemometer masts. The majority of these masts were equipped with cup anemometers at heights of 10 m, though several taller towers (extending up to 50 m) were deployed along with sonic anemometers to measure turbulence. The roughness length across this hill was approximately 0.03 m (as would be expected for a hill covered in grass and heather) and its characteristic length scale (L) varied between 215 - 380 m depending on wind direction (Taylor *et al*., 1987).

There are numerous evaluations of wind flow models using the Askervien Hill dataset (*e.g.* Castro *et al*., 2003; Taylor *et al*., 1987; Stangroom, 2004) and with a common parameter that is evaluated by most studies being the fractional speed-up ratio (FSR), defined in Equation 24.

$$FSR = \frac{U(z)}{U_{upwind}(z)} - 1 \qquad \text{Equation 24}$$

Plots of FSR collected over Askervien Hill for a South-westerly wind direction from Kim *et al*. (2000) are shown in Figure 11. These illustrate that the 10 m

[†] Task VI of the Internation Energy Agency Programme of Research and Development on Wind Energy Conversion Systems (WECS) according to Taylor and Teunissen (1987)

flow initially decelerates on the upwind slope, accelerating at the summit and then rapidly decelerates in the lee of the hill with the magnitude of the acceleration and deceleration being proportional to the slope. It can be seen from the model predictions by Kim *et al*. (2000) that the 3-dimensional numerical model predictions provide a good fit to the field data. These results can be compared with the predictions of the linear model FLOWSTAR from CERC (2001b) in Figure 12. It should be noted that the exact observational data contained in Figures 11 and 12 are not identical, though it is clear that the linear model predictions for the more realistic surface roughness (of 0.1 m) are in reasonably good agreement with the field data for most of the profile, with the main region of difference being in the lee of the hill. The CFD modelling results of Kim *et al*. (2000) show that flow separation was likely to have occurred in this region.

3.2 Studies of flow and dispersion over complex terrain

3.2.1 Cinder Cone Butte - Plume impaction on an isolated hill

Studies at the Cinder Cone Butte were conducted in 1980 as part of the US-EPA development programme for complex terrain models to evaluate dispersion in complex terrain during periods of stable stratification (Apsley and Castro, 1997; CERC, 2001c; Ross and Fox, 1991). This isolated hill is roughly 100 m high, with a radius of 500 m and is located in desert scrubland in Boise, Idaho, USA. Terrain gradients on the hill slopes have a magnitude of approximately 1:5 illustrating the likelihood of plume impaction occurring. Tracer gases (SF_6 and CF_3Br) were released from an elevated platform approximately 600 m from the summit of the hill with the intention of measuring the impaction of the plume on the hillside. The height of the release was varied so as to enable the collection of measurements data for situations where releases occurred above or below the dividing streamline. Meteorological data were collected on-site along with LIDAR and photographic data (Ross and Fox, 1991). Overall 45 hourly experiments were collected with measurements from a network of monitors illustrating the spread and position of the plume. These measurements were grouped into "case studies" illustrative of particular meteorological and source parameters.

The measurement data from Cinder Cone Butte have been compared by Ross and Fox (1991) with the predictions of a Gaussian Puff model coupled with a diagnostic wind field model and with a early derivative of the CTDM model (described by Perry *et al*., 1992). Normalised Mean Squared Errors (NMSEs) from the total dataset varied from 9.3 to 3.3, with generally a better agreement between the model predictions and field data when either the early version of CTDMPLUS was applied, or when the coupled model was run using a modified version of the code to simulate the impingement of the plume on the terrain. Values for Fractional Bias (FB) ranged between –0.16 (showing model overprediction) to 0.97 (showing model underprediction), with the early versions of CTDM and the (modified) coupled model providing FB values that were not significantly different from zero. It should be noted that full descriptions of the

statistical methods used to evaluate dispersion models can be found in Hanna (1998).

CERC (2001c) also used the Cinder Cone Butte database to evaluate ADMS 3.1. They noted that strong fluctuations occurred in the wind direction data for low wind speed conditions and, to account for this, corrected the direction data manually to ensure that the plume was advected towards the monitoring sites. The model predictions were compared with 19 hours of data (a different comparison to the use of "case studies" by Ross and Fox, 1991) with these hours being selected as those of best quality from the available dataset. The results of the CERC (2001c) comparison showed a value of fractional bias of 0.56 (*i.e.* the model underpredicted concentrations), a NMSE of 3.9 and that 27% of the observational data were within a factor of 2 of the model predictions. However, it is difficult to determine quantitatively whether the comparison of Ross and Fox (1991) provides a better fit to the data than that of CERC (2001c), as different assumptions were made regarding the use of observational datasets.

As a further note of caution, and possibly a reason for the adjustment to the wind direction data required by CERC (2001c), Apsley and Castro (1997) modelled Cinder Cone Butte using a RANS CFD model, comparing their data with both the observational dataset and with physical modelling in a towing tank. The physical and numerical studies showed that the direction in which the plume moved round the hill was highly sensitive to the incident wind angle, with a 10 degree variation in wind direction moving the plume path from one side of the hill to the other (see Figure 13). Due to the sensitivity of the flow to wind direction, it may be expected that the use of "case studies" by Ross and Fox (1991) would provide a better comparison due to the smoothing out of these considerable differences. The predictions of the CFD model of Apsley and Castro (1997) were generally found to compare well with the observational data and illustrated that (1) a region of flow separation and recirculation occurred in the lee of the hill (based on the terrain gradient and surface roughness, linear models may have been expected to provide a good approximation, however Apsley and Castro (1997) noted "*strong stability emphasises non-linear effects*"); and (2) the asymmetry of the flow and considerable horizontal divergence suggests that neither linear models or dividing streamline solutions are entirely valid for this site.

3.2.2 Lovett Power Plant - Long-term dispersion in moderately complex terrain

AERMOD and ADMS were both evaluated by Hanna *et al*. (2001) using the database of air concentrations collected during the model validation study at the Lovett power plant, situated on the banks of the Hudson river (Paumier *et al.,* 1992). Sulphur dioxide gas, produced from the combustion process, was discharged continuously throughout the year, providing a "real-word" tracer release. The emission rates of SO_2 were measured using continuous in-stack monitors and found to peak at 396 g s^{-1} with a mean emission and standard deviation of 137 g s^{-1} and 63 g s^{-1} respectively. The emission of approximately

4.3 kt of SO_2 per year clearly provides a strong signal to be used for model evaluation of hourly averaged air concentrations, though Venkatram *et al.* (2001) noted that, for daily averaged concentrations, many of the lower concentrations were not substantially greater than the background values.

The SO_2 plume was released from a 145 m stack and was highly buoyant, with a mean plume rise of a further 117 m in convective conditions and 242 m in stable conditions (Paumier *et al*., 1992). The rural terrain surrounding the Lovett Power Plant could be characterised as being moderately complex, with gradients of around 1:5, with the surrounding hills rising to a maximum height of 340 m, with typical hill heights being of the same order as the plume height.

It is interesting to note that the region comprises a considerable variation in surface roughness length, with wind from the Hudson River having a typical z_0 value of 0.001 m and the deciduous woodland over the hilltops having roughness lengths of around 1.5 m. Paumier *et al*. (1992) used a mean roughness length of 0.6 m in their model evaluation of CTDMPLUS, whilst it is not clear whether Hanna *et al*. (2001) considered the variability in surface roughness explicitly in their evaluation of ADMS. The latter point may be worthy of further investigation, as it would be useful to determine the sensitivity of the ADMS model's performance to the treatment of surface roughness data at this site.

Measurements were collected from a network of 12 continuous monitors, with 10 sited on the terrain at distances up to 3000 m from the stack and two being used as backgrounds. The monitors sited on the terrain were located based on the expectation that these sites would receive the maximum air concentration. The locations of these monitors are shown in Figure 14. Meteorological data were used from a single 100 m high tower located approximately 1 km South of the power plant. Data from this location included windspeed, wind direction and temperature at heights of 10 m, 50 m and 100 m, with the database being supplemented by measurements of cloud cover and radiosonde launches from more distant NWS sites (Paumier *et al*., 1992).

This dataset has been used to evaluate CTDMPLUS (Paumier *et al*., 1992; Perry *et al*., 2005), AERMOD (Paine *et al.* 1998; Hanna *et al.*, 2001; Venkatram *et al.* 2001; Perry *et al*., 2005) and ADMS (Hanna *et al.*, 2001) with the latter also including the ISCST-3 model. It is not certain which version of ADMS was used to conduct this validation, however it is believed ADMS version 3.0 was used (Williams, pers. comm.).

Model predictions using AERMOD and ADMS were evaluated using the direct quantitative comparison of observed and predicted maximum concentrations. Maximum concentrations were compared for two criteria: the maximum concentration observed at a given time and a given location and the maximum concentration at a given time over all measurement locations. The latter test is included because of legislation in the USA which focuses on the maximum air concentrations predicted and the test does not consider the effect of particular terrain conditions on the overall distribution of concentrations or the physical processes involved in the flow (Hall *et al*., 2000). For the comparison of

predicted maximum concentrations, tables of the ten highest observed and model predicted concentrations are presented in Hanna *et al.* (2001).

The results from Hanna *et al.* (2001) (see Table 1) show that ADMS under-predicted the maximum concentration by approximately 40% and AERMOD was within 1% of the highest concentrations. However the authors point out that this dataset was used by AERMOD developers for calibration of the model parameters for complex terrain (Paine *et al*., 1998) and AERMOD would therefore be expected to show a good agreement. When all the data are considered, ADMS showed a mean under-prediction of 14% and AERMOD showed a mean over-prediction of 37%. ADMS and AERMOD predictions were within a factor of two of the observations about 30% and 25% of the time respectively (Hanna *et al.*, 2001).

Additional results, provided by Perry *et al*. (2005), for AERMOD and CTDMPLUS are summarised in Table 2. These show a ratio of modelled to observed "robust highest concentrations" of 1.00 (AERMOD) and 2.37 (CTDMPLUS) for 3 hour averaged data. The "robust highest concentration" is a statistical estimator for the highest concentration. It is determined from an exponential fit to the high end of the frequency distribution of observed and predicted values (US EPA, 2003).

Venkatram *et al*. (2001) compared AERMOD and CTDMPLUS in terms of the concentration quantile-quantile distributions. This method is applied as the distributions of modelled and measured data are compared rather than a direct comparison of paired observations in space and time. This is a better metric for regulation in the USA, where the prediction of maxima are required. Their results (Figure 15) show that AERMOD provided an improved comparison with the observed data distribution than CTDMPLUS, though tended to slightly overpredict concentrations, as also found by Hanna *et al*. (2001).

3.2.3 Tracy Power Plant – Dispersion in complex terrain during stable conditions

Model validation experiments were conducted in 1984 at the Tracy Power Plant (27 km East of Reno, Nevada, USA) to evaluate dispersion in predominantly stable atmospheric conditions. As the measurements extended past daybreak, an additional 17 hours of data were collected in convective conditions, which followed sharp transitions in atmospheric stability. This site is located in a region of mountainous terrain with peaks to the North-East extending to nearly 1000 m above the valley floor. Gradients in this region were of the order of 1:4 or more and a constant roughness length of 0.1 m was assumed for AERMOD by (Paine *et al.* 1998) whilst a value of 0.2 m was applied by CERC (2001d) for the evaluation of ADMS.

The tracer gas SF_6 was released from a 91 m stack between 6 - 27 August 1984 (US EPA, 2003) with the stack efflux parameters being used to simulate a buoyant release with a 120 ^{o}C efflux temperature. A network of SF_6 monitors was deployed throughout the valley and on the surrounding terrain slopes as shown

in Figure 16, with a particularly high density of monitoring points at the constriction of the valley to the East of the stack. These monitors provided data on hourly average air concentrations with a collection of 128 hours of data in total over 14 discreet monitoring periods.

Meteorological data were collected from a 150 m tower located 1.2 km East of the power plant providing data on wind speed, wind direction, temperature and vertical and horizontal turbulence at heights of 10 m, 50 m, 75 m, 100 m, 125 m and 150 m. Additional data were collected from SODAR and tether-sonde measurements enabling the vertical profiles to be extended to a height of 400 m.

The wind rose (from the 10 m height) for the period of the tracer releases is shown in Figure 17. This clearly demonstrates the bias in this dataset for winds from the South-West, advecting the plume towards the constriction in the valley. Experiments also can be seen to have focussed on dispersion towards the hills to the North-West of the stack.

AERMOD was validated against this data (US EPA, 2003; Venkatram *et al*., 2001; Perry *et al*., 2005). In addition, the developers of ADMS used the Tracy Power Plant database to validate ADMS version 3.1 (CERC 2001d). A summary of the AERMOD and CTDMPLUS results (Table 2) shows the ratios of modelled to observed "robust highest concentration" were 1.07 and 0.77 respectively for a 1 hour average, indicating that the AERMOD model provided the closest estimate of maximum concentrations in the model domain.

Comparison of quantile-quantile plots by Venkatram *et al*. (2001) illustrated further that AERMOD provided improved predictions to those of the CTDMPLUS model (see Figure 18). Furthermore, Venkatram *et al*. (2001) modified the dividing streamline parameter (*f*) illustrating that the accurate prediction of concentrations by AERMOD could only be achieved if the plume was allowed to impact on the terrain features rather than flow over the terrain. This is useful to note as it illustrates that the concentrations measured at the Tracy Power plant are influenced strongly by the terrain and hence that this dataset is a good discriminator of the performance of the terrain algorithms in the models (rather than other parameters in the model, such as plume spread or the treatment of plume rise). The strong performance of AERMOD in this comparison is particularly encouraging as this dataset was not used in the development of the model and so provides an independent validation.

Model runs were conducted by CERC (2001d) for a sub-set of 79 hours of data for southwesterly winds and stable meteorological conditions using ADMS version 3.1. Results of the comparison between observations and modelled data were analysed using the BOOT statistical package. The statistics calculated include mean, standard deviation (sigma), bias, Normalised Mean Squared Error (NMSE), Correlation (Cor), fraction of results where the modelled and observed concentrations agree to within a factor of two (FA2), fractional bias (FB) and fractional standard deviation (FS). The results are shown for each experiment separately in Table 3, taken from CERC (2001d). Overall, a very variable model

performance was demonstrated with NMSE values ranging from 1710 to 1.9, FB ranging from –0.47 to 1.99, and FA2 values ranging from 0.4% to 27%.

The statistics presented by CERC (2001d) for the monitoring period "Stable 12" illustrate that the ADMS model did not provide a realistic prediction of the data observed in the field for this period whilst for other runs (e.g. "Stable 6") the model performed well. Quantile-quantile plots for these two periods are shown in Figure 19. An analysis of the results versus the wind speed indicated that ADMS performed better for higher wind speeds (experiments 6, 7, 8 and 9) than for lower wind speeds (experiments 2, 10 and 12) (CERC, 2001d). The poor performance for periods of low wind speed may have been related to uncertainties in the application of the linear flow field model FLOWSTAR, developed initially for moderate winds, neutral stability and flow over hills, which this case presents a significant departure from. It is also not clear from CERC (2001d) how the boundary conditions to the FLOWSTAR model were set, though it seems likely that the meteorological data from the power plant would have been used in the simulation. The correct representation of boundary condition for the FLOWSTAR model should reflect a wind-field undisturbed by flow perturbations induced by terrain. However, as the meteorological measurements at this location were collected within the perturbed flow field it is possible that the FLOWSTAR boundary conditions may not have been addressed adequately and that this uncertainty may have contributed to the variable quality of the model predictions. It is clear that further work is required to investigate the performance of FLOWSTAR and ADMS for this location.

3.2.4 Martins Creek – Long term dispersion in complex terrain

Model validation experiments have been conducted in 1992-1993 at the Martins Creek Powerplant using the discharge of SO_2 from the stack (Paine *et al*., 1998). The Martins Creek station is located within a valley basin on the border between Pennsylvania and New Jersey (USA). Terrain rises steeply to the South-East of the plant with maximum gradients of around 1:3 and attains a height of 334 m.

Discharges of SO_2 occurred from four relatively closely spaced stacks on the Martins Creek site, each having a physical height of 183 m. As with the study at the Lovett power plant, the discharges from this site were particularly high with an average discharge of 730 g s^{-1} (σ = 600 g s^{-1}) and a maximum discharge of 3500 g s^{-1}. This equates to an annual discharge of approximately 23 kt of SO_2. As the releases were buoyant, with efflux temperatures of 160^{o}C, it is likely that the plume height would be close to the height of the surrounding terrain and concerns over potential fumigation at these locations no-doubt motivated this study.

In addition to the release of SO_2 from the Martins Creek station, three other significant point sources were located within a radius of 10 km. These were the Metropolitan Edison Portland Station (ED), Hoffman-LaRoche (HL) and the Warren County Resource Recovery Facility (WC). Discharges of SO_2 from the

aforementioned facilities were approximately 16 kt, 0.7 kt and 0.3 t per year respectively.

Continuous monitoring of SO_2 was conducted for the period 1 May 1992 - 19 May 1993 at seven locations situated at between 3.0 and 5.6 km downwind of the Martins Creek facility in a South-Easterly direction. Background concentrations were estimated from the lowest reading of any of the monitors in each hour. The monitoring sites were located on a ridge at heights of between 340 – 377 m above sea level and well above the stack height. A contour map of the topography and the locations of the stacks and receptor points are shown in Figure 20.

Meteorological data for this area were obtained from an instrumented tower located on flat terrain, 2.5 km West of the plant, which provided the following data at a height of 10 m: hourly temperature, wind speed, wind direction and the horizontal and vertical standard deviations of the wind speed. These data were extended to determine vertical profiles to a height of 420 m using a SODAR located 3 km South-West of the Martins Creek station (US EPA, 2003).

Perry *et al*. (2005) evaluated the ratio of robust highest concentrations that were predicted by AERMOD with the observed dataset. The data presented in Table 2 show that the ratios of the 3-hour averaged robust highest concentrations range from 0.76 (annual peak) to 1.65 (24 hour) for AERMOD and 2.19 (annual peak) to 5.56 (24 hour) for CTDMPLUS. As found in the previous studies, AERMOD outperformed the more complex CTDMPLUS model.

A quantile-quantile comparison of measured and modelled data for the Martins Creek study was reported in Venkatram *et al*. (2001) and is shown in Figure 21. These data illustrate that the concentration distribution predicted by AERMOD was typically within a factor of 2 of the measured distribution and that AERMOD provided improved predictions across the concentration range.

3.2.5 Westvaco Corporation Pulp and Papermill - Long term dispersion in complex terrain

The Westvaco Corporation Pulp and Papermill is located at the base of a river valley in rural Maryland (USA). This area is shown in Figure 22 and comprises an area of highly complex terrain with gradients of around 1:2 between the stack and the nearest wall of the valley. The valley walls extend more than 300 m in height from the valley floor.

Buoyant discharges of SO_2, released from a 183 m stack on the site, were used for the evaluation of the predictions of complex terrain atmospheric dispersion models by Hanna *et al*. (1984). Emission rates from this source were 410 g s^{-1} (σ = 84 g s^{-1}) with an annual emission of 13 kt of SO_2.

Air concentrations were recorded using continuous monitoring devices at eleven receptors in the area surrounding the source. Figure 22 shows that eight of these monitors were situated on the elevated terrain to the East and South of the source at distances between 800 m to 1500 m. Hanna *et al*. (1984) reports that

SO_2 monitoring data were recorded between December 1979 – November 1981. Only data for the period from December 1980 – November 1981 have subsequently been used by Perry *et al*. (2005) and Venkatram *et al*. (2001).

Due to the complexity of the surrounding terrain, Hanna *et al*. (1984) paid particular attention to the collection of a detailed meteorological dataset for the area. Three meteorological towers were used for this area, these being:

- Beryl Tower: 400 m South-West of the site, with a height of 100 m and instrumented at 10 and 100 m levels.
- Luke Hill Tower: 900 m North-West of the site, with a height of 30 m, instrumented at 2, 10 and 30 m.
- Met Tower: located on a ridge 900 m east South-East of the site, with a height of 100 m and instrumented at 10, 50 and 100 m.

These data were supplemented by twice daily temperature-sonde data collected on weekdays during February, June and September 1980.

Hanna *et al*. (1984) compared the wind rose measured at a height of 100 m at "Met Tower" with data from the nearest NWS station (see Figure 23). It is apparent from the on-site data that the wind rose is aligned strongly to the axis of the valley, with blockage effects accounting for the low frequencies of winds from the North and South. This figure illustrates that if a model has no means of calculating the wind field (e.g. AERMOD), then on-site meteorological data, by definition, enables the inclusion of local-scale flows. However, as previously noted, when modelling the influence of terrain using a linear solution, care must be taken when attempting to apply locally measured meteorological data as boundary conditions.

Quantile-quantile plots were analysed by Venkatram *et al*. (2001) (see Figure 24) who concluded that AERMOD provided more accurate predictions than the CTDMPLUS model for all situations, with the exception of the upper end of the distribution of daily averaged SO_2 air concentrations. Perry *et al.* (2005) determined that the ratio of AERMOD predicted to observed robust highest concentrations range from 1.08 (3 hour average) to 1.65 (annual peak), see Table 2. The equivalent CTDMPLUS model predictions ranged between 2.14 (3 hour average) to 0.93 (annual peak), illustrating that the additional flowfield modelling in CTDMPLUS did not result in appreciable improvements in model predictions.

3.2.6 Brush Creek – Dispersion within deep high sided valleys in stable conditions

Tracer release experiments were conducted as part of the Atmospheric Studies in Complex Terrain (ASCOT) programme at Brush Creek Valley (Colorado) in July and August 1982 and September to October 1984. The experiments in 1984 were designed to investigate atmospheric dispersion within the valley during nocturnal periods and when morning transition flows occurred (Clements *et al*.,

1989). A considerable volume of information has been generated from these trials including the publication of a special issue of the Journal of Applied Meteorology (Vol. 28, Nos 6 and 7).

The topography of the valley is shown in Figure 25, illustrating that significant terrain gradients (close to 1:1 at places) occurred at the valley walls, which rose to 600 m above the floor level. Significant thermal winds were found to occur in this region (Allwine, 1993) with the night-time down-slope katabatic jet reaching a maximum speed of 5 to 6 m s^{-1}. Peak wind speeds within this jet occurred at a height of 80 to 100m from the valley floor, with wind speeds then decreasing with height, with zero wind speed being measured at 375 m above the floor level. Winds above this height represented boundary layer flows, with wind direction shear of up to 180^{o}. Further complexities to the flowfield were found to occur after sunrise, with full reversals in valley winds being found as anabatic upslope winds developed. Leone and Lee (1989) modelled the meteorology and fluid dynamics of the katabatic flow using a finite-element model. Their simulations showed a good agreement with the meteorological monitoring conducted during the 1984 experiments and illustrated that initially drainage flow on the side-walls of the canyon converged to form a coherent down-valley jet.

An overview of the tracer gas release experiments at Brush Creek is given in Allwine (1993). Figure 25 shows the locations of tracer gas release points and monitoring stations within the valley and along the valley side walls. Tracer gases were released from several different locations (and heights of up to 550 m from the valley floor) simultaneously, using different organic chemical species to relate downwind concentrations to a specific release point. Interestingly the tracer released during the night was confined within the valley, with concentration maxima typically occurring close to the valley floor irrespective of the original height of the release. For releases from 183 m Rao *et al.* (1989) suggested that this was caused by subsidence due to the increase in valley cross section with downwind distance. Only following the morning transition between up- and down- valley winds was the tracer vented from the valley, which then behaved essentially as if dispersion was occurring from a line source.

Allwine (1993) compared the concentrations measured at Brush Creek with the predictions of a Segmented Gaussian Plume model, with reflection terms on the crosswind dispersion parameter (σ_y) to account for the valley sidewalls and vertical dispersion being reflected between the valley floor and the overlying inversion layer. Overall a good agreement was found between the modelled and measured tracer concentrations when variations in vertical turbulence rates with distance down the valley were applied to account for changes in surface roughness.

Further numerical modelling of these tracer data have been conducted by Rao *et al.* (1989), Lange (1989) and Luhar and Rao (1994). Rao *et al*. (1989) used a Gaussian puff model, applying a subsidence velocity of 0.09 m s^{-1} to account for the reduction in the plume vertical centreline with down-valley distance. They concluded that their model agreed to within a factor of 2 to 6 with the measured

data. Lange (1989) used a coupled diagnostic wind field model and a Lagrangian particle model to study the flow and dispersion respectively. They found that 52% of the measurements were within a factor of 5 of the model predictions, though this increased to 78% when a 5^{o} angular uncertainty in the wind direction was included in the model. Luhar and Rao (1994) used a Lagrangian particle model to model dispersion within the valley, with the wind field provided through the interpolation of the detailed measured meteorological data. Overall 35% and 50% of the model predictions were within a factor of 2 of the observations for the surface release and elevated release respectively. The difference in model performance found by Luhar and Rao (1994) for the different release heights was attributed to the sensitivity of surface releases to the local terrain.

The releases at Brush Creek illustrate the features of the thermally-driven flow in deep valleys and, for such situations, the application of local meteorological wind data is required to evaluate dispersion. Clearly, the situation considered at Brush Creek represents something of an extreme, particularly in the context of regulatory point source modelling in the UK.

3.2.7 Rocky Flats – Dispersion downwind of complex terrain in stable conditions

A further set of field validation experiments were conducted as part of the ASCOT and Rocky Flats Winter Validation Study (RFWVS) programme at Rocky Flats in January – February 1991. The ASCOT programme was responsible for the collection of meteorological data to analyse the flow-field, whilst the RFWVS was responsible for the release of tracer gas (SF_6) from the Rocky Flats plant and the measurement of air concentrations at two arcs of approximately 65 samplers located 8 and 16 km from the plant (Poulos and Bossert, 1995).

The area that was studied is on the plains approximately 6 km to the East of the Rocky mountains in Colorado (USA), with measurements being taken to determine dispersion during nocturnal periods, when katabatic winds from the mountains dominated the surface level wind field and vertical dispersion was suppressed, such that the tracer plume was confined to within 100 m of the surface. Figure 26 shows radiosonde profiles from Rocky Flats illustrating the shear in wind speed and wind direction within the lower atmosphere (Poulos and Bossert, 1995). Overall 22 meteorological sites were operated in the study area including 10 towers, tether and radiosondes as well as LIDAR and SODAR stations.

Tracer gas was released on 4 nights from 2000 – 0700 hrs during the experimental period. Poulos and Bossert (1995) compared the observations with the predictions of the prognostic meteorological model RAMS, coupled with a Lagrangian particle dispersion model. They concluded that tracer concentrations would typically be predicted to within a factor of 2 and within +/- 50^{o} of the observed location.

Banta *et al*. (1996) evaluated horizontal LIDAR scan data and used a diagnostic wind-field model (MATHEW) coupled with a Lagrangian particle dispersion model to predict concentrations in the tracer plume. Their evaluation showed that katabatic jets, formed within canyons could penetrate distances of 20 km or more across the plains. These jets were narrow (of the order of 4 km wide) and were found to affect the advection of the tracer plume, though these effects were not captured by the diagnostic wind-field model due to the resolution of the observational dataset. It is interesting to note that similar conclusions over the influence of distant terrain features on the meteorology and pollution climate of the Swiss Plateau were reached by Lehning *et al*. (1996).

A further study by Luhar and Rao (1994) compared the tracer release data for a single night (4-5 February) with the predictions of a Lagrangian particle model coupled with an interpolated "terrain following" wind-field. They found that around 30% of the observations were predicted to within a factor of 2, with an overall NMSE of 3.21. A comparison of the model predictions of Luhar and Rao (1994) and Poulos and Bossert (1995) for the hour between 0300 – 0400 illustrates that the model predictions based on the interpolated wind-field provided a better estimate of the trajectory of the plume (see Figure 27).

The data from the Rocky Flats experiments illustrate the importance of considering terrain features that surround an area being modelled. In this case, the use of data from a distant meteorological site would have provided a poor representation of the surface level wind-field during overnight katabatic conditions and local (detailed) meteorological data would be likely to provide a better assessment for plume modelling. The study by Banta *et al*. (1996) also illustrates the pitfalls of using diagnostic wind-field models in regions where strongly localised flow features dominate.

3.2.8 TRACT – Dispersion in complex terrain in convective conditions

The TRAnsport of pollutants over Complex Terrain (TRACT) project was setup as a subproject of the European Union funded EUROTRAC programme. Experiments were conducted as part of this project through four main field studies: TRANSALP (1989, 1990, 1991) and TRACT (1992). TRANSALP (see Ambrosetti *et al*., 1998) comprised a series of studies within complex alpine topography in Switzerland, whilst TRACT (1992) evaluated dispersion in the Rhine valley.

TRANSALP experiments in 1989 focussed on dispersion within two valley forks (the Leventina and Biasca valleys) in southern Switzerland to distances of up to 25 km from a release point emitting a perfluorocarbon tracer. Ground level air concentrations were measured using a network of up to 60 samplers positioned along the floors of both valleys. In addition, meteorological measurements were made using a network of sites (approximately 12 anemometer masts, 3 SODARs, a sonic anemometer and a pilot balloon) (Ambrosetti *et al*., 1998).

The meteorological conditions that were measured during TRANSALP 1989 were compared with the predictions of two diagnostic wind-field models (MINERVE and CONDOR) by Desiato *et al*. (1998). They focused on the predictions of flow

during daytime convective conditions where transport through the Alps was likely and a thermal valley breeze (termed "Inverta") developed. The measurement data illustrated considerable local variability in the flow, with local wind speeds and directions being determining by the heat fluxes on the valley slopes, resulting in up-slope and also some cross-slope flows being recorded (Desiato *et al*. 1998). A schematic diagram illustrating the formation of up-slope thermally driven flows is shown in Figure 28. The diagnostic wind-field models were run to evaluate the sensitivity of the flow field predictions to the number and location of the meteorological sites used to derive the "initial guess" wind-field. Overall, there was little difference between the two diagnostic wind-field models and both performed well when run using a single vertical profile and three surface measurements (root mean squared error for wind speed and direction were less than 1 m s^{-1} and 40^{o} respectively). Desiato *et al*. (1998) concluded that the successful use of a diagnostic wind-field model depends on matching the scale of the meteorological input data to the scale of the flow being modelled. Hence, artefacts can be created when meteorological sites affected by localised flows are included or when vertical profile data that are unrepresentative of profiles elsewhere in the domain are applied.

Dispersion modelling during TRANSALP 1989 was conducted by Anfossi *et al*. (1998) using two Lagrangian particle models (ARCO and SPRAY) and the flow fields modelled using two diagnostic wind-field models (MINERVE and CONDOR) by Desiato *et al*. (1998), resulting in two combinations: CONDOR-ARCO and MINERVE-SPRAY. Anfossi *et al*. (1998) demonstrated that the ensemble properties of the measurement data were represented by both modelling systems, though artefacts in the diagnostic wind-field predictions occurred. These were due to failure to resolve localised flows and from unrepresentative vertical profile data and caused discrepancies in the time-series of modelled concentrations (in particular the more rapid emptying of the valleys than was measured), though it should be noted that the highest air concentrations were well represented by the models.

TRANSALP 1990 (Martilli and Graziani, 1998; Varvayanni *et al*., 1998; Ambrosetti *et al*., 1998) considered the flow and dispersion over a larger geographical area, with sampling points being located up to 45 km from the source of the tracer release. As found in TRANSALP 1989 thermal effects dominated, though in TRANSALP 1990 the valley breezes were strengthened by an overlying southerly flow generated by synoptic meteorology. The effect of these meteorological conditions on tracer dispersion was to enhance the transport over the mountains and even permitted the penetration of the inversion layer and entry of the tracer plume into the overlying free atmosphere (Ambrosetti *et al*., 1998).

Martilli and Graziani (1998) modelled the diurnal variation in valley meteorology during TRANSALP 1990 using the prognostic non-hydrostatic RAMS model, paying particular attention to the evaluation of first- and second-order turbulence closure models. As found by Desiato *et al*. (1998) for TRANSALP 1989, the main features of the flow field were found to be represented by the

RAMS model, though local scale flows, that were present in the measured meteorological dataset, were not able to be resolved. Furthermore, Martilli and Graziani (1998) were unable to draw a conclusion over the suitability of the turbulence closure schemes, suggesting that further work should focus on improving the parameterisations of soil characteristics and land use, that influence surface heat fluxes, and by the consideration of additional high resolution nested grids within regions where strong slope flows were likely.

Further work by Varvayanni *et al*. (1998) applied a "high-resolution ground/ low-resolution atmosphere" modelling concept to the TRANSALP 1990 dataset, through the application of a topography simulator (DELTA), a non-hydrostatic prognostic meteorological model (ADREA) and a Lagrangian particle model (DIPCOT). Although an improved fit to some of the measurement data was found when comparing the time-series graphs from Varvayanni *et al*. (1998) with the equivalent data from Desiato *et al*. (1998), it was difficult to conclude whether the application of the DELTA model improved the prediction accuracy. Furthermore, Varvayanni *et al*. (1998) also cites uncertainties in the parameterisation of surface properties as factors contributing to their under-prediction of the thermally-driven circulations.

Comparisons of predicted and measured tracer concentrations by Varvayanni *et al*. (1998) were limited by the availability of data (< 50% of the monitoring sites recorded non-zero values). The model was found to provide realistic predictions of the maximum values measured at each of the sites, particularly for those sites that recorded the highest air concentrations. However, the measured arrival and flushing times for the plume were not well represented, this being attributed to uncertainties in the wind-field predictions (Varvayanni *et al*., 1998). It is interesting to note that Ambrosetti *et al*. (1998) reported that the air concentration of tracer gas persisted for a considerable time (> 50 hours) from the time of release at a distance of 9 km from the release point. This was interpreted as being due to the recirculation of air within the valley system and illustrates the importance of the application of modelling techniques that can model dispersion in non-stationary conditions, even over relatively short distances, when considering the effects of complex terrain.

Tracer release experiments conducted during TRANSALP 1991 further confirmed the ability of pollutant plumes to disperse through and over regions of highly complex terrain. Measurements in September 1991 evaluated dispersion up to 100 km from Lake Lucerne to Lake Maggiore over the Gotthard Pass, whilst measurements in October 1991 evaluated dispersion over scales of up to 15 km in a region of thermally-driven flows around Lake Lucerne. Lamprecht and Berlowitz (1998) compared the results from this second set of measurements with the predictions of the diagnostic wind-field model CONDOR and the prognostic non-hydrostatic model MEMO, finding that errors occurred in the predictions of the diagnostic wind-field model due to insufficient resolution in the surface meteorological monitoring stations. Furthermore, accurate predictions from the prognostic model were only derived following sensitivity testing of the nesting of flow fields from different meteorological scales.

The TRACT field experiment was conducted in 1992 centred on the Rhine valley. This experiment evaluated meso–scale meteorology over a domain size of 300 × 300 km and also included a tracer dispersion experiment with the furthest sampling point being at a distance of approximately 60 km from the release point (Carvalho *et al*., 2002). As with the TRANSALP experiments, TRACT 92 was intended to evaluate dispersion during periods of convective meteorological conditions, though the topography studied during TRACT 92 was considerably simpler than the areas covered by TRANSALP.

The boundary layer structure during the TRACT 92 experiment was investigated using data from surface meteorological stations and from aircraft and balloon measurements (Kossmann *et al*., 1998). The aircraft and balloon measurements provided a particular insight into the spatial variability of boundary layer heights. Local reductions in the convective boundary layer height at the summit of the mountain (shown in Figure 29) due to the horizontal pressure gradient caused by the synoptic flow and also a reduction in convective turbulence occurred, caused by cooling due to the up-slope flows (Kossmann *et al*., 1998). It is also interesting to note in Figure 29 the formation of a gravity wave in the lee of the mountain during the second measurement period.

The tracer dispersion experiments that were conducted as part of TRACT 92 were discussed and compared with the predictions of a prognostic meteorological model (RAMS) coupled with a Lagrangian particle model (SPRAY) in Carvalho *et al*. (2002). The tracer release occurred between 0500 and 0800 hrs, with the experiment then tracking the dispersion of material over subsequent hours. The model predictions and measurements both showed the plume initially being advected along the valley then fragmenting due to wind direction shear. Subsequently material was re-circulated within the valley due to flow reversals in the afternoon. However, the model tended to underestimate air concentrations during the recirculation phase, in particular the re-emergence of the tracer at a location 2 km from the release point between 1130-1200 (up to 4 hours from the end of the tracer release). This was attributed by Carvalho *et al*. (2002) to local scale effects that were not resolved by the RAMS model.

3.2.9 Brasimone – Dispersion in complex terrain during nocturnal conditions

Field experiments were conducted in 1984 and 1985 at the Apennine mountains in Italy to evaluate nocturnal dispersion over a distance of approximately 6 km from a near ground level release of the tracer gas SF_6 (Desiato, 1991). The terrain heights in this region varied by up to 800 m within 6 km from the release with typical gradients of around 1:6. Meteorological data were collected at two surface towers and from three sites where vertical profiles were measured using tethersondes and a pilot balloon. These measurements showed a low lying (up to 100 m) layer of drainage flow close to the surface overlaid by airflow undergoing transition to geostrophic flow, similar to that observed at Rocky Flats (see Section 3.2.7). Overall Desiato (1991) found that 38% of the model predictions were within a factor of two of the field measurements, though this increased to

93% when a modelling uncertainty in the position of the plume of 10^{o} was accounted for. This demonstrates that dispersion rates during these trials were predicted accurately, with the most significant source of error being the prediction of the flowfield and hence the trajectory of the plume.

3.2.10 Sellafield – Dispersion over an area of complex terrain

An intensive programme of measurements of ^{85}Kr concentrations around the British Nuclear Group (Sellafield) Limited site in Cumbria (UK) has been conducted by Westlakes Scientific Consulting (WSC) since 1996 under contract to BNG (Sellafield) Ltd. In total 211 measurements of ^{85}Kr concentrations were collected over a total duration of 5401 hours, these are detailed in Table 4. Emissions of ^{85}Kr occur during reprocessing following the decanning of spent nuclear fuel and are discharged from two elevated release points on the site (stack heights of around 120 m). Meteorological data for the model validation study were obtained from a single tower close to the site (Hill *et al*., 2005).

Hill *et al*. (2005) evaluated subsets of the ^{85}Kr data, separating local dispersion to receptors within 3 km of the site and regional dispersion to receptors at distances of 12 km and 52 km from the site. For dispersion modelling in the far field, where terrain effects were likely to occur, the predictions of a simple Pasquill-Gifford type Gaussian Plume model (NRPB R-91) were compared with the predictions of the ADMS model (implementing the linear flowfield model FLOWSTAR) and AERMOD PRIME (using the dividing streamline method). Both ADMS and AERMOD were also configured in "flat terrain" mode as a comparison. Statistically significant differences were not observed between the model results assuming flat terrain and those cases where terrain modelling was included (Table 5). Furthermore, at these distances there was very little to differentiate between the performance of the different dispersion models, with all models underpredicting the measured air concentrations and being within a factor of 2 of the measurements for typically 27% of the time.

The results of Hill *et al*. (2005) suggest that the modelling of complex terrain effects by AERMOD and ADMS is of limited significance to the accuracy of the prediction of dispersion at the distances they considered, though it should be noted that their analysis was based on a relative small sample dataset of 11 samples.

4 A COMPARISON OF THE PREDICTIONS OF ADMS AND AERMOD FOR DIFFERENT TERRAIN TYPES

The performance of the terrain modules of the Gaussian Plume models ADMS and AERMOD was compared by calculating dispersion from idealised point sources at six sites in Cumbria corresponding to complex, moderate and simple terrain. The study considered the effect of release height on dispersion in complex terrain by considering both a low stack (20 m) located within an area of

complex terrain and a tall stack (100 m) located in a coastal site with emissions that impinge on an area of complex terrain. For both these situations, unit release rates (of 1 g s^{-1}) were applied and the releases were modelled at ambient conditions without any plume rise.

The locations of the sites selected are presented in Table 6 and are illustrated in Figure 30. For the case of simple terrain, an inland site with gradients of less than 1:20 and a site on a coastal plain with nearby terrain with average gradients of approximately 1:10 were chosen. For the moderate terrain case, an inland site with gradients of approximately 1:7 and a coastal location with average gradients of 1:7 or less were chosen. For the case of steep terrain, an inland site featuring a stack located in a valley surrounded by steep mountains, with gradients averaging 1:2, and a stack located on a coastal plane close to steep hills, experiencing gradients of 1:2 or less, were selected. Variations in roughness length were not taken into account in these model runs.

It should be noted that the terrain gradients for the "steep terrain" case are likely to be outside the limits that the analytical solution applied by FLOWSTAR is valid for (see Section 2.2). However, the steep terrain simulations were considered to be a useful test of the performance of regulatory models in extreme terrain, highlighting the major differences between the techniques.

The models were run using hourly sequential meteorological data taken from Manchester (Ringway) Airport for 2000. These data are binned into 10^{o} sectors and wind directions during the period were biased towards the South and also the West (see Figure 31). Further details of this dataset can be found in the review of Auld *et al*. (2003).

A terrain domain size of 8 km $\times$ 8 km was used in ADMS in the model calculations in the inland areas, though due to the offset between the source and the terrain features for the coastal sites slightly larger terrain domains were required (typically 12 km $\times$ 12 km). ADMS has the capability to allow the terrain to be modelled at different resolutions. In the first set of model runs a resolution of 64 $\times$ 64 nodes (labelled "64N" in Table 6) was used. In addition, sensitivity studies were conducted to investigate the effect of reducing the terrain resolution on the results by conducting runs at resolutions of 32 $\times$ 32 nodes (labelled "32N") and 16 $\times$ 16 nodes (labelled "16N"). The effect of changing the terrain domain size was also investigated by running the model with domain sizes of 16 km ("16D") and 32 km ("32D") for the inland steep and moderate terrain cases.

Output data from all the model simulations were determined on 5 km $\times$ 5 km output grids at a grid resolution of 64 $\times$ 64 output nodes. It should be noted that in ADMS the output grid is defined independently of the terrain grid and the use of a consistent terrain grid herein enabled the direct comparison of concentrations for different terrain types, terrain resolution and terrain domain sizes. For AERMOD, calculations of dividing streamline height and terrain height are only determined at each of the output grid nodes, hence modifications to the terrain domain and terrain resolution were not possible. AERMOD was run with

the same specification of output points as were applied in ADMS. Full details of these model setups can be found in Table 6.

Ground level air concentrations were calculated for a baseline case with no terrain calculations included and for a case with terrain calculations included. Amplification factors were determined from the ground level air concentrations (GLCs) modelled with terrain present ($C_{terrain}$) and from GLCs modelled without the consideration of terrain effects ($C_{no\_terrain}$) using Equation 24.

$$AF = \frac{C_{terrain}}{C_{no\_terrain}} \qquad \text{Equation 24}$$

Results were produced for annual average concentrations (termed "long-term") and for the 99.8th percentile of hourly concentrations (termed "short-term"). Values of the maximum and median short term and long term concentrations are presented in Table 7.

Predictions of dispersion in flat terrain (shown in Table 7) were all calculated for the same specification of grid (a 5 km $\times$ 5 km output grid resolved at 64 $\times$ 64 nodes). Obvious differences can be seen between the coastal and inland cases, due to the application of different stack heights in the models. However, it is also apparent that the concentrations output were not identical within each case. These effects are particularly apparent for the predictions of maximum concentrations for the inland sites, where stack heights of 20 m were used, with difference between cases of up to 6% in ADMS and up to 20% in AERMOD due to small changes to the positions of the sources within each output grid.

4.1 Simple terrain

4.1.1 Inland site

The modelled air concentrations for the inland site with simple terrain (gradients of 1:10 or less) are shown in Figures A1 and A2, whilst Figures 32 and 33 show the terrain amplification factor plots. A statistical summary of the data is presented in Table 7.

Contour plots of the air concentrations modelled with AERMOD and ADMS showed broadly similar patterns for the case with hills included and for the flat terrain case (Figure A1 and A2). ADMS predicted slightly higher maximum short-term concentrations (with and without terrain) than AERMOD. However, AERMOD predicted higher median short-term concentrations and higher median and maximum long-term concentrations for cases with and without terrain (Table 7). In addition, the AERMOD results showed narrow bands in the short-term air concentration contour plots that were not observed in the ADMS results. These are likely to be due to AERMOD predicting narrow plumes in stable conditions. The disparities in the concentration data for flat terrain illustrate that some fundamental differences occur between these two models in their treatment of atmospheric dispersion.

A comparison of amplification factors in Figures 32 and 33 (long-term and short-term averages) and Table 7 shows differences in the overall predicted effects of the terrain. ADMS showed overall increases in median concentrations of 52% and 62% for short-term and long-term averages, though little effect of terrain on concentration maxima was manifest. AERMOD showed small reductions in median short-term and maximum long-term concentrations, whilst median long-term concentration increased slightly (4%) and no change occurred to the maximum short-term concentration due to the effects of terrain.

4.1.2 Coastal site

Air concentrations at this site showed similar magnitudes and distributions for both AERMOD and ADMS, with some localised differences in the spatial pattern of concentrations occurring due to modelling the effects of terrain (Figures A3 and A4). The data in Table 7 show that ADMS predicted increases in median short-term and long-term concentrations by 38% and 33%, though only small changes in maximum concentrations occurred due to terrain effects. The equivalent model predictions from AERMOD showed that terrain influences did not affect any of the concentration statistics by more than 2%.

Figures 34 and 35 show disparities in the spatial pattern of terrain amplification factors, with ADMS predicting amplification of concentrations to the East of the model domain and no change in concentrations, or a small reduction in concentrations, to the West of the model domain for both short-term and long-term averages. The AERMOD results showed a much smaller area to the East of the source where concentrations were slightly raised as a result of terrain.

Table 7 illustrates that median amplifications were predicted by AERMOD to reduce slightly, whilst increases were predicted by ADMS. The difference between the two models in median and maximum short-term amplification factors was small however, with a maximum short-term amplification factor of 2.89 being predicted by AERMOD, compared to 2.63 predicted by ADMS.

4.1.3 Summary

Maximum air concentrations were in reasonable agreement between ADMS and AERMOD with both models predicting no significant increase in maximum concentration due to the effects of terrain. However, ADMS predicted increases in median short-term and long-term air concentrations due to the effects of terrain, which were not matched by AERMOD. These increases in median air concentrations were not expected, due to the very shallow gradients that were modelled. Such increases may be significant for certain types of air pollution assessments where spatial averages are important, such as deposition studies, and illustrate that the cut-off point for determining whether to assume flat terrain in dispersion modelling studies is not well defined.

The predicted maximum short- and long-term amplification factors were also in good agreement. The spatial distributions of terrain amplification factors were

found to differ, which is unsurprising since AERMOD is designed to predict the magnitude of maximum concentrations rather than their location.

4.2 Moderate terrain

4.2.1 Inland site

In this section the high-resolution ADMS results (listed in Table 7 as Run MI 64N) are compared with the predictions from AERMOD (MI). It should be noted that the sensitivity cases (MI 32N and MI 16N) are discussed later.

Long-term air concentrations (both the median and maximum) were found to be in good agreement between the two models when hills were included in the simulations (Table 7). This agreement may be somewhat fortuitous, as the predictions of long-term concentrations in flat terrain show more pronounced disparity between the two models (see Figures A5 and A6). When terrain effects were included in the simulations ADMS predicted that long-term concentrations would increase, whilst AERMOD predicted that concentrations would reduce. Both models did however predict that the maximum short-term air concentrations would be increased due to the effects of terrain, though in this case a considerable higher increase (167%) was predicted by AERMOD than ADMS (17%).

A comparison of the amplification factors (Figures 36 and 37 and Table 7) shows disparities between the two models both in magnitude and in the general structure of the contour plots. In Figures 36 and 37, ADMS predicts large areas of either concentration amplification or no change in air concentration, whereas AERMOD predicts large areas of reduction in concentration and some areas of no change. The top of the stack is located on the western slope of a ridge and the release height is less than the height of the summit. In the case of AERMOD the amplification factor contours follow the shape of the terrain (Figures 36 and 37) and the plume can be seen to impinge on the side of the ridge producing a narrow band of concentration amplification. In the case of ADMS the flow is channelled around the hill producing concentration amplification around the sides of the hill.

The statistical comparison of the amplification factors in Table 7 showed that AERMOD predicted higher maximum amplification factors of 7.6 (short-term) and 3.7 (long-term) than ADMS (3.0 and 2.2 for short-term and long-term averages). It is also interesting to note that AERMOD predicts reductions in median short-term and long-term concentrations due to the effects of terrain (shown by the median amplification factors being less than unity) whilst ADMS predict median concentration increases.

4.2.2 Coastal site

The ADMS and AERMOD models were found to be in good agreement with respect to the magnitude and spatial distributions of ground level air

concentrations for both long-term and short-term simulations (Figures A7 and A8). Both models predicted similar median and maximum long- and short-term concentrations for flat terrain and when modelling hill effects (Table 7).

As with previous simulations, some discrepancies were found in the amplification factors (Figures 38 and 39 and Table 7). ADMS predicted an amplification of air concentrations over the hills in the North and East of the model domain (though by less than a factor of 2) and little change in concentration over the area of flat terrain in the South and West of the model domain. In contrast, AERMOD predicted a terrain-following flow, with little change in air concentration due to interaction between the plume and underlying topography, with small areas of slightly enhanced air concentrations being modelled to the North-East of the domain where the plume impacted on the higher ground.

The statistical comparison of the amplification factors showed that ADMS predicted a median concentration increase in all the recorded statistics, with a maximum short-term amplification factor of 2.1. AERMOD predicted median concentration amplifications of unity both in the short and long-term and a maximum short-term amplification factor of 1.8. Again the AERMOD and ADMS maximum amplification factors were found to be similar though the locations and geographical extent that these occurred were not well matched.

4.2.3 Summary

AERMOD and ADMS predict similar magnitudes of median and maximum long-term concentrations for inland and coastal sites of moderate terrain. At the inland site (where a lower stack height was applied) AERMOD predict a higher median and maximum short-term air concentrations than ADMS. For the coastal site (with a taller stack height), the air concentrations are of a similar magnitude although the spatial patterns vary between the models. AERMOD's dividing streamline concept is illustrated in Figures 36 and 37 where the plume can be seen to impact on an adjacent hill. In contrast, in Figures 38 and 39 the majority of the plume is above the dividing streamline and consequently there is a reduced interaction between the plume and the underlying terrain.

4.3 Complex terrain

4.3.1 Inland site

This section compares the ADMS baseline results (listed in Table 7 as run CI 64N) to the AERMOD results (CI). The ADMS sensitivity cases CI 32N, CI 16N, CI 64 N 16D and CI 64 N 32D are discussed later. AERMOD was found to predict higher median short-term concentrations in the flat terrain case, but lower median short-term concentrations in the case with terrain effects included. However, the ADMS model predicted higher median and maximum concentrations when terrain effects were considered (see Table 7).

The influence of the FLOWSTAR model in ADMS was apparent in Figures A9 and A10 where channelling of the plume within the valleys was observed. The simpler approach included in AERMOD is well illustrated in Figures A11 and A12 showing that this model was unable to resolve the channelled flow, with the terrain causing blocking effects which severely restricted the dispersion of the plume within the model domain.

Figures 40 and 41 show that ADMS predicts higher air concentration amplification in the valley due to the effects of terrain compared to AERMOD, shown as a narrow ring of concentration amplification near the foot of the slopes. The statistical comparison of concentrations (Table 7) demonstrated that ADMS provided higher maximum short- and long-term averaged concentrations when terrain effects were included. ADMS also predicted a maximum short-term amplification factor of 20 compared to a value of 11 predicted by AERMOD. However, the ratio of the maximum concentrations predicted with and without the inclusion of terrain (using the values presented in Table 7) provides a ratio of approximately 3.0 for both ADMS and AERMOD.

4.3.2 Coastal site

The air concentration contour plots (shown in Figures A13 and A14 and Table 7) showed good agreement in both the spatial distribution and magnitude of the concentrations predicted by AERMOD and ADMS for the situation where terrain effects were not considered. However, it is clear from the spatial patterns shown in Figures A13 and A14 that ADMS generally predicted higher air concentrations than AERMOD when terrain effects were included. This was particularly noticeable at locations close to the summit of the terrain. The effect of the dividing streamline approach in AERMOD is clearly illustrated as a band of high air concentrations near the base of the terrain features, though it is interesting to note that this band extends around the lee side of the hill (Figure A14).

The contour plots of amplification factors (Figures 42 and 43) showed that widespread increases in air concentrations were predicted by ADMS. In contrast, AERMOD predicted a narrow band of amplification around the entire base of the hill, though with concentrations reducing higher up the hill. The amplification of air concentrations in the lee of the terrain is difficult to reconcile from a theoretical perspective and may well illustrate an artefact of the AERMOD methodology.

ADMS predicted a short-term maximum amplification factor of approximately 50 compared to a value of approximately 120 predicted by AERMOD. The peak long-term amplification factors were higher still with values greater than 33,000 being predicted by ADMS and 30 being predicted by AERMOD. However, when terrain amplification was expressed as the ratio of long-term concentration maxima using the values presented in Table 7, the agreement between the models improved, with values of 10 being calculated for ADMS and 15 for AERMOD.

4.3.3 Summary

Clearly the gradients being modelled in these cases are outside the intended scope of these models; AERMOD in particular does not exhibit the expected median increase in concentration in the inland case. It does however predict high maximum increases in concentration due to terrain effects. The dividing streamline approach in AERMOD is again illustrated by the plume impacting on the hill close to the stack height and concentrations above this height are reduced from their flat terrain values. The increases in concentration found in the lee of the hill that were predicted by AERMOD are somewhat difficult to reconcile from a theoretical standpoint and may be an artefact of the application of a methodology designed to predict the magnitude but not location or extent of the maximum concentration.

4.4 Effects of changing grid resolution

The effect of reducing the terrain grid resolution in ADMS on the moderate and complex terrain cases was investigated by changing the terrain grid resolution from the baseline case of "high resolution" with 64 × 64 nodes (termed "64N") to "medium resolution" with 32 × 32 nodes ("32N") and "low resolution" with 16 × 16 nodes ("16N").

4.4.1 Steep terrain, inland site

Comparison of the terrain amplification factors determined at the high resolution for long-term and short-term concentrations (Figures 40 and 41) with the equivalent data determined using medium and low resolution terrain data (Figures 44 and 45) illustrates that the spatial pattern and magnitude of terrain influences were relatively insensitive to resolution of the terrain modelling, especially when the transition from high to medium resolution was considered. This is further demonstrated by the median concentrations (short and long-term), shown in Table 7, that were found to vary by less than 10% when medium resolution terrain data were applied.

The maximum short-term and long-term concentrations in Table 7 were found to be more sensitive to the terrain resolution than the median air concentrations with the maximum long- term concentration increasing by 19% and 56% when medium and low resolution terrain were applied. Interestingly, the largest increase in the maximum short-term concentration was predicted to occur for medium resolution terrain data (an increase of 26%). The low resolution terrain data provided a maximum short-term concentration that was 14% greater than when high resolution terrain data were applied.

A further effect that changing the grid resolution has on the performance of the ADMS model is of course the impact on the model run times[‡]. The following run-times were recorded for the various model simulations considered above:

64×64 nodes	8 hours 10 minutes
32×32 nodes	2 hours 11 minutes
16×16 nodes	42 minutes

4.4.2 Moderate terrain, inland site

The results of the sensitivity tests to determine the effect of terrain resolution are presented in Figures 46 and 47 and Table 7. Reducing the grid resolution from high to medium resolution makes very little difference to the spatial patterns and magnitudes of the air concentrations. This is illustrated by the median concentrations (short and long-term) which vary by less than 1%. Only a moderate difference is seen in the low-resolution case where median air concentrations vary by less than 10% of the high resolution value. The maximum concentrations that were predicted for medium and low resolution terrain differ by less than 10% from those determined for the high resolution terrain modelling, though a slightly higher sensitivity was found for the short-term case (a reduction in concentration of 14%).

The greatest variation in amplification factor was observed in the long-term averages at low resolution, where the median and maximum amplification factors differed by 7% from those determined at high resolution.

4.4.3 Recommendations on the selection of grid resolution

As the ADMS model did not show a strong sensitivity in either the concentration predictions or the predictions of the influences of terrain on dispersion, it is recommended that for moderate terrain, a 32×32 resolution terrain file is sufficient. A greater sensitivity of the ADMS model to terrain resolution was found for the situation where steep terrain was encountered. From Sections 2 and 3 the uncertainties in the model due to the violation of the assumptions of linear flow and from not considering thermal effects would potentially be more significant than the effects of changing model resolution shown herein, hence even for a situation of steep terrain, a 32×32 resolution would be likely to be sufficient.

[‡] Run times were for a Pentium-4 Personal Computer with a 3 Ghz processor and 1 Gb of RAM.

4.5 Effect of changing domain size

The effect that topographical features outside the domain area may have on dispersion was investigated by changing the size of the model domain from 8 km × 8 km (termed standard domain size) to 16 km × 16 km (termed medium domain size) and 32 km × 32 km (termed large domain size). The terrain resolution was 64 × 64 cells for this sensitivity study, though as the domain size increases the distance between grid nodes also increases thus reducing the overall resolution. This was illustrated by the grid nodes shown in Figure 48, though it should be noted that this figure does not show the full extent of the revised terrain domains. The inland steep terrain site (CI) and the inland moderate terrain site (MI) were used to evaluate the effect of different domain sizes on the predictions of terrain effects, as these site have been shown in the previous sections to be sensitive to terrain effects and changes in grid resolution.

4.5.1 Steep terrain, inland site

Contour plots of terrain amplification were determined for the medium and large domain sizes and are shown for long-term and short-term averages in Figures 48 and 49 respectively. The modification of the domain size can be seen to have relatively little influence when compared with the standard domain size (shown in Figure 40), with the main effects being to reduce the magnitudes of any increases or reductions in concentrations occurring due to terrain effects. The statistical comparison of concentrations shown in Table 7 confirms that the changes in domain size had relatively little influence on concentrations, with the largest change being an increase in maximum long-term concentration of 48% for the medium domain size. Interestingly, the results for the larger domain size show a closer agreement with the concentrations determined using the standard domain size than those determined using the medium sized domain. This illustrates that the relationship between the concentration statistics and domain size for this location is non-linear. In addition, this suggests that the variation described previously is due to the modelling compromises between terrain resolution and the influences of surrounding features.

4.5.2 Moderate terrain, inland site

Medium and large domain sizes were also investigated for the moderate terrain site in order to establish the sensitivity of the ADMS model for a location with gradients more typical of those to which the model is usually applied. It should be noted that for this location the application of a 16 km × 16 km domain ensured that the edges of the Cumbrian mountains to the East and South and the sea cliffs to the West of the stack were included. The 32 km × 32 km domain captured a greater proportion of the surrounding complex terrain.

Figures 50 and 51 show terrain amplification factor contour maps determined for the different domain sizes for long-term and short-term averaging. These figures illustrate that only minor differences occurred between the medium and large domain sizes. This is also shown in Table 7 by the good agreement between

concentration statistics. Comparing Figures 50 and 51 with the data for the standard domain size, shown in Figures 36 and 37, indicates that the influence of terrain has increased for the larger domain sizes, especially in areas to the North, North-East and North-West of the stack. These areas correspond with the locations where wake effects from the surrounding terrain may occur. However, these increases also may have been caused partially by the reduction in model grid resolution as shown in Figures 44 and 45. Data from Table 7 illustrate that increases of between 17 – 34% occurred in median concentrations due to the application of the enlarged terrain domains. However, maximum long-term concentrations were almost unaffected and maximum short-term concentrations reduced by up to 25%.

It is useful to note that the model predictions were found to be less sensitive to the specification of terrain resolution than they were to domain size for this location. As the ADMS model requires that the incoming wind-field at the domain boundaries represents that which is undisturbed by local terrain features it is likely that the inclusion of the surrounding terrain in the larger domain may have introduced artefacts within the model, contributing to the sensitivity to domain size that was observed. It is, unfortunately, not possible to draw a definitive conclusion about this point, though this would be a useful avenue for further investigation.

4.5.3 Recommendations on the selection of domain size

The selection of an appropriate domain size should involve the consideration of the significance of the scale of surrounding terrain. For a situation where a source is affected by the immediately surrounding terrain (such as discussed in Section 4.5.1), the domain size needs to be large enough to resolve these features, with more distant terrain having only minor effects. Where the source is located within an area of undulating terrain or where significant terrain features are some distance from the source then it may be appropriate to apply a larger domain size, though it should be recognised that undisturbed flow at the edge of the domain is an assumption included within the model. Furthermore, as FLOWSTAR assumes that the wind-field is stationary during any particular hour, domain sizes significantly greater than the distance over which the plume is likely to be advected during an hour should be avoided.

4.6 Summary comments

It is apparent that substantial differences in the predictions of the effects of terrain on atmospheric dispersion occur between ADMS and AERMOD despite both these models being widely used for addressing regulatory compliance issues in the UK. These disparities were particularly obvious for the predictions of dispersion within extremely complex terrain where the lack of a detailed horizontal flow-field model within AERMOD led to concentration contour plots that did not realistically represent the channelled flow that would be expected within the model domains. AERMOD did however predict similar patterns of near-

field plume impaction on terrain features to those found with ADMS and predictions of maximum concentrations that were within 20% of those of ADMS for dispersion within highly complex terrain. More significant differences were found for the case where a plume interacted with a downwind region of highly complex terrain. In this situation the predictions of AERMOD were a factor of 2.6 higher than those derived from ADMS.

The flow field model applied in ADMS was found to require careful consideration of the domain size, node resolution and the geographical area that was modelled. For simulations in "moderate" terrain, the influences of terrain features at the edges of the domain were hypothesised to be responsible for the model showing an increased sensitivity to domain size and geographical extent than to grid resolution. For dispersion in "complex" terrain disentangling the effects of resolution and domain extent was more difficult, though the sensitivities of the model to changes in these parameters (of the order of 50 – 60%) were anticipated to be less than the errors due to the violation of the linear flow assumption and the exclusion of thermal winds.

The effects of terrain on dispersion were generally found to be less significant for the releases from the "coastal" terrain cases. This was likely to be due to the higher stack height that was applied in these simulations, leading to more of the plume being above the dividing streamline height and thus being carried over, rather than impacting on, terrain features. The dependence of terrain amplification factors on source height has also been observed in other numerical and wind tunnel studies (e.g. Etling *et al*., 1986).

The maximum amplification factors illustrate the highest relative increases in concentrations due to the effects of complex terrain. The moderate and simple terrain cases represent terrain types that are more typically experienced in the UK and situations that the algorithms contained in ADMS and AERMOD are better suited to. For these simulations the maximum short-term terrain amplification factors were approximately a factor of 3 and the maximum long-term amplification factors were of the order of a factor of 2. It is useful to note that even for the situation where very shallow terrain gradients were modelled (< 1:10), significant amplification of concentrations occurred at points within the model domains, illustrating that care should be taken when deciding whether or not to model terrain influences.

Often the focus is on the effects of terrain on the maximum concentrations that are predicted around a source. The simulation results shown in Table 7 illustrate that the maximum concentrations are not as sensitive to terrain influences as the amplification factors were. This was due to the peaks in air concentration (caused by vertical dispersion in the atmosphere) not corresponding with the locations where the highest terrain amplification occurs in these simulations. For the case of simple terrain, very little change in maximum concentrations occurred due to terrain influence. Even for the situation of dispersion in moderate terrain, the ADMS simulations showed that maximum air concentrations did not increase significantly, with the largest increase being of 17% for the "moderate inland" simulation. A more significant increase in

concentration was modelled by AERMOD for this site, an increase by a factor of 2.7, which was due to a closer match between the locations of peak concentration and peak terrain amplification.

5 RECOMMENDATIONS

5.1 General recommendations

This review has made a detailed consideration of the types of models used to determine flow and dispersion in regions of complex terrain and their validation. A sensitivity test was also conducted to compare two Gaussian Plume models, typically used for regulatory purposes in the UK for a range of terrain types.

The strength of interaction between a dispersing plume and the underlying terrain is a function of the release height. Stronger terrain interactions occur where plumes are released at heights less than or equal to those of the surrounding terrain. Conversely, modelling of terrain effects will most likely not be required for elevated releases that disperse over relatively low lying terrain features.

One of the key areas that has been highlighted in this review is that, for the robust assessment of dispersion in regions of complex terrain, it is of primary importance to be able to predict the wind-field accurately. All modelling methods for determining flow in complex terrain were found to have their benefits and limitations and none should be applied without detailed consideration of the suitability of the model to the terrain features being modelled. Guidance on model suitability is presented in this report, though it should be noted that the report from the European Union project COST 710 (Finardi *et al*., 1997) also provides useful information. The conclusions of Finardi *et al*. (1997) regarding the applicability of different model types are summarised below:

- Single low hill or hilly terrain with moderate slopes (linear flow model).
- Single simple large valley or non-homogeneous flat terrain with 3D circulations (diagnostic mass consistent model or hydrostatic prognostic model).
- Complex terrain including mountains or steep slopes (diagnostic mass consistent model, hydrostatic prognostic model or non-hydrostatic prognostic model).
- Very complex terrain such as canyons or alpine regions (diagnostic mass consistent model (with care) or non-hydrostatic prognostic model).

5.2 Regulatory modelling

For situations where locally-representative meteorological data are available and where the assessment of impacts to local receptors is required, then models,

such as AERMOD, that do not model the wind-field explicitly (just the interaction of the dispersing plume with the underlying terrain) can be applied. This is demonstrated by the performance of the AERMOD model during field validation trials where detailed local meteorological data were available. It is also apparent that the predictions of concentration maxima by AERMOD, when run using annual meteorological data, also compare well with those from a more complex dispersion model run using a linear analytical solution to determine the wind-field (ADMS). However, as may be expected, the spatial patterns of air concentration predicted by AERMOD are very different to those predicted by ADMS, in particular the inability of AERMOD to predict channelled flows. Consequently, the interpretation of air concentrations predicted by AERMOD at specific receptors in complex terrain should be avoided for situations other than where the input meteorological data capture the mean properties of flow between the source and receptor.

Disparities were also found to exist in the meteorological requirements of ADMS and AERMOD for studies where the influences of complex terrain may be significant. AERMOD requires meteorological data to be specified within the model domain, whilst ADMS requires that data are provided for undisturbed flow at the domain boundaries. Locally-derived meteorological data, that reflect flows affected by terrain within the domain, are therefore well suited for use in AERMOD though would be unsuitable for use in ADMS.

The linear analytical flow-field module contained within ADMS enables this model to predict terrain-influenced plume trajectories for situations where the flow is disturbed by low lying hills of moderate slope and where thermal effects can be ignored. It is also noted that care should be taken to ensure that the model domain includes the terrain features that are likely to affect flow. For a situation where a source is affected by the immediately surrounding terrain, the domain size needs to be large enough to resolve these features, with more distant terrain having only minor effects. Where the source is located within an area of undulating terrain or where significant terrain features are some distance from the source then it may be appropriate to apply a larger domain size. Furthermore, as FLOWSTAR assumes that the wind-field is stationary during any particular hour, domain sizes significantly greater than the distance over which the plume is likely to be advected during an hour should be avoided.

The requirement of analytical models for predicting flows over "moderate" slopes is addressed herein using the simple approximation method of Wood (1995) that accounts for the effects of surface roughness on the critical gradient of the slope. Whilst the analytical models may not be strictly valid for flows over slope gradients greater than around 1:3, comparisons with non-linear models demonstrate that predictions of flow and dispersion on the windward slope and close to the summit of a hill are approximated reasonably well, though wind speeds in the recirculation region in the lee side of a hill may be over-predicted.

It is also noteworthy that this review has highlighted the importance of thermally-driven winds which are not considered by ADMS. These types of winds may affect dispersion of material within an area of complex terrain and may also

create significant meso-scale flows that may affect dispersion in adjacent regions of simple terrain. Much of the meteorological data applied in the UK for regulatory modelling is derived from distant meteorological sites. As such, consideration should be given to the possible effects of such flows when assessing how representative the meteorological data may be when applied for pollutant modelling. It would be useful to have guidance from the Met. Office on the accuracy to which thermally-driven meso-scale flows are modelled in the Numerical Weather Prediction (NWP) codes.

The application of diagnostic wind-field models to evaluate flows has been found to provide a useful alternative method to the application of linear models, particularly for flows over steep complex terrain or where thermal effects may be important. However the predictions of these models may be sensitive to the selection of meteorological sites and care has to be taken to ensure that meteorological data are representative of the mean flows over the areas that data are interpolated. Thus, the potential exists for the inclusion of too many, or too few, meteorological observations in diagnostic wind-field models and the output from the model may be a reflection somewhat of the skill of the modeller.

The review of the performance of regulatory dispersion models when compared with model validation datasets has shown that further work is required in order to establish the cause of the disparities highlighted. Particular attention should be paid to the following areas:

1) The sensitivity of model predictions for Lovett Power Plant to the specification of surface roughness or the use of a roughness length map.
2) The performance of FLOWSTAR and ADMS for the Tracy Power Plant study in order to establish the cause of the somewhat variable performance of the model during specific monitoring periods.
3) The typical range of influence of nocturnal katabatic flows for UK meteorological conditions and topography.

5.3 Short-term release modelling

Air concentration peaks over short time periods can be of significant concern for regulatory modelling, where compliance with a short-term assessment level is required, and for modelling the dispersion of accidental releases to the atmosphere. The literature reviewed in Section 3 and the numerical modelling studies presented in Section 4 both showed that short-term air concentrations were particularly sensitive to the effects of complex terrain, especially during periods where geostrophic wind speeds are low and where significant thermal influences occurred.

Much of the research reviewed herein focussed on the prediction of dispersion in nocturnal conditions with katabatic flows and where dividing streamline heights were sufficiently low to cause the impaction of pollutant plumes on terrain features. Such conditions would often represent a "worst-case" as atmospheric dispersion would be relatively inefficient due to the suppression of turbulence

and the influence of a capping inversion layer. Prediction accuracies for modelling local dispersion in such conditions may be expected to be of the order of 20 - 40% of the model estimates being within a factor of 2 of monitoring data based on studies by CERC (2001c); CERC (2001d) and Luhar and Rao (1994). Much of the uncertainty in these estimates of model accuracy relates to the uncertainty in the prediction of wind trajectories in complex terrain. Accuracy for the prediction of air concentrations increases markedly when wind trajectory uncertainty is accounted for, as shown by Desiato (1991) and Lange (1989). Uncertainty in wind trajectories was found to vary with location, meteorological conditions and modelling technique, though from the research of Apsley and Castro (1997), Desiato (1991), Desiato *et al*. (1998), Lange (1989) and Poulos and Bossert (1995), may be expected to be in the range of +/- 10^{o} to +/- 50^{o}.

A further uncertainty in short-term release modelling relates to the prediction of the arrival time of a plume and the exposure duration, the latter may be particularly relevant where accumulated doses may be required to be calculated. Estimates of such properties for areas of complex terrain have been found by Anfossi *et al*. (1998) and Carvalho *et al*. (2002) to be particularly inaccurate and care should be exercised in their estimation.

5.4 Further development of models for dispersion in complex terrain

As previously noted, where sites are located within an area of moderately complex terrain and where only near-field concentrations are required (within 1 – 2 km), then it is likely that the most accurate flow-field prediction would be obtained from using detailed meteorological measurements collected off-site and preferably between the source and receptor. It should be noted though that attention would need to be paid to ensure that such measurements were not unduly affected by unrepresentative local-scale flows.

In contrast, prognostic meteorological models represent the most promising avenue for the accurate prediction of flow-fields in regions of complex terrain in the absence of local measurement data and where dispersion has to be modelled over scales of tens of kilometres. In particular, these models are well suited for nesting within the NWP models, the output from which are increasingly being applied as National Weather Services continue to reduce the number of surface observational sites. Of course, the prognostic calculations remain computationally intensive, though speeds continue to increase as technology improves. Development of prognostic models should focus on improving the accuracy of the input datasets (in particular the land-use and surface flux schemes) to enable better estimation of the smaller scale flow features that have been found to be important for modelling atmospheric dispersion. Furthermore, issues regarding the coupling of prognostic models with dispersion codes remain and further work should be directed to verification that such errors are reduced or eliminated.

Further intercomparison work should be conducted on linear flow-field models, comparing their dispersion predictions with those of prognostic and/or CFD simulations to address quantitatively the inaccuracies that develop in these models as they are applied for situations where the original assumptions implicit in their development do not hold. To recap, these assumptions are of flow over moderate, low-lying terrain in a neutral atmosphere with relatively strong winds. Further work comparing the predictions of linear flow models with the model validation datasets discussed in Section 3 could be used to highlight any limitations within the modelling methodologies and to assess areas for future improvements.

For many situations, where flow and dispersion modelling are required to consider regions of moderately complex terrain, linear models may remain an appropriate technique. These models could be extended to consider additional flow properties, such as localised thermal slope flows and the treatment of the effects of downwind recirculation areas in entraining material close to the ground. Perhaps also, techniques for incorporating more of the data available from NWP models within linear flow models could improve the specification of flow at domain boundaries for situations where meso-scale influences are important. It is noted however that care should be taken when applying linear models to ensure that the model domain includes the terrain features that are likely to affect flow. However, domain sizes that are greater than the distance a plume is likely to be advected during a single hour should be avoided.

Diagnostic meteorological models also may provide realistic estimates of flow and dispersion over areas of complex terrain, with the benefits of the speed of linear models, but without (apparently) sacrificing much of the accuracy of prognostic models when compared with field data. Again these models could benefit from improvements to the specification of surface flux schemes, though the most significant improvements for the prediction of plume dispersion may be achieved through the correct inclusion of measured data. As National Weather Services continue to improve upon the resolution of NWP data, then perhaps the interfacing of this data-source within the context of simple diagnostic models that treat the most significant localised influences on flow (such as slope flows, blocking effects etc.) may provide an alternative practical option for regulatory modelling in the near-future.

In conclusion, the improvements in model physics must be matched by improvements in the input data supplied to the models. In this context, these improvements should include improvements to the data supplied to specify the underlying surface and also the meteorological data that drives the flows within the model.

6 REFERENCES

Allwine, K. J., 1993: Atmospheric Dispersion and Tracer Ventilation in a Deep Mountain Valley. Journal of Applied Meteorology, 32, 1017-1037.

Ambrosetti, P., D. Anfossi, S. Cieslik, G. Graziani, R. Lamprecht, A. Marzorati, K. Nodop, S. Sandroni, A. Stingele, and H. Zimmermann. 1998: Mesoscale transport of atmospheric trace constituents across the central Alps: TRANSALP tracer experiments. Atmospheric Environment, 32, 1257-1272.

Anfossi, D., F. Desiato, G. Tinarelli, G. Brusasca, E. Ferrero, and D. Sacchetti, 1998: TRANSALP 1989 experimental campaign - II. Simulation of a tracer experiment with Lagrangian particle models. Atmospheric Environment, 32, 1157-1166.

Apsley, D. D. and I. P. Castro, 1997: Numerical modelling of flow and dispersion around Cinder Cone Butte. Atmospheric Environment, 31, 1059-1071.

Aria, 1995: MINERVE Version 4.0 Theory Manual: Theoretical description of the objective analysis system MINERVE. Aria technologies report.

Auld, V., R. Hill, and T.J. Taylor (2003) Uncertainty in deriving dispersion parameters from meteorological data. Atmospheric Dispersion Modelling Liaison Committee report ADMLC-R2. ISBN 0-85951-525-7.

Baklanov, A., 2000: Application of CFD methods for modelling in air pollution problems: Possibilities and gaps. Environmental Monitoring and Assessment, 65, 181-189.

Banta, R. M., L. D. Olivier, P. H. Gudiksen, and R. Lange, 1996: Implications of small-scale flow features to modeling dispersion over complex terrain. Journal of Applied Meteorology, 35, 330-342.

Belcher, S. E. and J. C. R. Hunt, 1998: Turbulent flow over hills and waves. Annual Review of Fluid Mechanics, 30, 507-538.

Belcher, S. E., D. P. Xu, and J. C. R. Hunt, 1990: The Response of a Turbulent Boundary-Layer to Arbitrarily Distributed 2-Dimensional Roughness Changes. Quarterly Journal of the Royal Meteorological Society, 116, 611-635.

Beljaars, A. C. M., J. L. Walmsley, and P. A. Taylor, 1987: A Mixed Spectral Finite-Difference Model for Neutrally Stratified Boundary-Layer Flow over Roughness Changes and Topography. Boundary-Layer Meteorology, 38, 273-303.

Bitsuamlak, G. T., T. Stathopoulos, and C. Bedard, 2004: Numerical evaluation of wind flow over complex terrain: Review. Journal of Aerospace Engineering, 17, 135-145.

Bradley, E. F., 1980: An experimental study of the profiles of wind speed, shearing stress and turbulence at the crest of a large hill. Quarterly Journal of the Royal Meteorological Society, 106, 101-124.

Carruthers, D. J. and J. C. R. Hunt, 1990: Fluid mechanics of airflow over hills: turbulence, fluxes, and waves in the boundary layer. Meteorological Monographs, 23(45), 83-103.

Carruthers, D. J., C. A. McHugh, S. Dyster, A. Stidworthy and W. Oates, 2001: ADMS, Fundamental Aspects, Validation and Comparisons to Other Models. AWMA Guideline on Air Quality Models: A New Beginning. April 2001, Rhode Island.

Carruthers, D. J., J.C.R. Hunt, R. E. Britter, R. J. Perkins, P. F. Linden, and S. B. Dalziel, 1991: Fast models on small computers of turbulent flows in the environment for non-expert users. Computer Modelling in the Environmental Sciences, 199-214, Ed. Farmer & Rycroft, Oxford University Press.

Carruthers, D. J., R. J. Holroyd, J. C. R. Hunt, W. S. Weng, A. G. Robins, D. D. Apsley, D. J. Thomson, and F. B. Smith, 1994: UK-ADMS: a new approach to modelling dispersion in the earth's atmospheric boundary layer. Journal of Wind Engineering and Industrial Aerodynamics, 52, 139-153.

Carruthers, D. J., W.S. Weng, S.J. Dyster, R. Singles, and H. Higson, 2000: The Complex Terrain Module. CERC Report P14/01H/00.pdf. Cambridge Environmental Research Consultants, UK.

Carvalho, J. C., D. Anfossi, S. T. Castelli, and G. A. Degrazia, 2002: Application of a model system for the study of transport and diffusion in complex terrain to the TRACT experiment. Atmospheric Environment, 36, 1147-1161.

Castelli, S. T., S. Morelli, D. Anfossi, J. Carvalho, and S. Z. Sajani, 2004: Intercomparison of two models, ETA and RAMS, with TRACT field campaign data. Environmental Fluid Mechanics, 4, 157-196.

Castro, F. A., J. Palma, and A. S. Lopes, 2003: Simulation of the Askervein flow. Part 1: Reynolds averaged Navier-Stokes equations (k-epsilon turbulence model). Boundary-Layer Meteorology, 107, 501-530.

Castro, I. P. and D. D. Apsley, 1997: Flow and dispersion over topography: A comparison between numerical and laboratory data for two-dimensional flows. Atmospheric Environment, 31, 839-850.

CERC, 2001a: The advantages of ADMS3 over other models. Cambridge Environmental Research Consultants, UK.

CERC, 2001b: ADMS 3 Complex Terrain Flow Field Validation: Comparison of ADMS to Askervein Hill Field Data. Cambridge Environmental Research Consultants, UK.Cambridge Environmental Research Consultants, UK.

CERC, 2001c: ADMS 3 Hills Validation: Cinder Cone Butte. Cambridge Environmental Research Consultants, UK.

CERC, 2001d: ADMS 3 Hills Validation: Tracy Power Plant. Cambridge Environmental Research Consultants, UK.

Chandrasekar, A., C. R. Philbrick, R. Clark, B. Doddridge, and P. Georgopoulos, 2003: Evaluating the performance of a computationally efficient MM5/CALMET system for developing wind-field inputs to air quality models. Atmospheric Environment, 37, 3267-3276.

Chow, F. K. and R. L. Street, 2004: Evaluation of turbulence models for large-eddy simulations of flow over Askervein hill. In: Proceedings of the 16th Symposium on Boundary Layers and Turbulence, Portland, USA.

Cimorelli, A. J., S.G. Perry, A. Venkatram, J.C. Weil, R.J. Paine, R.B. Wilson R.F. Lee, W.D. Peters, R.W. Brode, J.O. Pauimer, 2002: AERMOD, Description of model formulation. Version 02222 EPA 454/R-02-002d. October 21 2002.

Clements, W. E., J. A. Archuleta, and P. H. Gudiksen, 1989: Experimental-Design of the 1984-Ascot Field-Study. Journal of Applied Meteorology, 28, 405-413.

Cox, R. M., J. Sontowski, C. M. Dougherty, and J. C. Boutet, 2003: The use of diagnostic and prognostic wind-fields for atmospheric transport calculations: an evaluation of the DIPOLE EAST 169 field experiment. Meteorological Applications, 10, 151-164.

CSU, 1997: RAMS, The Regional Atmospheric Modelling System, Technical Description. Colorado State University.

Danard, M., 1976: A simple model for mesoscale effects of topography on surface winds. Monthly Weather Review, 105, 572-581.

Davakis, E., M. Varvayanni, P. Deligiannis, and N. Catsaros, 1998: Diagnosis of wind flow and dispersion over complex terrain based on limited meteorological data. Environmental Pollution, 103, 333-343.

Dawson, P., D. E. Stock, and B. Lamb, 1991: The Numerical-Simulation of Air-Flow and Dispersion in 3-Dimensional Atmospheric Recirculation Zones. Journal of Applied Meteorology, 30, 1005-1024.

Desiato, F., 1991: A Dispersion Model Evaluation Study for Real-Time Application in Complex Terrain. Journal of Applied Meteorology, 30, 1207-1219.

Desiato, F., S. Finardi, G. Brusasca, and M. G. Morselli, 1998: TRANSALP 1989 experimental campaign - I. Simulation of 3D flow with diagnostic wind field models. Atmospheric Environment, 32, 1141-1156.

Dudhia, J., Gill D., Manning K., Wang W., Bruyere C., Kelly S. and Lackey K., 2005: PSU/NCAR Mesoscale Modeling System Tutorial Class Notes and User's Guide: MM5 Modeling System Version 3. National Centre for Atmospheric Research, Boulder, CO.

Duynkerke, P. G., 1988: Application of the E-Epsilon Turbulence Closure-Model to the Neutral and Stable Atmospheric Boundary-Layer. Journal of the Atmospheric Sciences, 45, 865-880.

Egan, B. A. and F. A. Schiermeier, 1986: Dispersion in Complex Terrain - a Summary of the Ams Workshop Held in Keystone, Colorado, 17-20 May 1983. Bulletin of the American Meteorological Society, 67, 1240-1247.

Etling, D., J. Preuss, and M. Wamser, 1986: Application of a Random-Walk Model to Turbulent-Diffusion in Complex Terrain. Atmospheric Environment, 20, 741-747.

Finardi, S., M. G. Morselli and P. Jeannet, 1997: Wind flow models over complex terrain for dispersion calculations. Cost Action 710 Pre-processing of meteorological data for dispersion models. Report of Working Group 4.

Gariazzo, C., A. Pelliccioni, M. P. Bogliolo, and G. Scalisi, 2004: Evaluation of a Lagrangian particle model (SPRAY) to assess environmental impact of an industrial facility in complex terrain. Water Air and Soil Pollution, 155, 137-158.

Gross, G., 1996: On the applicability of numerical mass-consistent wind field models. Boundary-Layer Meteorology, 77, 379-394.

Hall, D. J., A. M. Spanton, F. Dunkerley, M. Bennet and R.F. Griffiths, 2000: A Review of Dispersion Model Intercomparison Studies using ISC, R91, AERMOD and ADMS. Environment Agency R&D Technical Report P362.

Hanjalic, K. and B. E. Launder, 1972: A Reynolds stress model for turbulence and it's application to thin shear flows. Journal of Fluid Mechanics 52, 609-638.

Hanna, S. R., 1988: Air-Quality Model Evaluation and Uncertainty. Japca-the International Journal of Air Pollution Control and Hazardous Waste Management, 38, 406-412.

Hanna, S. R., B. A. Egan, C. J. Vaudo, and A. J. Curreri, 1984: A Complex Terrain Dispersion Model for Regulatory Applications at the Westvaco Luke Mill. Atmospheric Environment, 18, 685-699.

Hanna, S. R., B. A. Egan, J. Purdum and J. Wagler, 2001: Evaluation of the ADMS, AERMOD and ISC3 Models with the Optex, Duke Forest, Kincaid, Indianapolis and Lovett Field Data Sets. International Journal of Environment and Pollution, 16 (1-6), 301-314.

Hewer, F. E., 1998: Non-linear numerical model predictions of flow over an isolated hill of moderate slope. Boundary-Layer Meteorology, 87, 381-408.

Hill R., J. Taylor, I. Lowles, K. Emmerson and T. Parker, 2005: A new model validation database for evaluating AERMOD, NRPB R91 and ADMS using krypton-85 data from BNFL Sellafield. International Journal of Environment and Pollution, 24 (1/2/3/4), 75 – 87.

Homicz G.F. (2002) Three-dimensional wind field modelling: a review. SAND Report. SAND2002-2597.

Hunt, J. C. R., F. Tampieri, W. S. Weng, and D. J. Carruthers, 1991: Air-Flow and Turbulence over Complex Terrain - a Colloquium and a Computational Workshop. Journal of Fluid Mechanics, 227, 667-688.

Hunt, J. C. R., S. Leibovich, and K. J. Richards, 1988a: Turbulent Shear Flows over Low Hills. Quarterly Journal of the Royal Meteorological Society, 114, 1435-1470.

Hunt, J. C. R., K. J. Richards, and P. W. M. Brighton, 1988b: Stably Stratified Shear-Flow over Low Hills. Quarterly Journal of the Royal Meteorological Society, 114, 859-886.

Hurley P.J., 2005: The Air Pollution (TAPM) version 3. Part 1: Technical Description. CSIRO, Australia.

Iizuka, S. and H. Kondo, 2004: Performance of various sub-grid scale models in large-eddy simulations of turbulent flow over complex terrain. Atmospheric Environment, 38, 7083-7091.

Jackson, P.S. and J.C.R. Hunt, 1975: Turbulent wind flow over a low hill. Quarterly Journal of the Royal Meteorological Society, 101, 929-955.

Jenkins, G. J., P. J. Mason, W. H. Moores, and R. I. Sykes, 1981: Measurements of the Flow Structure around Ailsa-Craig, a Steep, 3-Dimensional, Isolated Hill. Quarterly Journal of the Royal Meteorological Society, 107, 833-851.

Jones, W. P. and B. E. Launder, 1972: The prediction of laminarization with a two-equation model of turbulence. International Journal of Heat and Mass Transfer, 15, 301-314.

Kim, H. G. and V. C. Patel, 2000: Test of turbulence models for wind flow over terrain with separation and recirculation. Boundary-Layer Meteorology, 94, 5-21.

Kim, H. G., V. C. Patel, and C. M. Lee, 2000: Numerical simulation of wind flow over hilly terrain. Journal of Wind Engineering and Industrial Aerodynamics, 87, 45-60.

King, D. S. and S. S. Bunker, 1984: Application of Atmospheric Transport Models for Complex Terrain. Journal of Climate and Applied Meteorology, 23, 239-246.

Kossmann, M., R. Vogtlin, U. Corsmeier, B. Vogel, F. Fiedler, H. J. Binder, N. Kalthoff, and F. Beyrich, 1998: Aspects of the convective boundary layer structure over complex terrain. Atmospheric Environment, 32, 1323-1348.

Lamprecht, R. and D. Berlowitz, 1998: Evaluation of diagnostic and prognostic flow fields over prealpine complex terrain by comparison of the Lagrangian prediction of concentrations with tracer measurements. Atmospheric Environment, 32, 1283-1300.

Lange, R., 1989: Transferability of a 3-Dimensional Air-Quality Model between 2 Different Sites in Complex Terrain. Journal of Applied Meteorology, 28, 665-679.

Lee, S. M., S. C. Yoon, and D. W. Byun, 2004: The effect of mass inconsistency of the meteorological field generated by a common meteorological model on air quality modeling. Atmospheric Environment, 38, 2917-2926.

Lehning, M., H. Richner, and G. L. Kok, 1996: Pollutant transport over complex terrain: Flux and budget calculations for the POLLUMET field campaign. Atmospheric Environment, 30, 3027-3044.

Leone, J. M. and R. L. Lee, 1989: Numerical-Simulation of Drainage Flow in Brush-Creek, Colorado. Journal of Applied Meteorology, 28, 530-542.

Leschziner, M. A. and W. Rodi, 1981: Calculation of Annular and Twin Parallel Jets Using Various Discretization Schemes and Turbulence-Model Variations. Journal of Fluids Engineering-Transactions of the Asme, 103, 352-360.

Luhar, A. K. and K. S. Rao, 1994: Lagrangian Stochastic Dispersion Model Simulations of Tracer Data in Nocturnal Flows over Complex Terrain. Atmospheric Environment, 28, 3417-3431.

Luhar, A. K. and P. J. Hurley, 2003: Evaluation of TAPM, a prognostic meteorological and air pollution model, using urban and rural point-source data. Atmospheric Environment, 37, 2795-2810.

Mahrt, L., 1982: Momentum balance of gravity flows. Journal of Atmospheric Science, 39, 2701 – 2711.

Martilli, A. and G. Graziani, 1998: Mesoscale circulation across the Alps: Preliminary simulation of TRANSALP 1990 observations. Atmospheric Environment, 32, 1241-1255.

Mason, P. J. and J. C. King, 1985: Measurements and Predictions of Flow and Turbulence over an Isolated Hill of Moderate Slope. Quarterly Journal of the Royal Meteorological Society, 111, 617-640.

Mason, P. J. and R. I. Sykes, 1979: Flow over an isolated hill of moderate slope. Quarterly Journal of the Royal Meteorological Society, 105, 383 – 395.

McIlveen R., 1998: Fundamentals of weather and climate. Stanley Thornes (Publishers) Ltd.

McQueen, J. T., R. R. Draxler, and G. D. Rolph, 1995: Influence of Grid Size and Terrain Resolution on Wind-Field Predictions from an Operational Mesoscale Model. Journal of Applied Meteorology, 34, 2166-2181.

Paine J., R. F. Lee, R. Brode, R. B. Wilson, A. J. Cimorelli, S. G. Perry., J. C. Weil, A. Venkatram and W. D. Peters, 1998: Model Evaluation Results for AERMOD. USEPA Report NC 27711.

Paumier, J. O., S. G. Perry, and D. J. Burns, 1992: CTDMPLUS - a Dispersion Model for Sources near Complex Topography .2. Performance-Characteristics. Journal of Applied Meteorology, 31, 646-660.

Perry, S. G., 1992: CTDMPLUS - a Dispersion Model for Sources near Complex Topography .1. Technical Formulations. Journal of Applied Meteorology, 31, 633-645.

Perry, S. G., A. J. Cimorelli, R. J. Paine, R. W. Brode, J. C. Weil, A. Venkatram, R. B. Wilson, R. F. Lee, and W. D. Peters, 2005: AERMOD: A dispersion model for industrial source applications. Part II: Model performance against 17 field study databases. Journal of Applied Meteorology, 44, 694-708.

Poulos, G. S. and J. E. Bossert, 1995: An Observational and Prognostic Numerical Investigation of Complex Terrain Dispersion. Journal of Applied Meteorology, 34, 650-669.

Rao, K. S., R. M. Eckman, and R. P. Hosker, 1989: Simulation of Tracer Concentration Data in the Brush Creek Drainage Flow Using an Integrated Puff Model. Journal of Applied Meteorology, 28, 609-616.

Robinson L. M., 1996: Turbulent structure of the atmosphere in a region of complex terrain and near to a major industrial installation. Ph. D. Thesis submitted to the University of Manchester Institute of Science and Technology.

Ross, D. G. and D. G. Fox, 1991: Evaluation of an Air-Pollution Analysis System for Complex Terrain. Journal of Applied Meteorology, 30, 909-923.

Ryan, W., B. Lamb, and E. Robinson, 1984: An Atmospheric Tracer Investigation of Transport and Diffusion around a Large, Isolated Hill. Atmospheric Environment, 18, 2003-2021.

Salmon, J. R., H. W. Teunissen, R. E. Mickle, and P. A. Taylor, 1988: The Kettles Hill Project - Field Observations, Wind-Tunnel Simulations and Numerical-Model Predictions for Flow over a Low Hill. Boundary-Layer Meteorology, 43, 309-343.

Scire, J. S., F. R. Robe, M. E. Fernau, and R. J. Yamartino, 2000: A users guide for the CALMET meteorological model (version 5). Earth Tech Inc. Report.

SMHI, 1997: Airviro User Documentation. Swedish Meteorological and Hydrological Institute, Norrköping, Sweden.

Snyder, W. H. , R. S. Thompson, R. E. Eskridge, R. E. Lawson, I. P. Castro, J. T. Lee, C. R. Hunt and Y. Ogawa, 1985: The structure of the strongly stratified flow over hills: Dividing streamline concept. Journal of Fluid. Mechanics, 152, 249-288.

Stangroom, P., 2004: CFD Modelling of Wind Flow Over Terrain. Thesis submitted to the University of Nottingham.

Sykes, R.I., (1980): An asymptotic theory of incompressible flow turbulent boundary-layer flow of a small hump. Journal of Fluid Mechanics, 101, 647-670.

Taylor, P. A. and H. W. Teunissen, 1987: The Askervein Hill Project - Overview and Background Data. Boundary-Layer Meteorology, 39, 15-39.

Taylor, P. A., J. L. Walmsley, and J. R. Salmon, 1983: A Simple-Model of Neutrally Stratified Boundary-Layer Flow over Real Terrain Incorporating Wavenumber-Dependent Scaling. Boundary-Layer Meteorology, 26, 169-189.

Taylor, P. A., P. J. Mason, and E. F. Bradley, 1987: Boundary-Layer Flow over Low Hills. Boundary-Layer Meteorology, 39, 107-132.

US EPA, 2003: AERMOD: Latest Features and Evaluation Results. US EPA Report 454/R-03-003.

Varvayanni, M., J. G. Bartzis, N. Catsaros, G. Graziani, and P. Deligiannis, 1998: Numerical simulation of daytime mesoscale flow over highly complex terrain: Alps case. Atmospheric Environment, 32, 1301-1316.

Venkatram, A., R. Brode, A. Cimorelli, R. Lee, R. Paine, S. Perry, W. Peters, J. Weil, and R. Wilson, 2001: A complex terrain dispersion model for regulatory applications. Atmospheric Environment, 35, 4211-4221.

Walmsley, J. L., J. R. Salmon, and P. A. Taylor, 1982: On the Application of a Model of Boundary-Layer Flow over Low Hills to Real Terrain. Boundary-Layer Meteorology, 23, 17-46.

Weber, R. O. and P. Kaufmann, 1998: Relationship of synoptic winds and complex terrain flows during the MISTRAL field experiment. Journal of Applied Meteorology, 37, 1486-1496.

Wood, N., 1995: The onset of separation in neutral, turbulent flow over hills. Boundary-Layer Meteorology, 76, 137-164.

Wood, N., 2000: Wind flow over complex terrain: A historical perspective and the prospect for large-eddy modelling. Boundary-Layer Meteorology, 96, 11-32.

Wroblewski, A., A. Coppalle, and R. Guillermo, 2001: Comparison of two different operational models for complex terrain in neutral flow. International Journal of Environment and Pollution, 16, 328-334.

Yakhot, V. and S. A. Orszag, 1986: Renormalization-Group Analysis of Turbulence. Physical Review Letters, 57, 1722-1724.

7 SYMBOLS AND NOTATION

α	Angle of the terrain
$C_{es}\{x_r, y_r, z_t\}$	Contribution in convective and stable conditions from the terrain following plume state at a receptor point
$C_{es}\{x_r, y_r, z_r\}$	Contribution in convective and stable conditions from the horizontal plume states at a receptor point
C_d	Drag coefficient
C_μ , C_1, C_2	Constants used in the k-ε turbulence model
C_p	Specific heat capacity of air
$C_T\{x_r, y_r, z_r\}$	Total concentration (CBL) at a receptor point
C_s	Concentration in the absence of the hill for stable conditions
ε	Energy dissipation rate, or,
ε	Angle between the surface and geostrophic winds
f	Plume state weighting function

F	Friction force
F_r	Froude number
ϕ_p	Fraction of plume mass below H_c
g	Acceleration due to gravity
γ	Lapse rate
H	Boundary layer height
h_c,	Height scale characterises the height of the surrounding terrain that most dominates the flow in the vicinity of he receptor
h_{max}	Maximum height of the hill
h_{mean}	Mean height of the hill
h_t	Terrain height
Δh_t	Effective obstacle height
k	Turbulent kinetic energy
k_{sf}	Entrainment coefficient on the top of the slope flow layer
K_m	Eddy diffusivity for momentum
K_t	Horizontal thermal diffusivity
l	Terrain length scale
L	Monin-Obukhov length
L_e	Equilibrium length scale
L_v and L_w	Vertical and transverse length scales
M_a	Height of the plume above H_c
M_b	Height of the plume below H_c
N	Buoyancy frequency, or,
N	Brunt-Väisälä frequency
Q	Rate of temperature change due to heating or cooling
Q_H	Surface heat flux
ρ_s	Surface pressure
ρ_g	Geostrophic pressure
ρ_0	Reference-state pressure
ρ_τ	Pressure at the top of the domain
ρ_{s0}	Reference-state pressure at the surface
S	Slope speed for downslope flows, or,
S	Source term
σ	Terrain following vertical co-ordinate
σ_u, σ_v, σ_w	Local root mean square velocity scales
R_γ	Specific gas constant
T_g	Geostrophic temperature
T_L	Lagrangian time scale
T_s	Surface temperature
τ	Time interval over which the heating occurs
U_{hmax}	Wind speed at the maximum height of the hill
u	Wind component in the x direction
U_i and U_j	Instantaneous horizontal winds
u'_i and u'_j	Fluctuations in the horizontal winds
v	Wind component in the y direction

V_g	Geostrophic wind
V_s	Wind at the surface
w	Wind component in the z direction
θ_{crit}	Critical gradient
θ_s	Potential temperature at the surface
z_o	Roughness length
$z_p = z_r - z_t$	Receptor flagpole height
z_r	Height of the receptor above local source base
z_t	Height of the terrain above mean sea level
Z_g	Geostrophic height
Z_s	Surface height

8 TABLES

Table 1 Overview of Model Evaluation Results for ADMS and AERMOD for the Lovett database (from Hanna *et al.*, 2001)

	Value
Number of Points	2595
Max Concentration Observations ($\mu g\ m^{-3}$)	447
Max Concentration ADMS ($\mu g\ m^{-3}$)	267
Max Concentration AERMOD ($\mu g\ m^{-3}$)	441
Geometric mean ADMS	0.14
Geometric mean AERMOD	-0.37
Geometric variance ADMS	3.6
Geometric variance AERMOD	3.6
Fraction of predictions within a factor of two of the observations ADMS	0.3
Fraction of predictions within a factor of two of the observations AERMOD	0.25

Table 2 Summary of AERMOD and CTDMPLUS evaluation results for the SCRAM databases (from Perry *et al.*, 2005)[§]

Database	Model Validated	Ratio of Modelled / Observed Robust Highest Concentrations
Lovett (SO_2)	AERMOD	1.00 (3 hour average)
		1.00 (24 hour average)
		0.79 (annual peak)
	CTDMPLUS	2.37 (3 hour average)
		2.01 (24 hour average)
		1.34 (annual peak)
Martins Creek (SO_2)	AERMOD	1.06 (3 hour average)
		1.65 (24 hour average)
		0.76 (annual peak)
	CTDMPLUS	4.80 (3 hour average)
		5.56 (24 hour average)
		2.19 (annual peak)
Tracy (SF_6)	AERMOD	1.07 (1 hour average)
	CTDMPLUS	0.77 (1 hour average)
Westvaco (SO_2)	AERMOD	1.08 (3 hour average)
		1.14 (24 hour average)
		1.65 (annual peak)
	CTDMPLUS	2.14 (3 hour average)
		1.54 (24 hour average)
		0.93 (annual peak)

[§] The model evaluation databases used to validate AERMOD can be downloaded from the Support Centre for Regulatory Atmospheric Modelling (SCRAM). http://www.epa.gov/scram001/dispersion_prefrec.htm

Table 3 Summary of ADMS evaluation results for the Tracy databases (from CERC, 2001d)

Experiment	Model	Mean	Sigma	Bias	NMSE	R	FA2	FB	FS
Stable 1	Obs	431	489	0	0	1	1	0	0
	ADMS	439	661	-8.31	2.89	0.199	0.2	-0.019	-0.298
Stable 2	Obs	838	1270	0	0	1	1	0	0
	ADMS	203	490	634.65	11.78	0.2	0.149	1.219	0.886
Stable 3	Obs	219	208	0	0	1	1	0	0
	ADMS	354	602	-134.9	5.28	0.061	0.197	-0.471	-0.973
Stable 4	Obs	210	266	0	0	1	1	0	0
	ADMS	11	34	198.62	48.92	-0.158	0.058	1.799	1.547
Stable 5	Obs	473	985	0	0	1	1	0	0
	ADMS	294	496	178.76	9.06	-0.01	0.221	0.466	0.661
Stable 6	Obs	537	590	0	0	1	1	0	0
	ADMS	461	766	76.66	1.9	0.522	0.267	0.154	-0.261
Stable 7	Obs	569	859	0	0	1	1	0	0
	ADMS	356	614	212.56	3.07	0.511	0.183	0.46	0.332
Stable 8	Obs	391	476	0	0	1	1	0	0
	ADMS	233	541	158.55	5	0.171	0.184	0.508	-0.127
Stable 9	Obs	309	363	0	0	1	1	0	0
	ADMS	351	557	-41.58	2.55	0.413	0.219	-0.126	-0.421
Stable 10	Obs	380	523	0	0	1	1	0	0
	ADMS	29	95	351.57	36.49	0.087	0.072	1.72	1.387
Stable 11	Obs	291	598	0	0	1	1	0	0
	ADMS	119	432	172.29	15.94	0.045	0.064	0.841	0.322
Stable 12	Obs	227	444	0	0	1	1	0	0
	ADMS	0.6	3.1	226.36	1709.58	-0.009	0.004	1.989	1.972
Stable 13	Obs	513	856	0	0	1	1	0	0
	ADMS	166	337	347.63	10.36	0.151	0.116	1.024	0.869
Stable 14	Obs	551	731	0	0	1	1	0	0
	ADMS	146	287	405.22	9.17	0.107	0.173	1.163	0.873

FA2 is the fraction of model predictions within a factor of 2 of the field measurements respectively, R is the correlation statistic, FB is the fractional bias, FS is the Fractional Standard Deviation and NMSE is the Normalised Mean Squared Error.

Table 4 Details of the field measurements of ^{85}Kr air concentrations compiled in the model validation database (All) and those included in the ADMS and AERMOD validation study (Local sites, Westlakes and Greystoke). From Hill *et al.* (2005).

Location	Number of measurements	Duration (hours)	Air concentration (Bq m^{-3})		
			Maximum	Minimum	Average
Local sites	188	2 to 24	5510.0	1.3	243.9
Greystoke	5	24	17.9	4.0	11.4
Westlakes	6	24	302.4	26.2	141.9
All	211	2 to 168	5510.0	1.2	221.7

Table 5 Statistical comparison between the predictions of the atmospheric dispersion models ADMS and AERMOD and the field measurements of ^{85}Kr air concentrations. From Hill *et al.* (2005).

Model	Configuration	Mean Bias	FA2	FA5	FA10	R^2	NMSE
Regional dispersion over complex terrain (number of samples = 11)							
NRPB R-91	FLAT	0.60	0.27	0.64	0.82	0.17	2.64
ADMS 3.1	FLAT	0.17	0.18	0.45	0.64	0.11	13.26
	TERRAIN	0.22	0.27	0.64	0.82	0.60	3.55
AERMOD	FLAT	0.37	0.27	0.64	0.82	0.60	3.55
	TERRAIN	0.30	0.27	0.55	0.82	0.53	5.18

FA2, FA5 and FA10 are the fraction of model predictions within factors of 2, 5 and 10 of the field measurements respectively, R^2 is the square of the correlation statistic and NMSE is the Normalised Mean Squared Error.

Table 6 Locations selected for model inter-comparison and model set-ups.

Terrain	Location	Simulation Key	OS Co-ordinates	Stack height	Grid resolution (nodes)	Domain size (km)	Indicative gradient
Simple	Inland	SI	343485, 539565	20 m	64 × 64	8 × 8	<1:20
	Coastal	SC	301520, 531880	100 m	64 × 64	11 ×12	1:10
Moderate	Inland	MI 64N	303000, 521000	20 m	64 × 64	8 × 8	1:7
		MI 32N	303000, 521000	20 m	32 × 32	8 × 8	1:7
		MI 16N	303000, 521000	20 m	16 × 16	8 × 8	1:7
		MI 64N 16 D	303000, 521000	20 m	64 × 64	16 × 16	1:7
		MI 64N 32 D	303000, 521000	20 m	64 × 64	32 × 32	1:7
	Coastal	MC	320270, 470000	100 m	64 × 64	12 × 12	<1:7
Complex	Inland	CI 64N	318785, 508660	20 m	64 × 64	8 × 8	1:2
		CI 32N	318785, 508660	20 m	32 × 32	8 × 8	1:2
		CI 16N	318785, 508660	20 m	16 × 16	8 × 8	1:2
		CI 64N 16 D	318785, 508660	20 m	64 × 64	16 × 16	1:2
		CI 64N 32 D	318785, 508660	20 m	64 × 64	32 × 32	1:2
	Coastal	CC	311450, 483450	100 m	64 × 64	13 × 12	1:3

Simulation key is determined as follows: character 1 (S = simple terrain, M = moderate terrain, C = complex terrain); character 2 (I = inland location, C = coastal location); optional (N = node resolution; optional (D = domain size in kilometres).

Table 7 Statistical comparison of concentrations (μg m^{-3}) predicted by ADMS and AERMOD. See Table 6 for definitions of the simulation keys.

Simulation Key	Concentrations (no terrain) (μg m^{-3})				Concentrations (terrain) (μg m^{-3})				Amplification factor = C_{terr} / C_{flat}			
	Median short-term	Max short-term	Median long-term	Max long-term	Median short-term	Maximum short-term	Median long-term	Maximum long-term	Median short-term	Maximum short-term	Median long-term	Maximum long-term
ADMS												
SI	7.59	220.35	0.13	6.41	11.57	228.79	0.21	6.19	1.46	2.90	1.56	2.27
SC	1.09	10.89	0.03	0.13	1.50	11.06	0.04	0.13	1.10	2.63	1.27	1.82
MI 64N	7.63	207.91	0.13	6.17	9.48	242.46	0.18	6.79	1.28	2.95	1.34	2.22
MI 32N					9.44	258.19	0.18	6.50	1.22	2.97	1.32	2.25
MI 16N					10.29	209.65	0.19	7.07	1.32	3.01	1.43	2.07
MI 64N 16 D					12.74	188.69	0.22	7.04	1.60	3.05	1.62	2.21
MI 64N 32 D					12.53	182.29	0.21	6.49	1.59	3.53	1.62	2.20
MC	1.04	11.61	0.03	0.13	1.20	11.52	0.04	0.14	1.05	2.08	1.16	1.67
CI 64N	7.59	220.35	0.13	6.41	13.97	701.66	0.17	21.00	2.09	20.61	1.58	24.33
CI 32N					15.01	887.19	0.18	24.90	2.25	22.57	1.67	23.11
CI 16N					15.91	801.30	0.19	32.75	2.27	25.45	1.76	16.98
CI 64N 16 D					13.11	921.89	0.18	31.10	2.04	21.35	1.66	23.12
CI 64N 32 D					13.41	774.64	0.18	23.72	1.79	13.73	1.53	10.04
CC	1.11	10.91	0.03	0.13	2.70	101.80	0.04	1.29	1.95	51.84	1.34	33230.94
AERMOD												
SI	27.26	189.86	0.28	8.53	24.81	189.86	0.29	7.18	0.89	2.72	0.94	2.46
SC	0.98	7.51	0.02	0.16	0.97	7.66	0.02	0.16	0.98	2.89	0.97	1.84
MI	27.39	205.33	0.28	9.02	20.84	549.22	0.23	7.81	0.75	7.59	0.80	3.65
MC	0.92	7.50	0.03	0.16	0.92	7.33	0.03	0.16	0.99	1.79	0.98	1.56
CI	21.77	166.25	0.24	7.21	2.36	592.74	0.04	11.39	0.12	10.91	0.17	5.93
CC	0.96	7.41	0.03	0.16	0.83	266.47	0.02	2.34	0.91	119.21	0.91	29.81

9 FIGURES

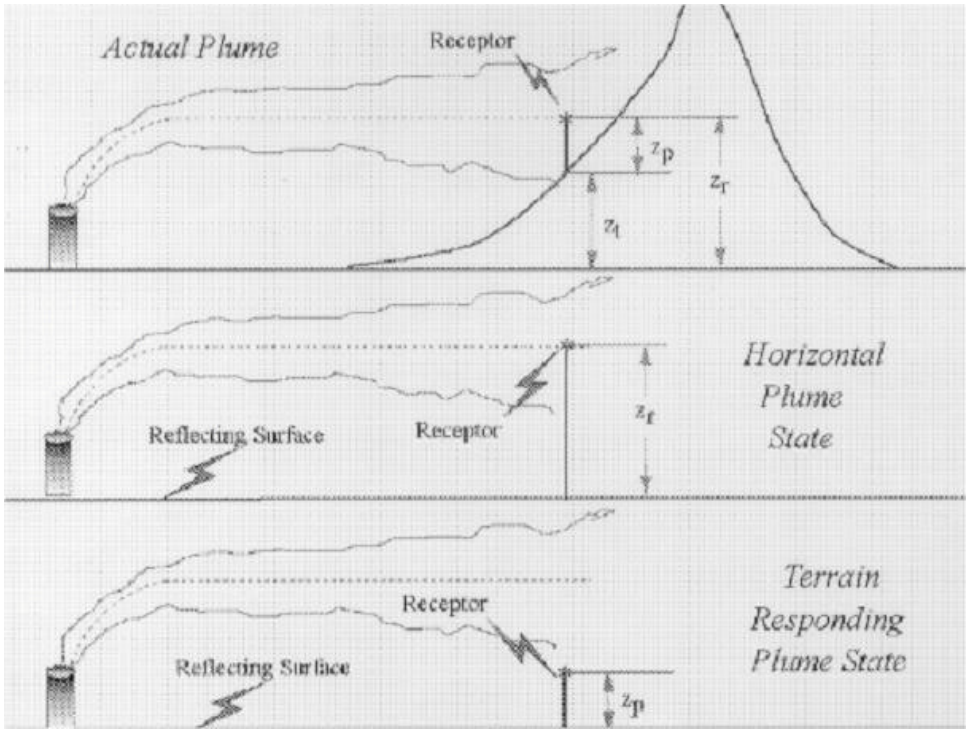

Figure 1 AERMOD Two state approach. The total concentration is the weighted sum of two extreme possible plume states. From Cimorelli *et al.*, 2002.

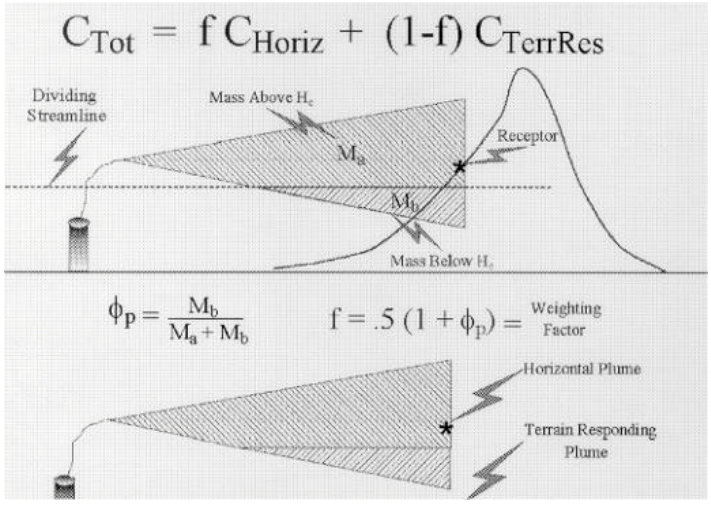

Figure 2 Treatment of Terrain in AERMOD. Construction of the weighting factor used in total concentration. From Cimorelli *et al.*, 2002.

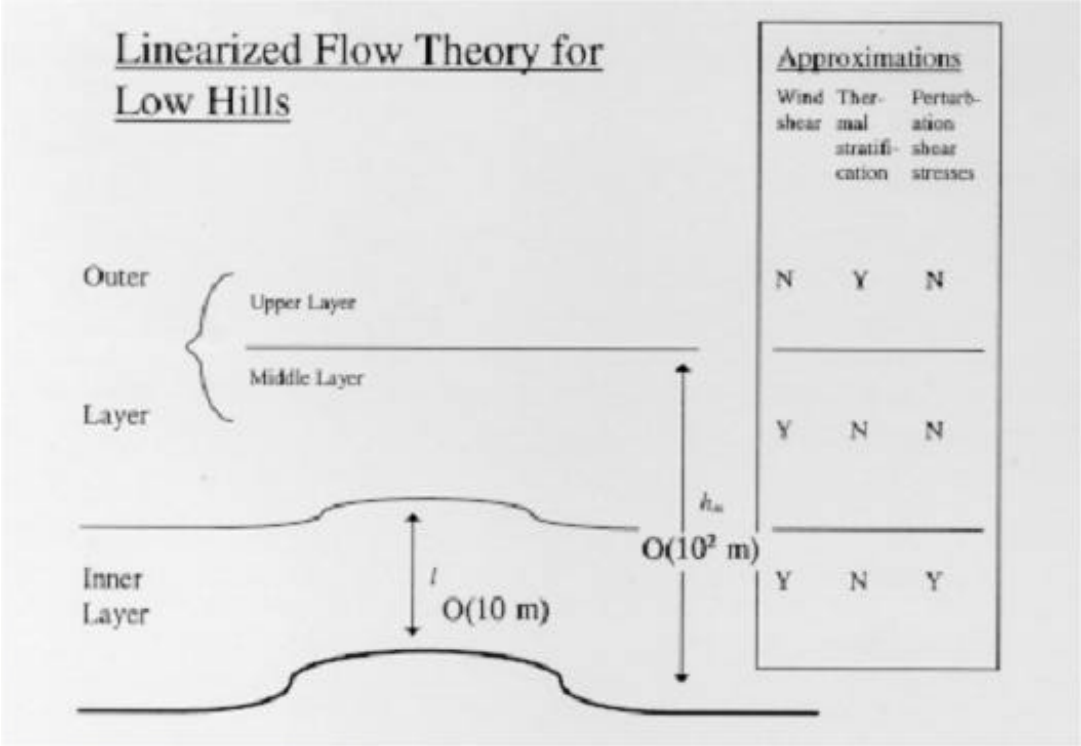

Figure 3 Division of the flow in FLOWSTAR into layers and the approximations applied within each. From Robinson (1996).

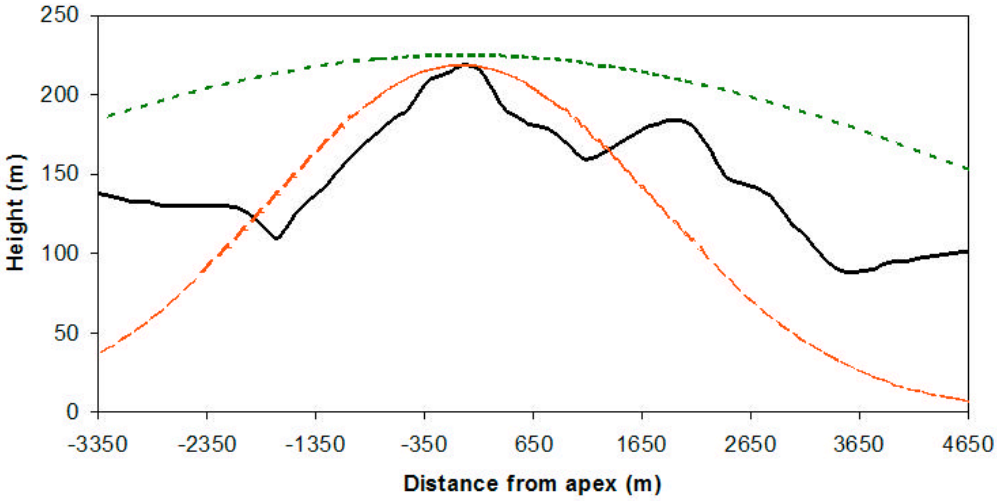

Figure 4 Incorporation of the dividing streamline concept within the linear flow-field model FLOWSTAR showing the actual terrain height (in black) the idealised terrain height (in red) and the height of the dividing streamline (in green).

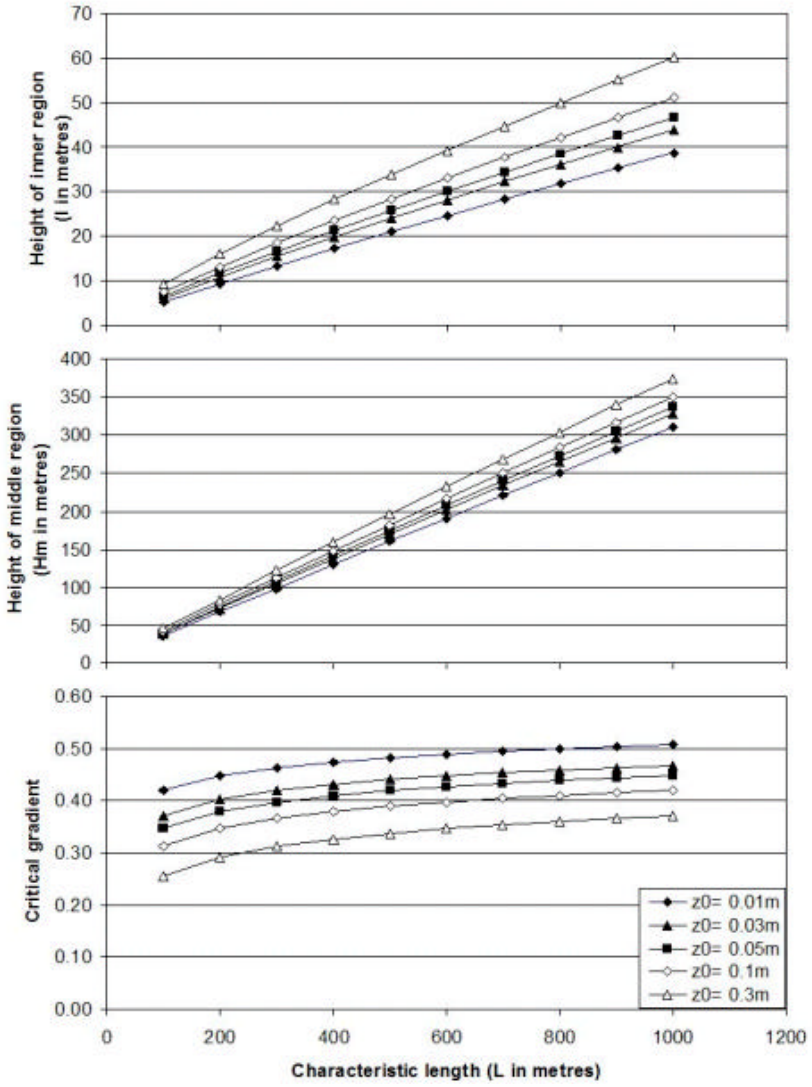

Figure 5 Approximate critical gradients using the Wood (1995) equation (Equation 5) for 3-dimensional flow (assumed by Hewer, 1998, to be approximately 20% greater than for 2-dimensional flow) for the onset of non-linear flow for a range of surface roughness lengths and terrain length scales.

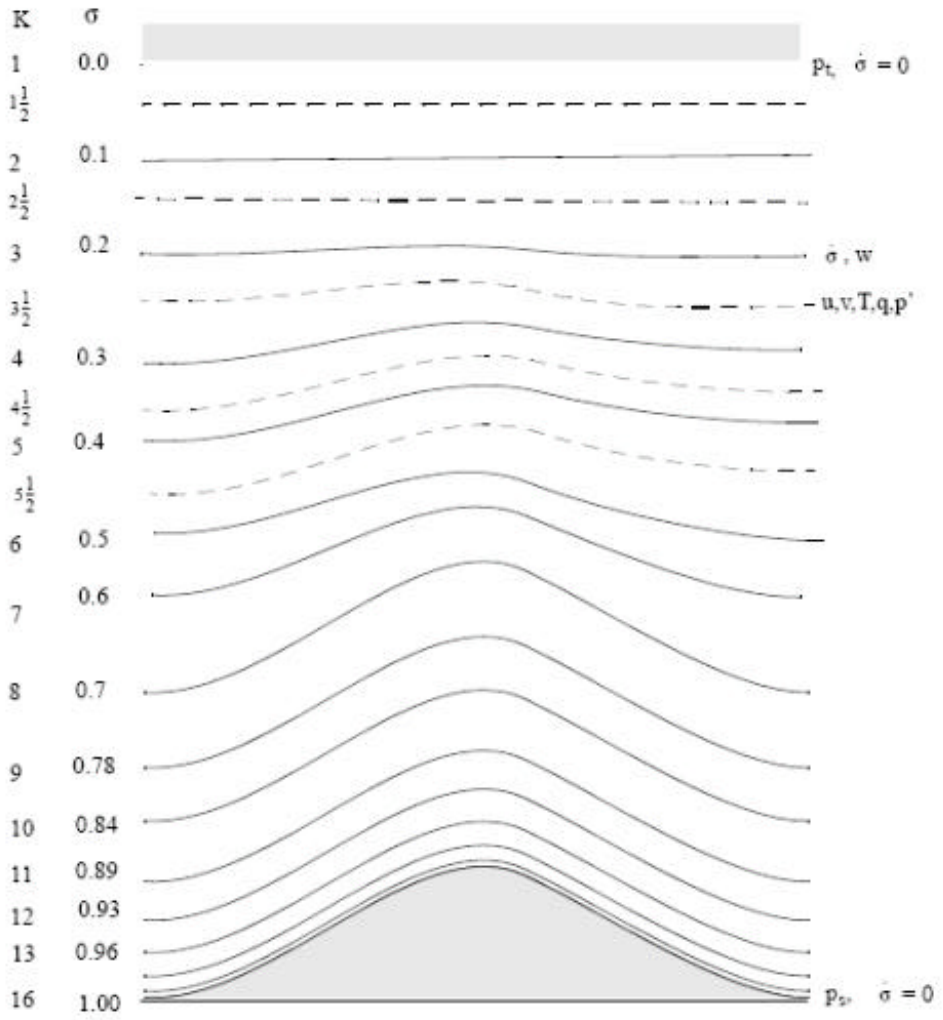

Figure 1.2 Schematic representation of the vertical structure of the model. The example is for 15 vertical layers. Dashed lines denote half-sigma levels, solid lines denote full-sigma levels.

Figure 6 Vertical structure of the MM5 prognostic meteorological using sigma co-ordinates. From Dudhia *et al*. (2005).

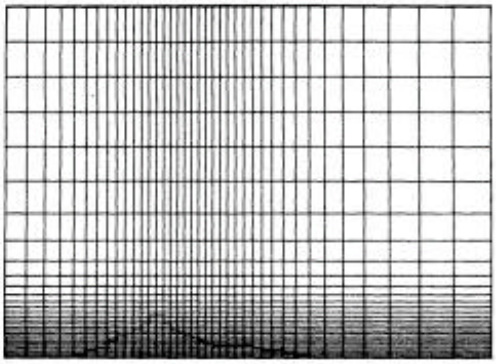

Cartesian Mesh (Dawson *et al*., 1991)

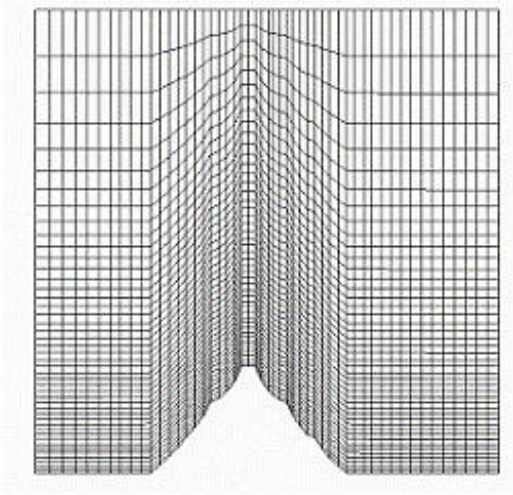

Structured BFC mesh

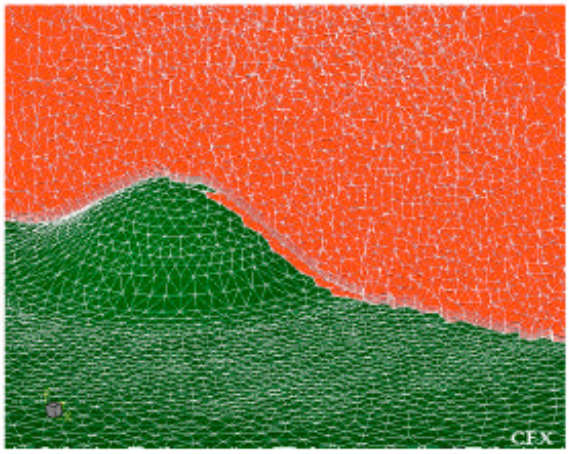

Unstructured BFC mesh (Stangroom, 2004)

Figure 7 Comparison of three different CFD mesh types used to model flow over an isolated hill.

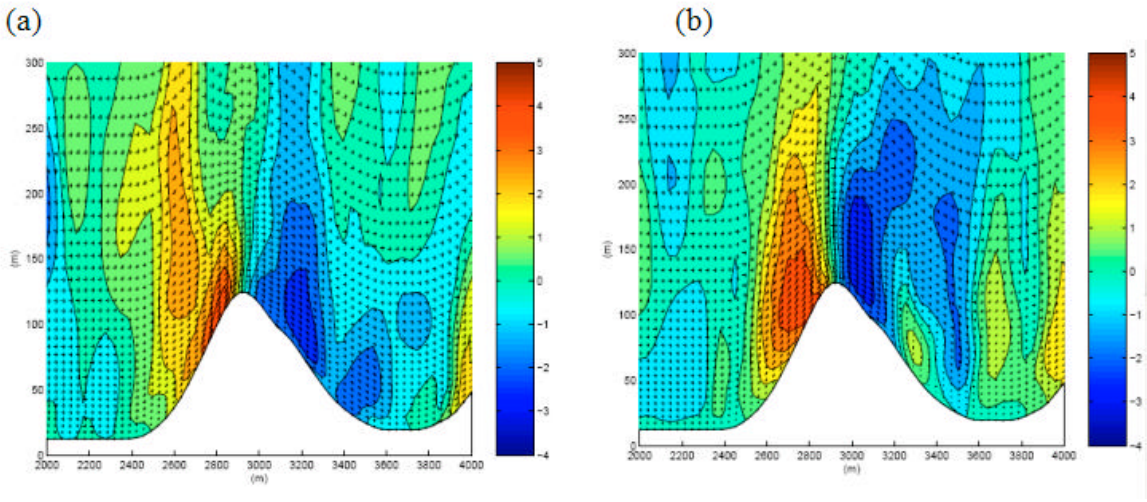

Figure 8 Comparison of instantaneous LES results for flow over Askervein Hill, from Chow and Street (2004), illustrating period of gust (a) and recirculation (b). Velocity vectors are shown along with contours of vertical wind speed.

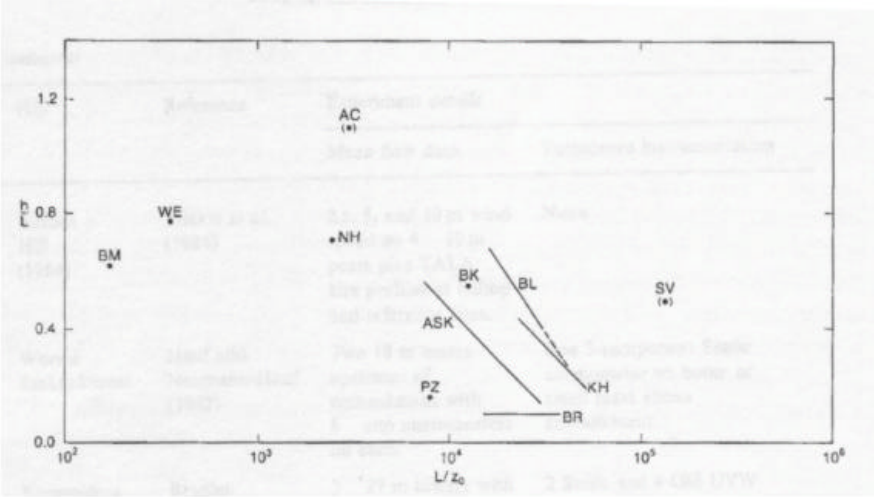

Figure 9 Parameter space evaluation of terrain complexity for studies of air-flow from Taylor *et al*. (1987). Studies referred to are: AC: Ailsa Craig; ASK: Askervein Hill; BK: Brent Knoll; BL: Blashaval Hill; BM: Black Mountain; BR: Bungendore Ridge; KH: Kettles Hill; NH: Nyland Hill; PZ: Pouzauges Hill; SV: Sirhowy Valley; WE, Worms Embankment.

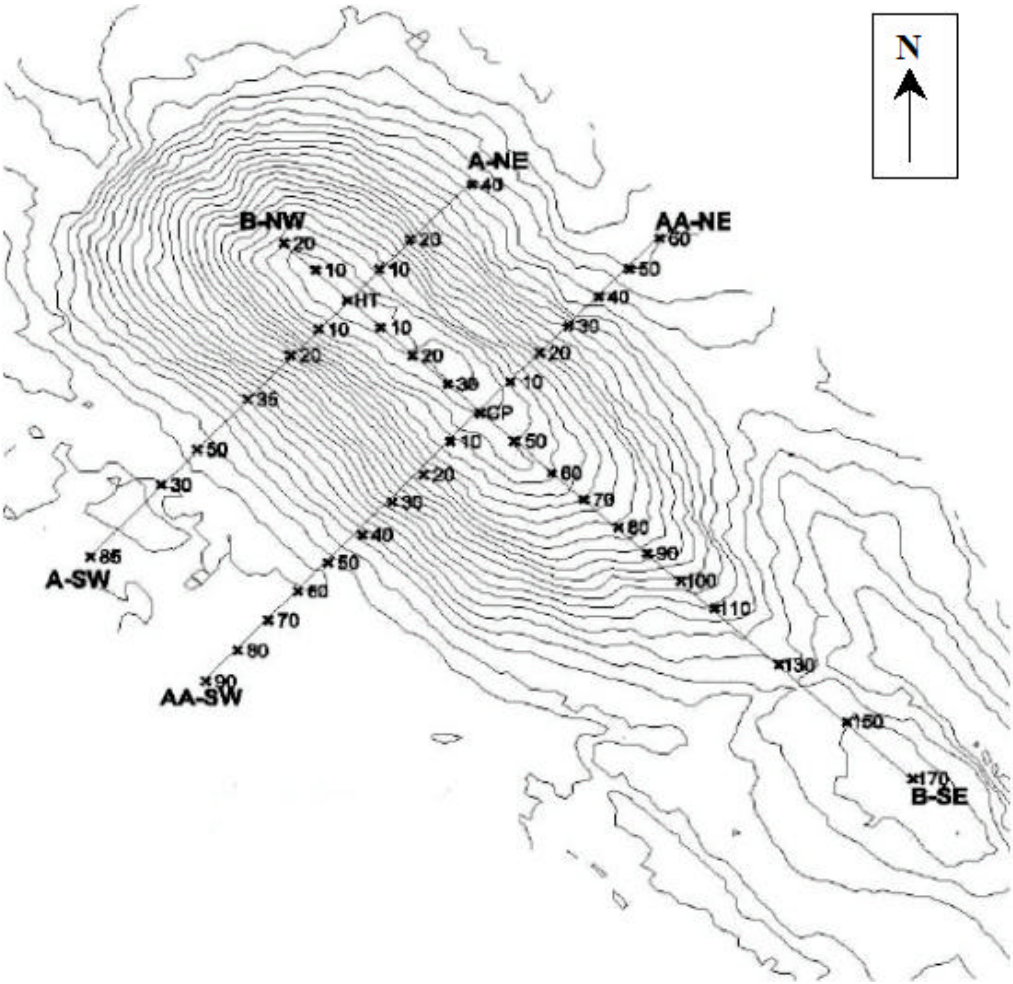

Figure 10 Contour plot and experimental measurement arrays from the Askervien Hill experiment. Reproduced from Stangroom (2004).

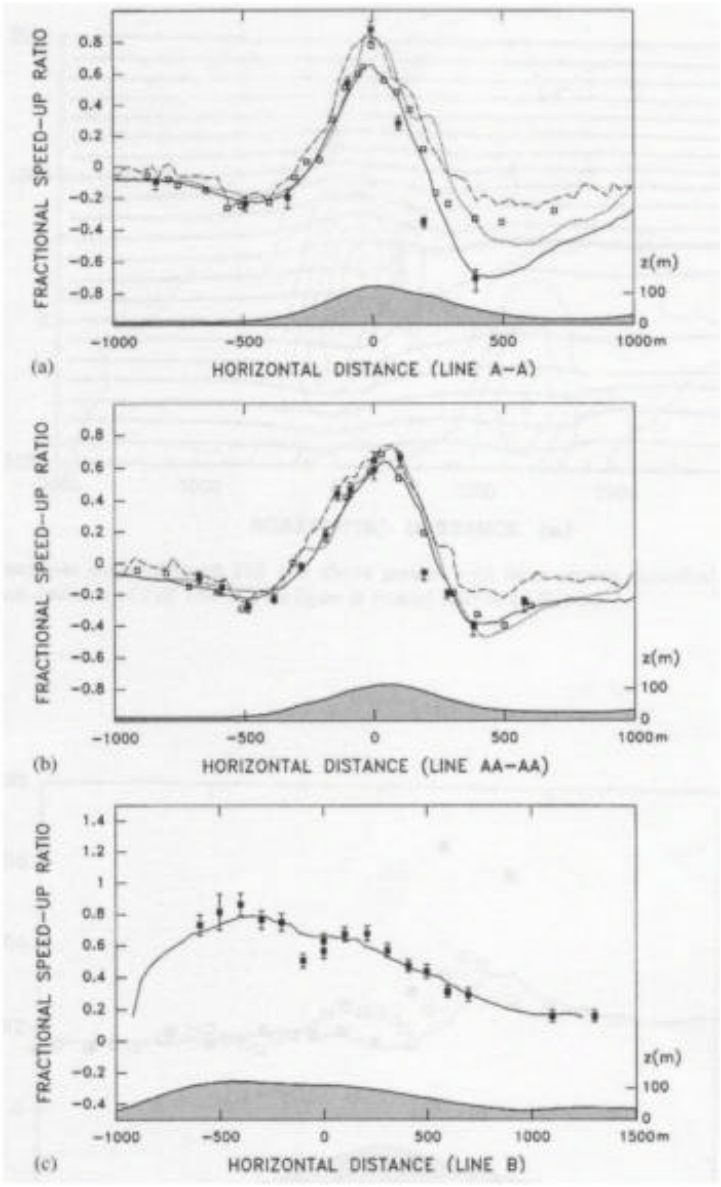

Figure 11 Fractional speed-up ratios over Askervien Hill at 10 m above ground level for a 210 degree incident wind. Solid points show measurement data, solid and dotted lines show 3D and 2D CFD model predictions respectively and dashed lines show the predictions of the linear model of Beljaars *et al*. (1987). From Kim *et al*. (2000).

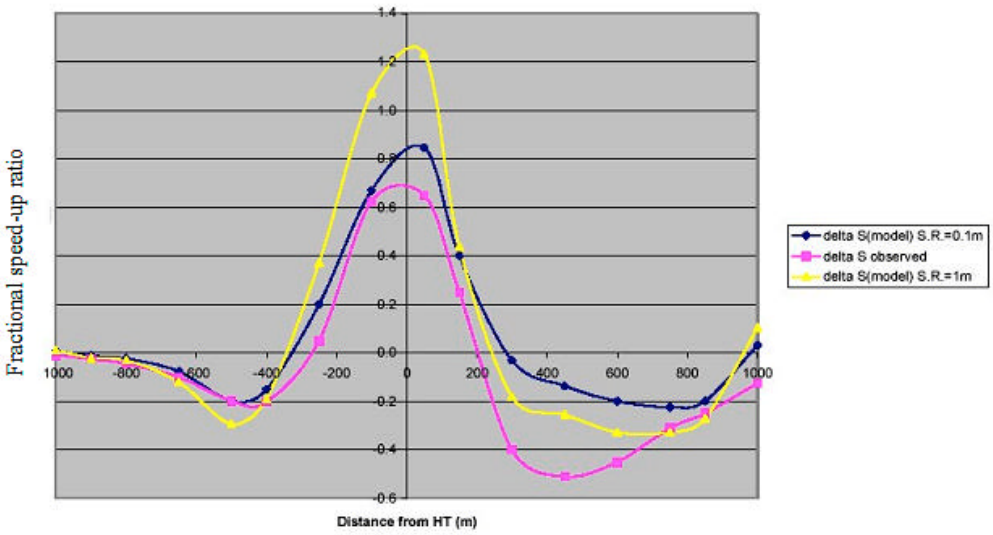

Figure 12 Fractional speed up ratios measured at 10 m height over Askervien Hill for line A for a 210 degree incident wind. From CERC (2001b).

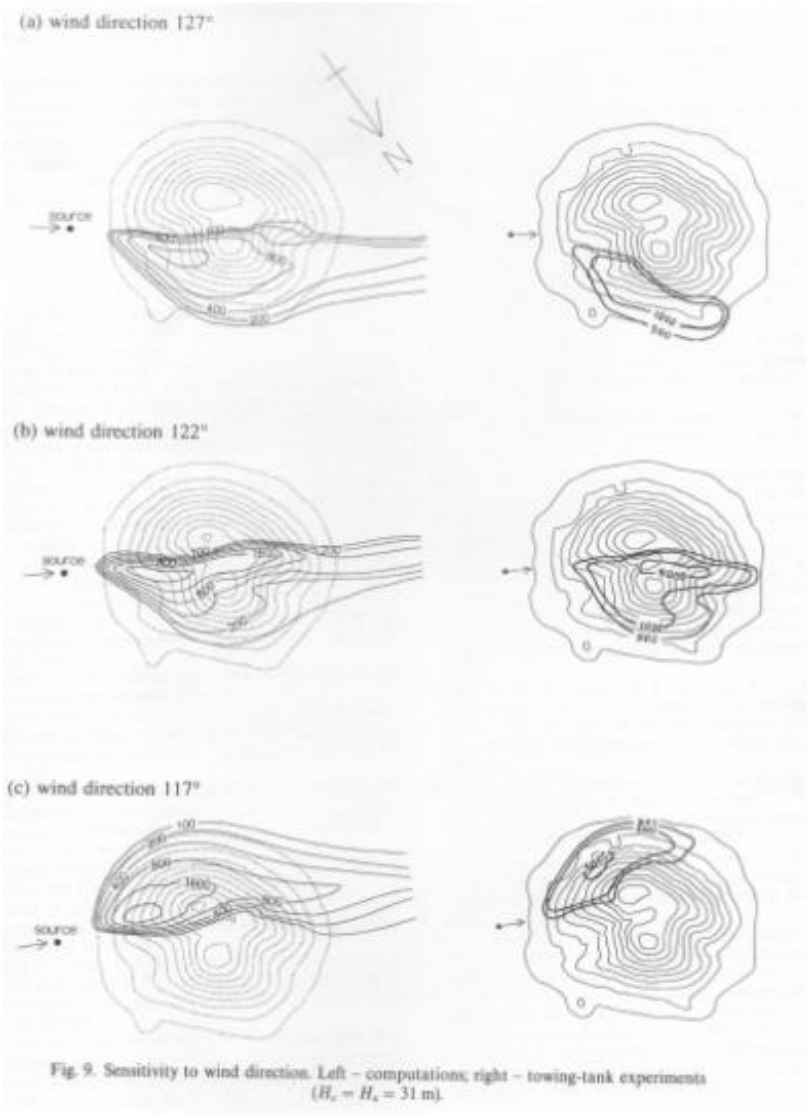

Fig. 9. Sensitivity to wind direction. Left – computations; right – towing-tank experiments ($H_c = H_s = 31$ m).

Figure 13 Sensitivity of flow round Cinder Cone Butte to incident wind direction from CFD modelling results (left) and towing tank experiments (right). From Apsley and Castro (1997).

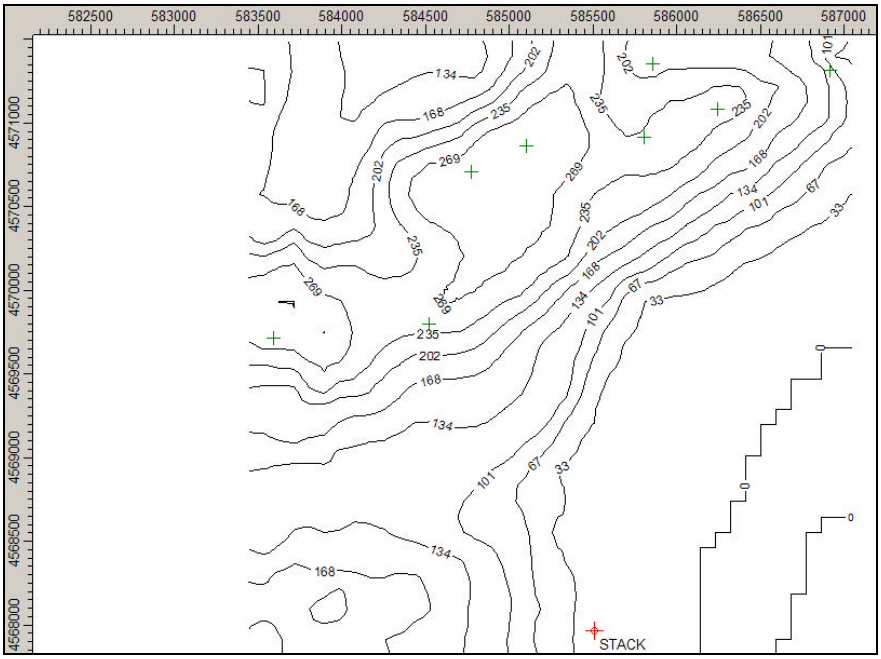

Figure 14 Terrain surrounding the Lovett Power Plant (USA) and the locations of the sampling points.

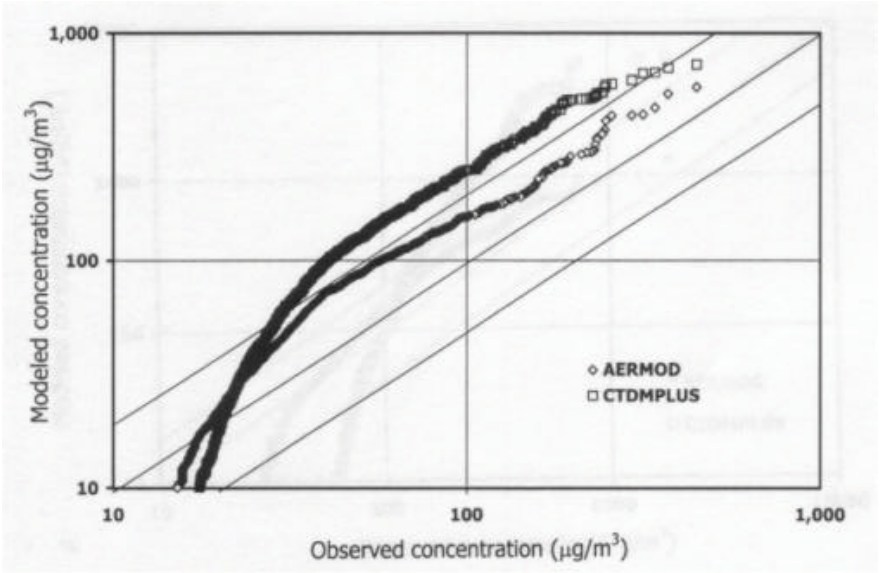

Figure 15 Quantile-quantile plots comparing distributions in hourly air concentrations observed at the Lovett Power plant with the predictions of AERMOD and CTDMPLUS. From Venkatram *et al*. (2001).

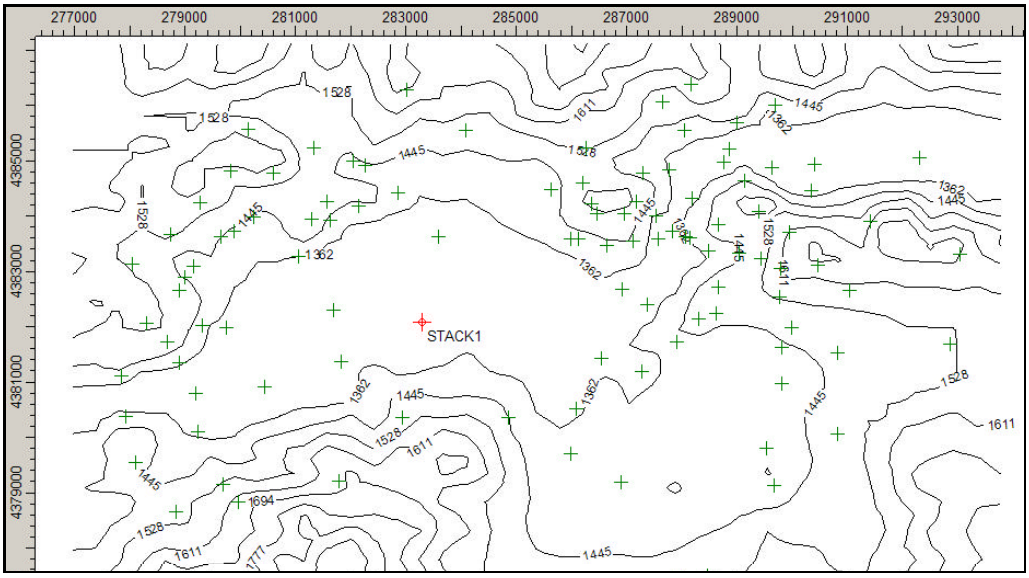

Figure 16 Terrain surrounding the Tracy Power Plant, Reno and the locations of the sampling points.

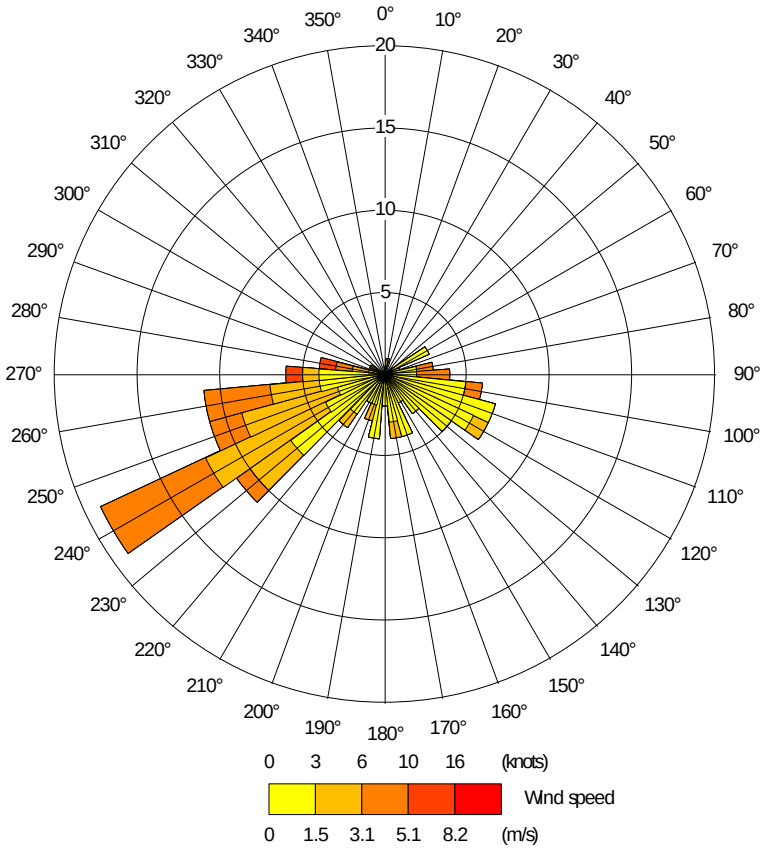

Figure 17 Wind rose for the experiments at the Tracy Power Plant.

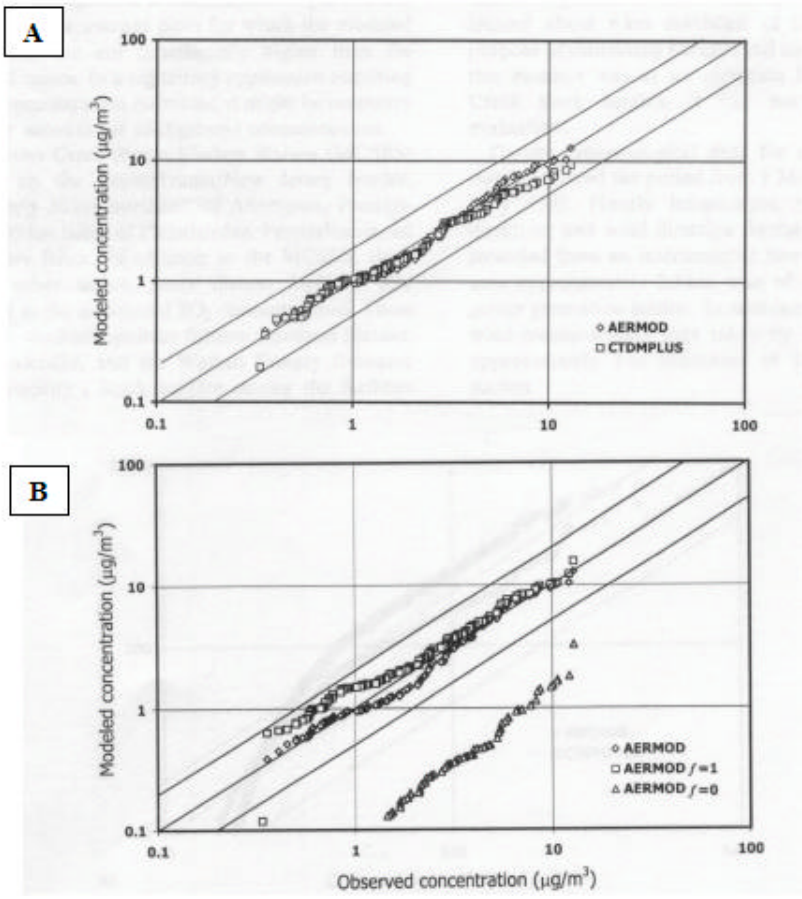

Figure 18 Quantile-quantile plots comparing distributions in hourly air concentrations observed at the Tracy Power plant with (A) the predictions of AERMOD and CTDMPLUS and (B) for AERMOD in standard configuration and when configured to simulate the plume passing over the terrain (*f*=0) or impacting on the terrain (*f*=1). From Venkatram *et al*. (2001).

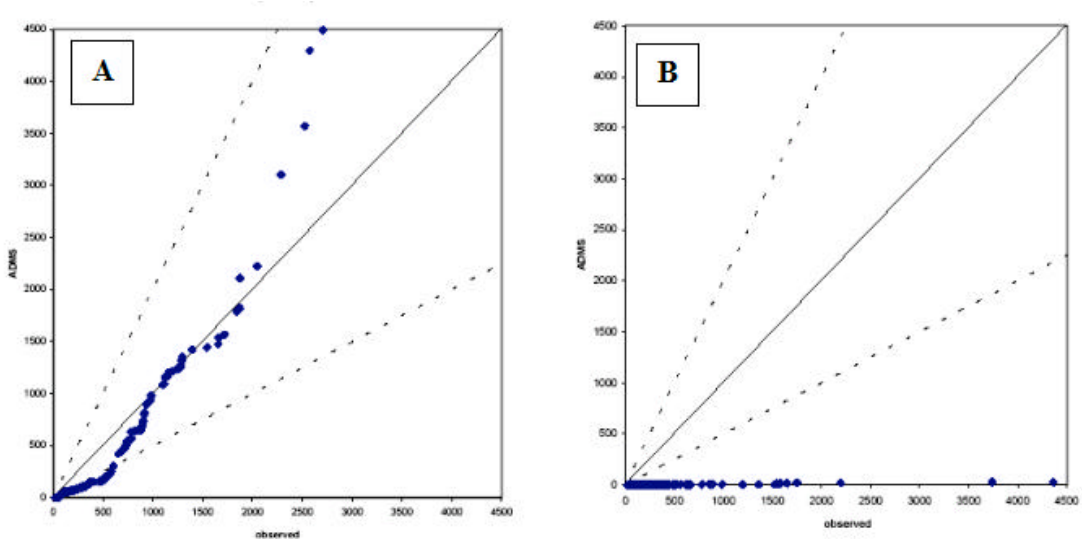

Figure 19 Comparison of quantile-quantile plots from CERC (2001d) showing the performance of ADMS for periods when the model agreed reasonably well with the monitoring data (A- Stable 6) and when severe disparities were observed (B- Stable 12).

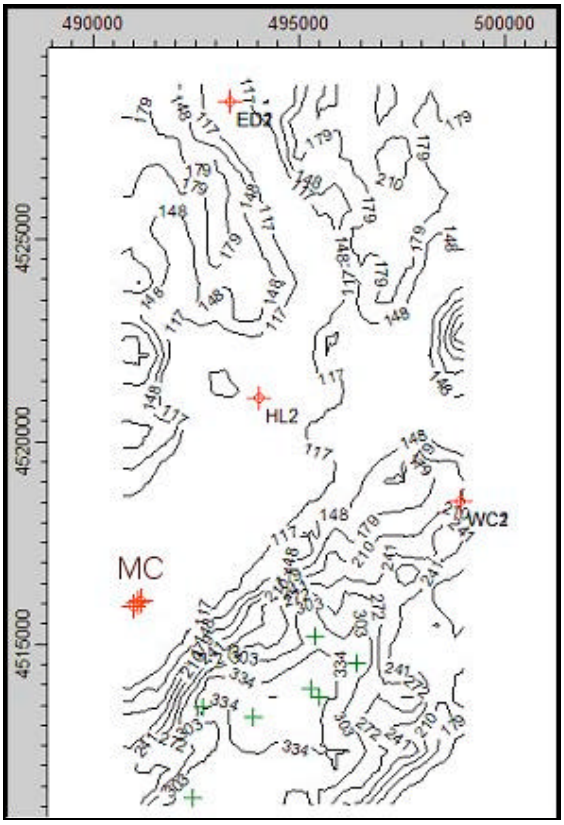

Figure 20 The terrain surrounding the Martins Creek Steam Electric Station (MC), the Metropolitan Edison Portland Station (ED, Hoffman-LaRoche (HL) and the Warren County Resource Recovery Facility (WC) in red and the locations of the monitoring points (in green).

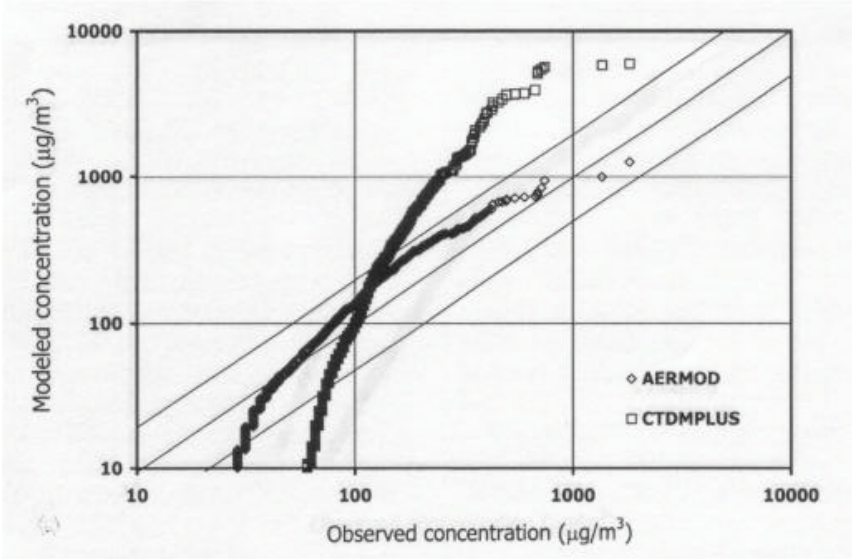

Figure 21 Quantile-quantile plots comparing distributions in hourly air concentrations observed at the Martins Creek Power plant with the predictions of AERMOD and CTDMPLUS. From Venkatram *et al*. (2001).

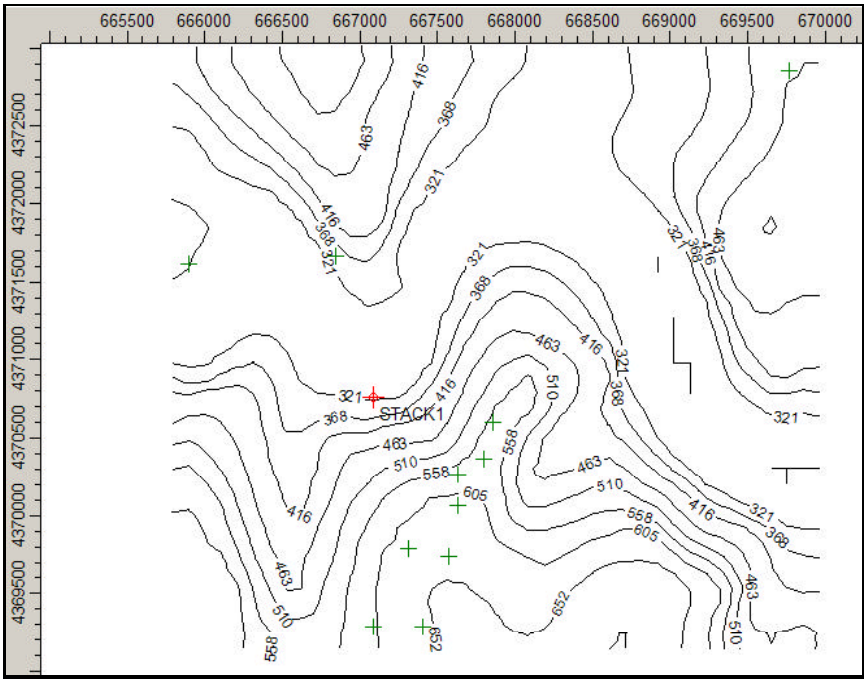

Figure 22 The terrain surrounding the Westvaco Corporation Pulp and Papermill, and the locations of the sampling points.

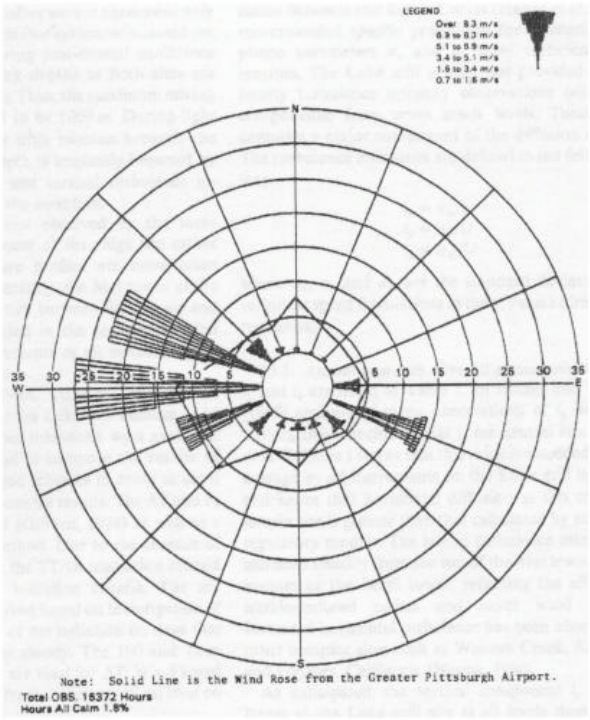

Figure 23 Comparison between wind roses measured at the 100 m level at "Met Tower" at the Westvaco model validation study with airport meteorological data (solid line). From Hanna *et al*. (1984).

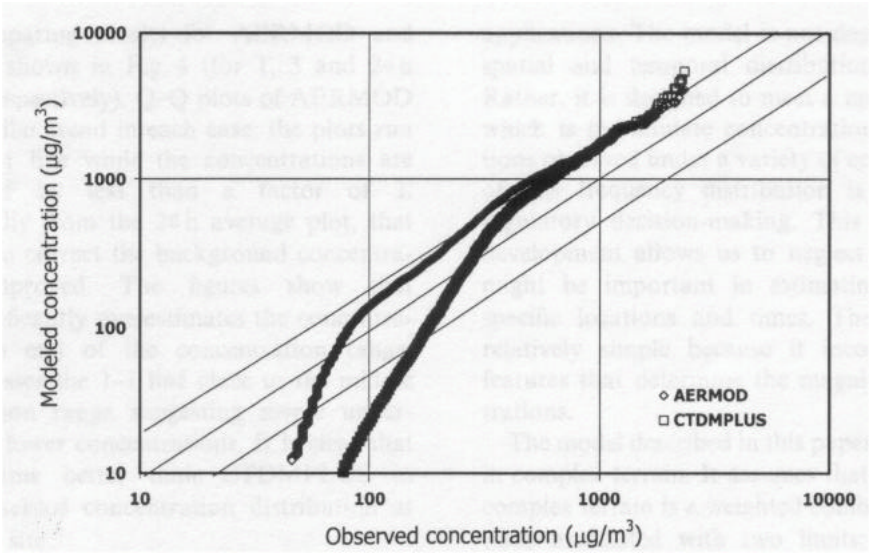

Figure 24 Quantile-quantile plots comparing distributions in hourly air concentrations observed at the Westvaco with the predictions of AERMOD and CTDMPLUS. From Venkatram *et al*. (2001).

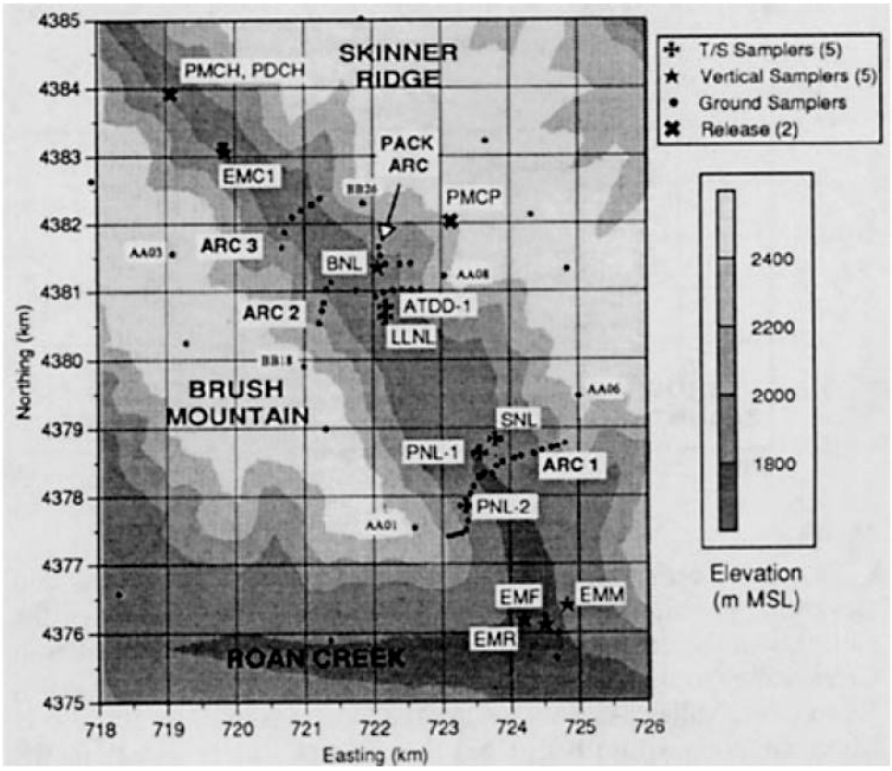

Figure 25 The terrain around Brush Creek and the locations of sampling points. From Allwine (1993).

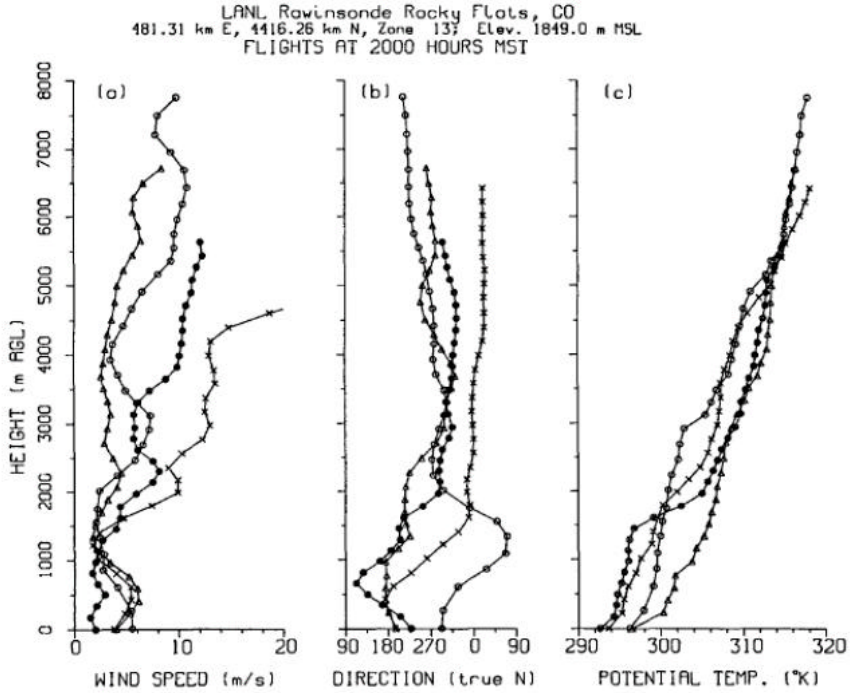

Figure 26 Radiosonde profiles from Rocky Flats showing the variation in wind speed, wind direction and potential temperature with height above ground level. From Poulos and Bossert (1995).

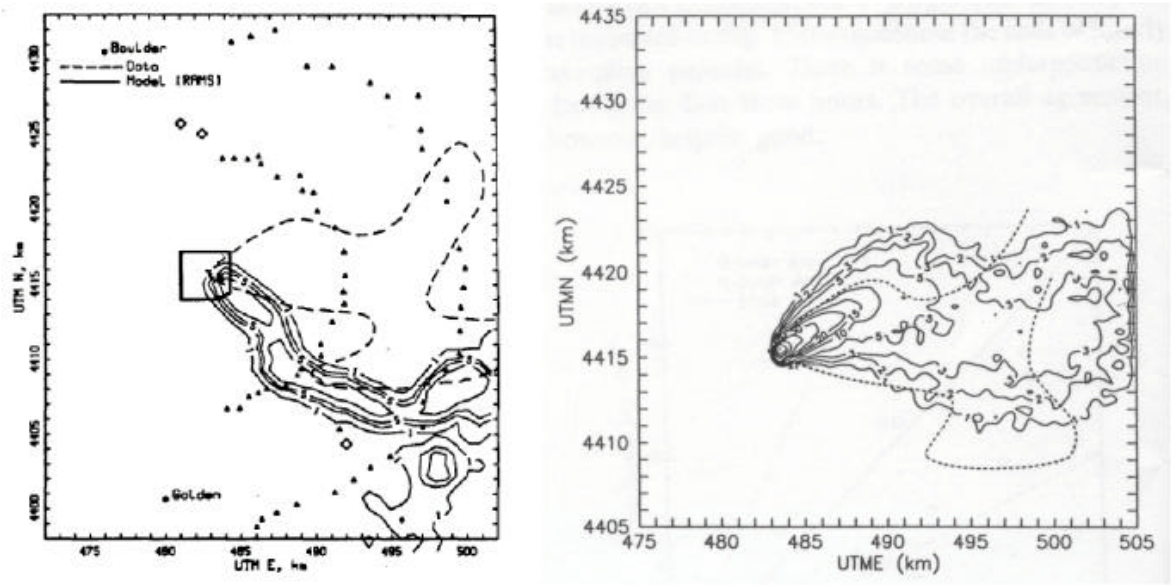

Figure 27 Poulos and Bossert (1995) (left) and Luhar and Rao (1994) (right) predictions of dispersion during 0300-0400 of the 5th of February 1991 at Rocky Flats. Dotted line shows measured concentrations interpolated at 1 mg m^{-3}.

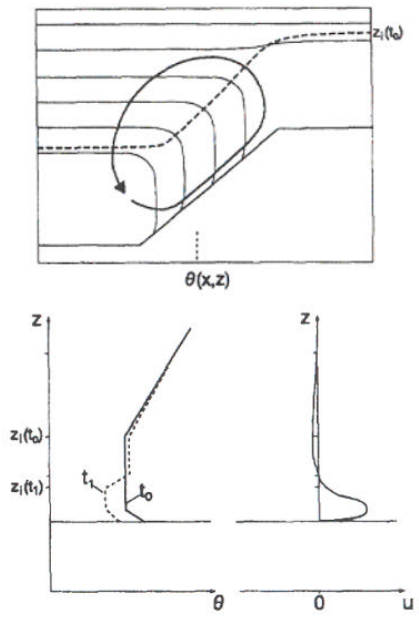

Figure 28 Temperature and wind flows in a region of upslope flow during convective conditions. From Kossmann *et al*. (1998).

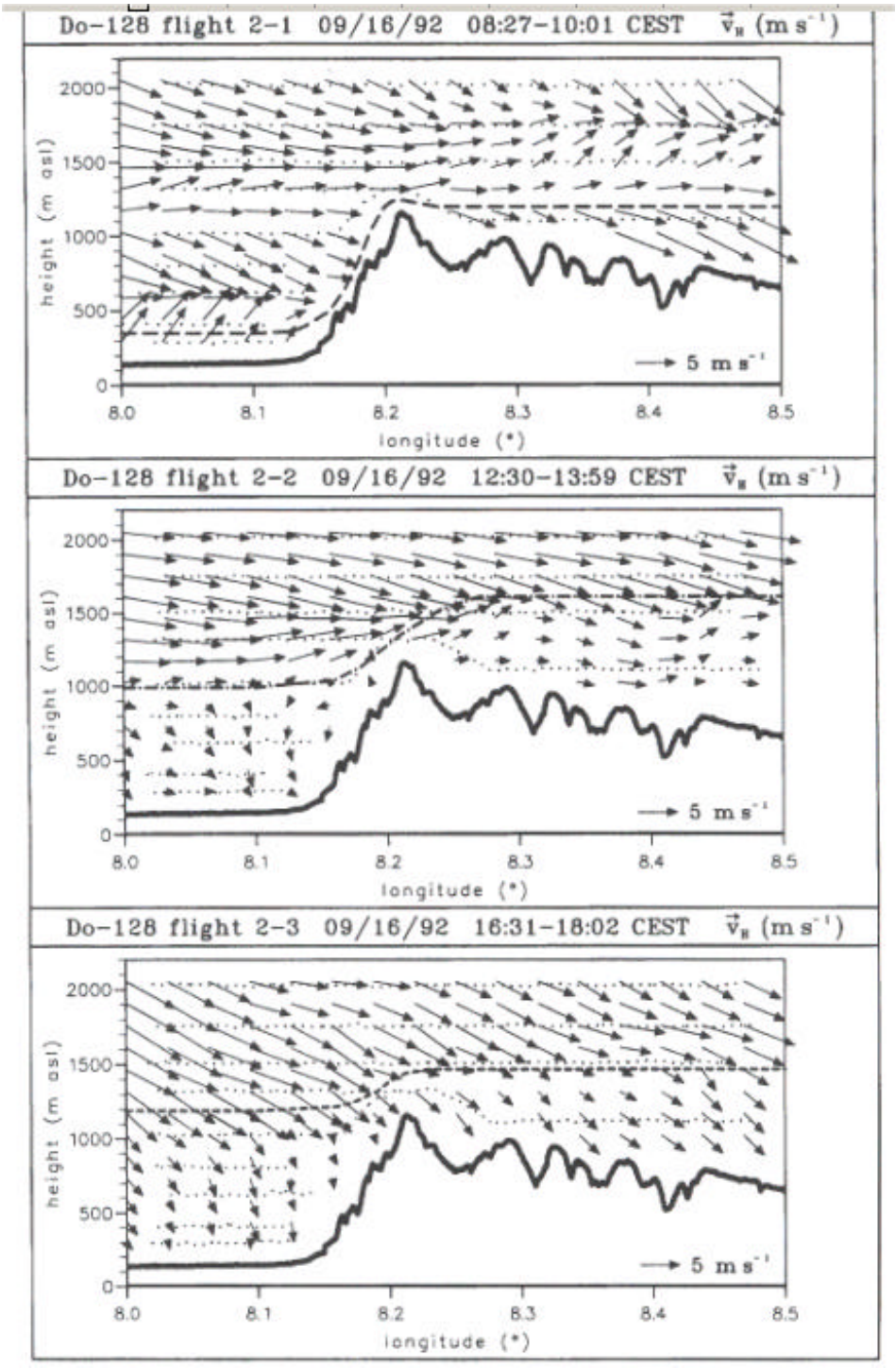

Figure 29 Wind vectors measured during three experimental flights (flightpaths shown as dotted lines) at the TRACT 92 experiment. The dashed lines show the boundary layer height. From Kossmann *et al*. (1998).

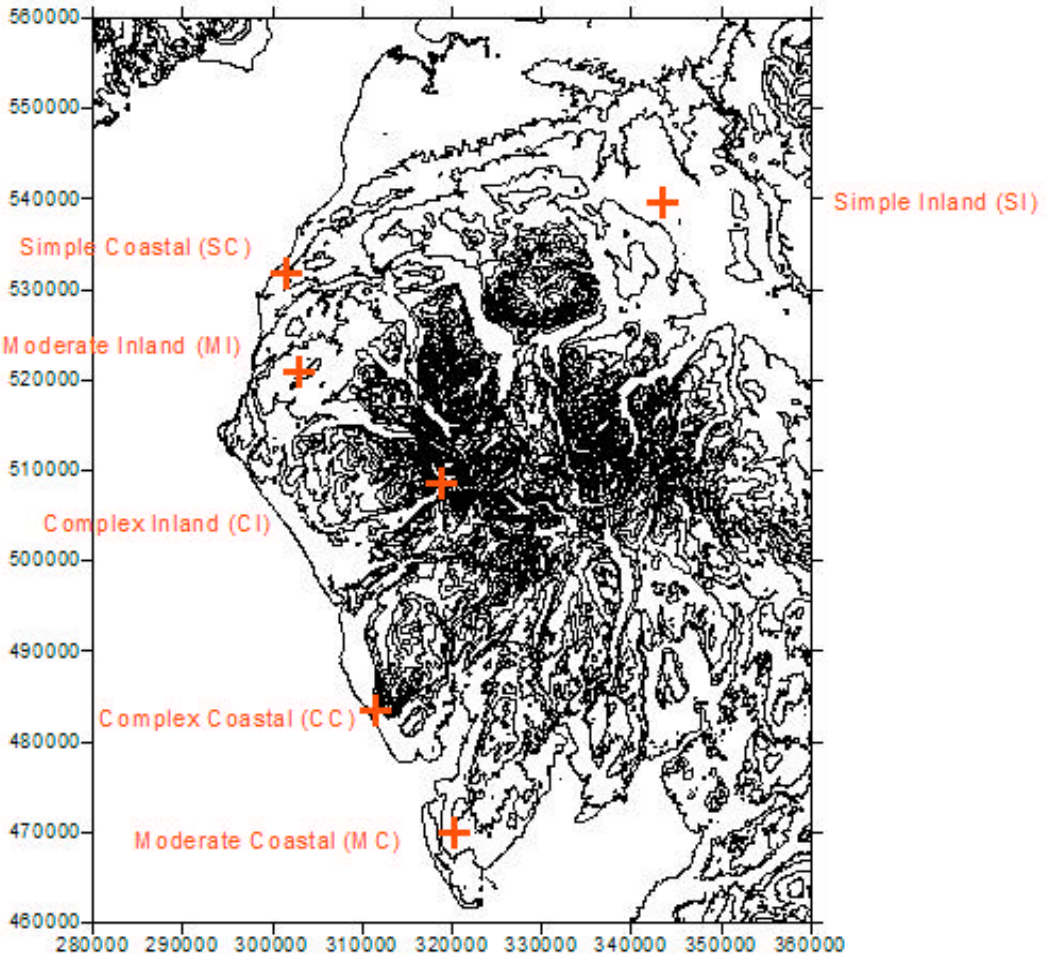

Figure 30 Locations used for ADMS and AERMOD assessments.

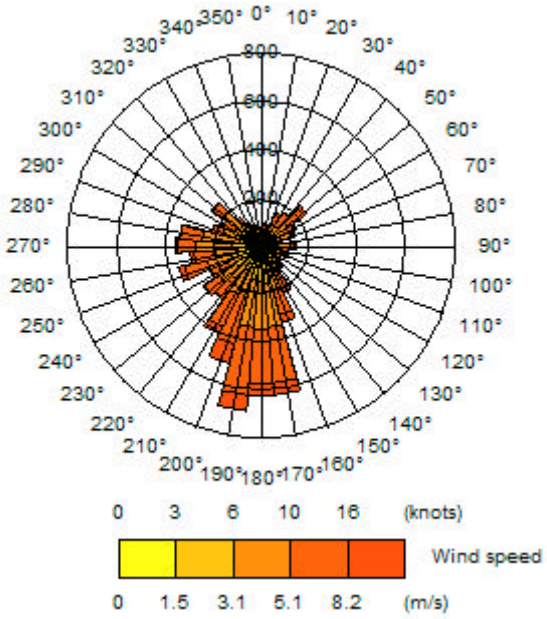

Figure 31 Wind rose for the ADMS and AERMOD assessments

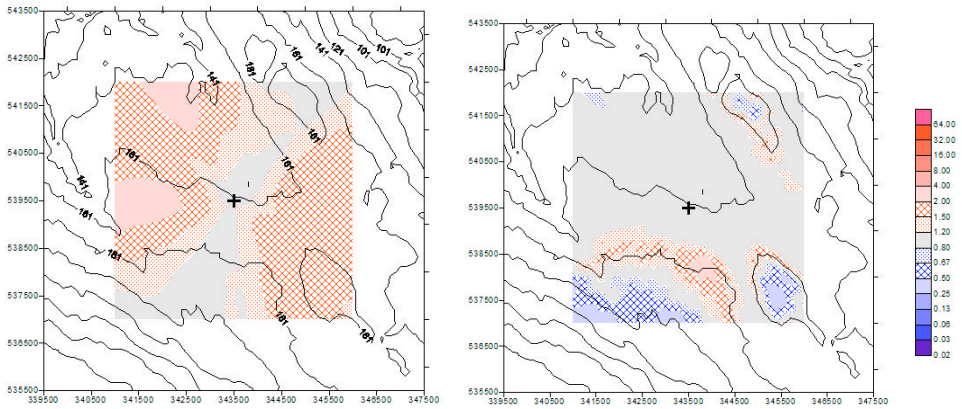

Figure 32 Amplification factors predicted by ADMS (left) and AERMOD (right) for simple terrain (inland). Annual averaged concentrations. Contour intervals = 20 m.

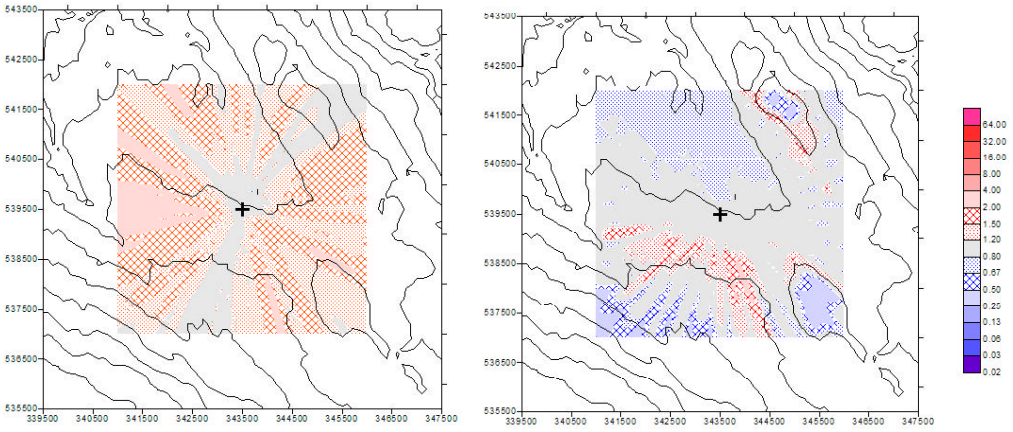

Figure 33 Amplification factors predicted by ADMS (left) and AERMOD (right) for simple terrain (inland). Data shown as the 99.8th percentile of hourly averaged concentrations. Contour intervals = 20 m.

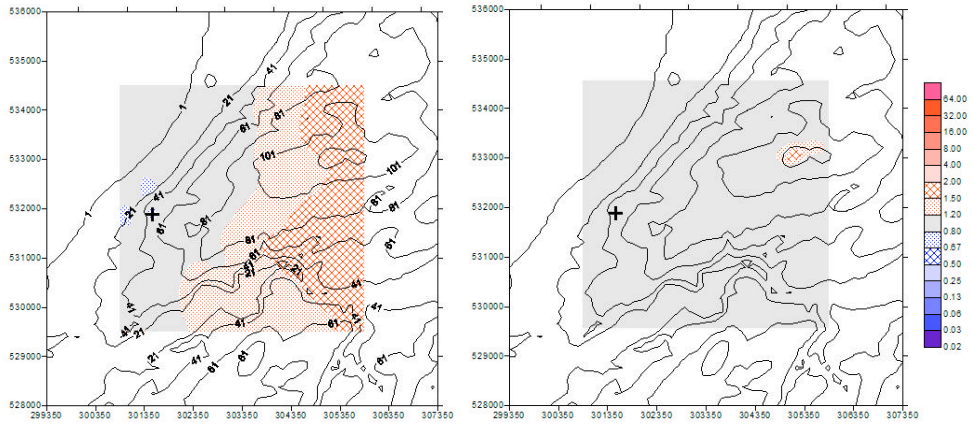

Figure 34 Amplification factors predicted by ADMS (left) and AERMOD (right) for simple terrain (coastal). Annual averaged concentrations. Contour intervals = 20 m.

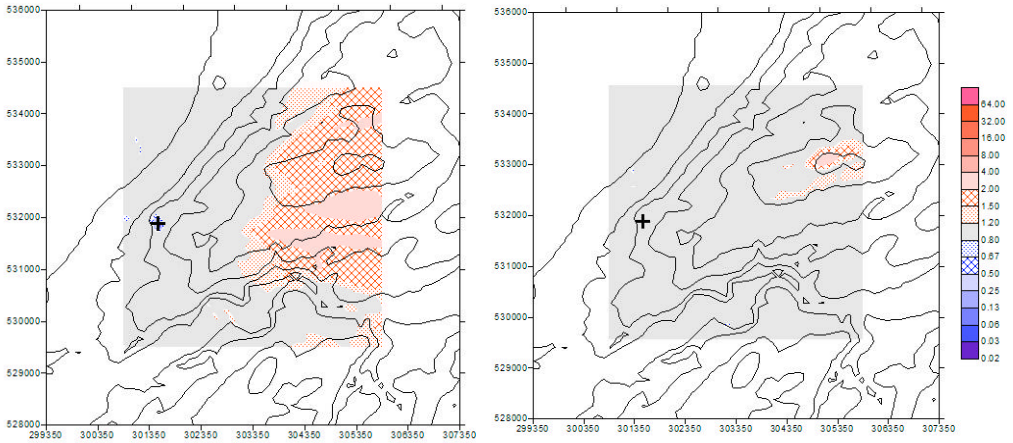

Figure 35 Amplification factors predicted by ADMS (left) and AERMOD (right) for simple terrain (coastal). Data shown as the 99.8th percentile of hourly averaged concentrations. Contour intervals = 20 m.

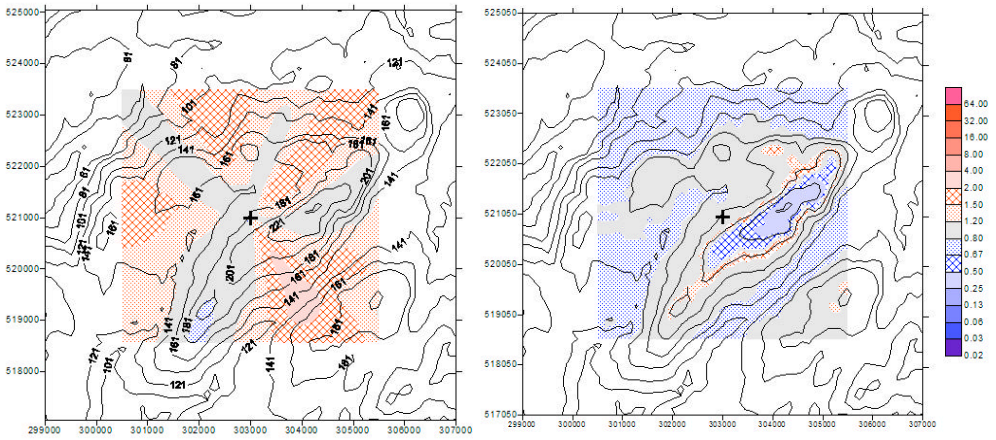

Figure 36 Amplification factors predicted by ADMS (left) and AERMOD (right) for moderate terrain (inland). Annual averaged concentrations. Contour intervals = 20 m.

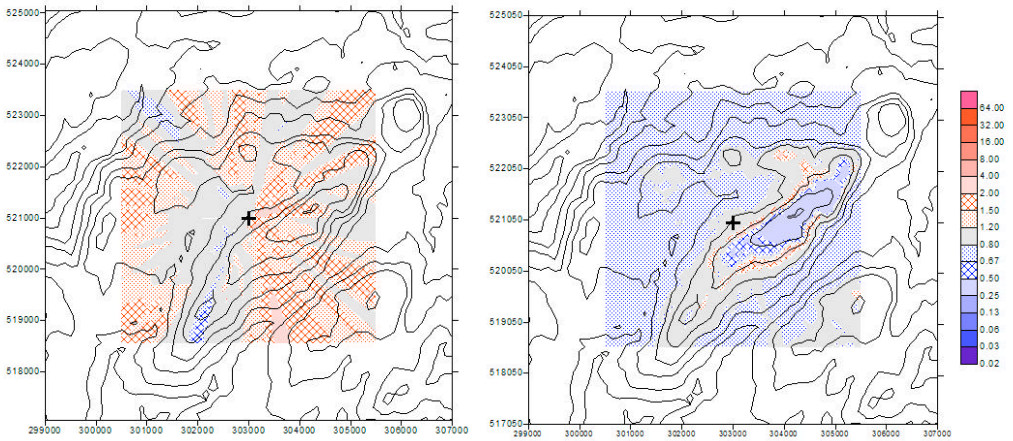

Figure 37 Amplification factors predicted by ADMS (left) and AERMOD (right) for moderate terrain (inland). Data shown as the 99.8th percentile of hourly averaged concentrations. Contour intervals = 20 m.

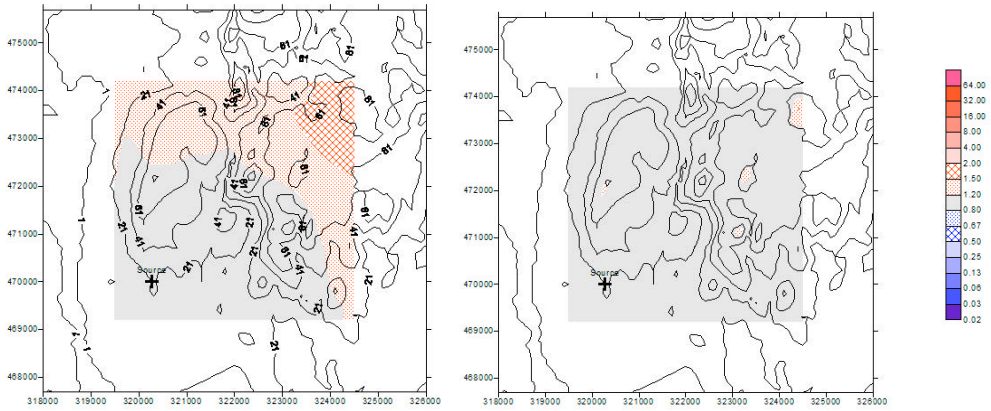

Figure 38 Amplification factors predicted by ADMS (left) and AERMOD (right) for moderate terrain (coastal). Annual averaged concentrations. Contour intervals = 20 m.

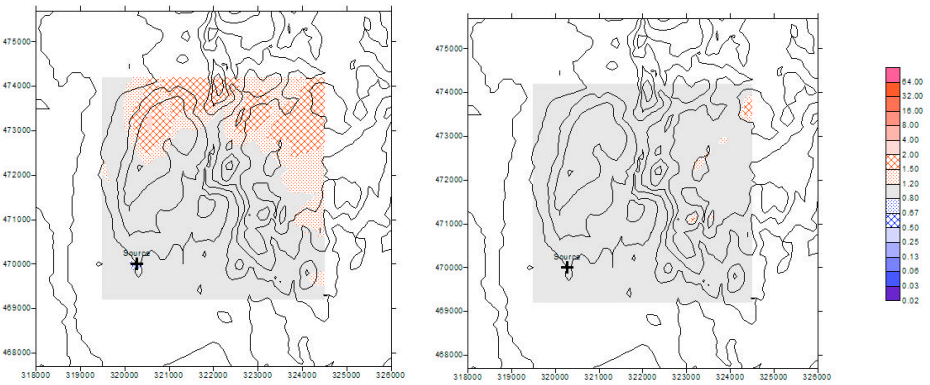

Figure 39 Amplification factors predicted by ADMS (left) and AERMOD (right) for moderate terrain (coastal). Data shown as the 99.8th percentile of hourly averaged concentrations. Contour intervals = 20 m.

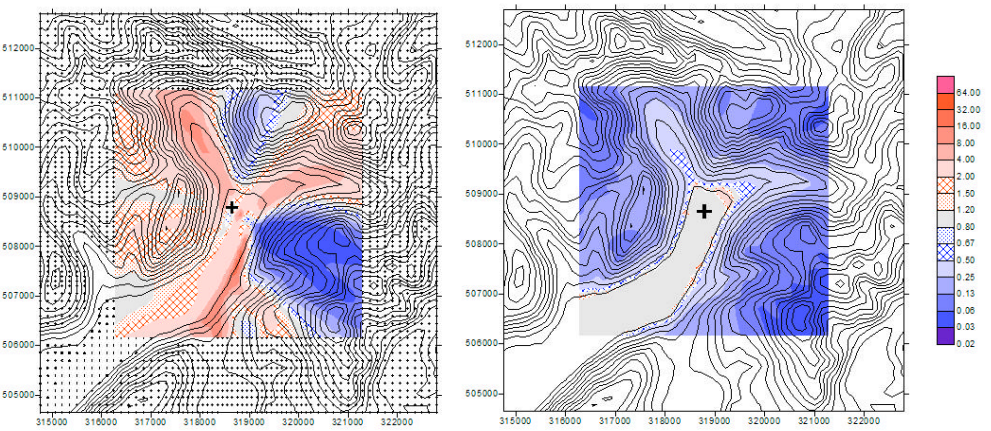

Figure 40 Amplification factors predicted by ADMS (left) and AERMOD (right) for complex terrain (inland). Annual averaged concentrations. Contour intervals = 50 m. Terrain nodes marked to illustrate the 64 ´ 64 cell terrain resolution.

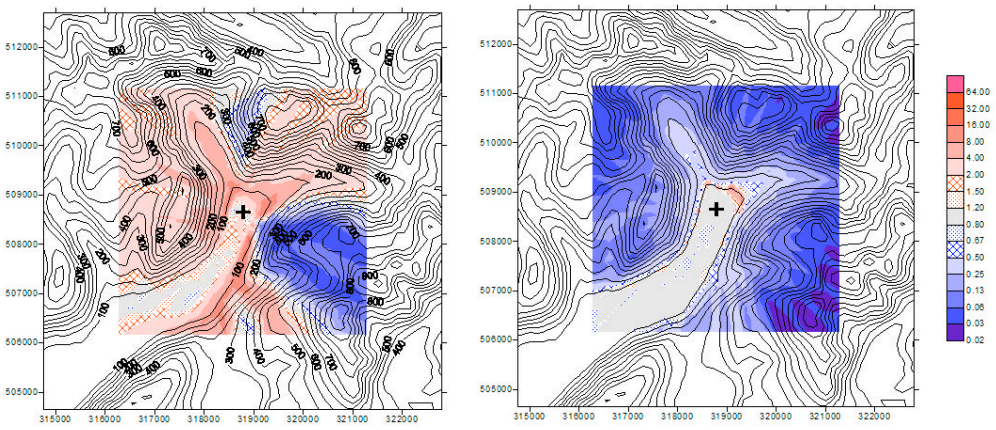

Figure 41 Amplification factors predicted by ADMS (left) and AERMOD (right) for complex terrain (inland). Data shown as the 99.8th percentile of hourly averaged concentrations. Contour intervals = 50 m.

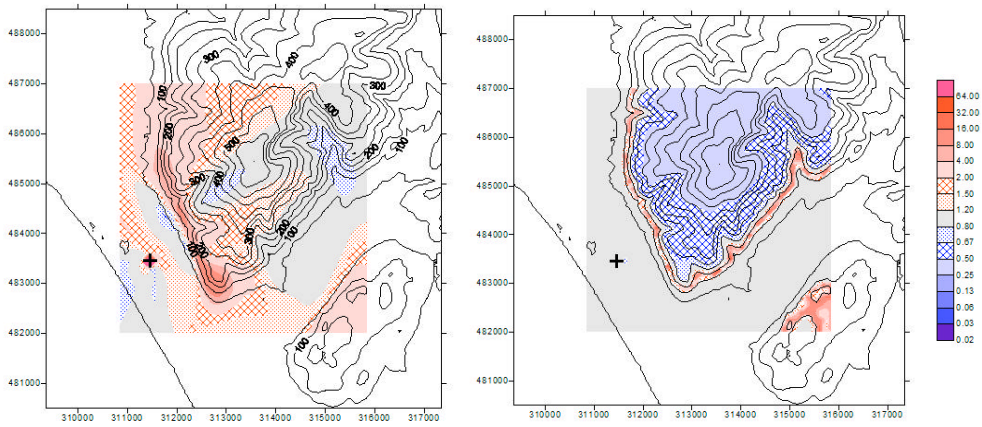

Figure 42 Amplification factors predicted by ADMS for complex terrain (coastal). Annual averaged concentrations. Contour intervals = 50 m.

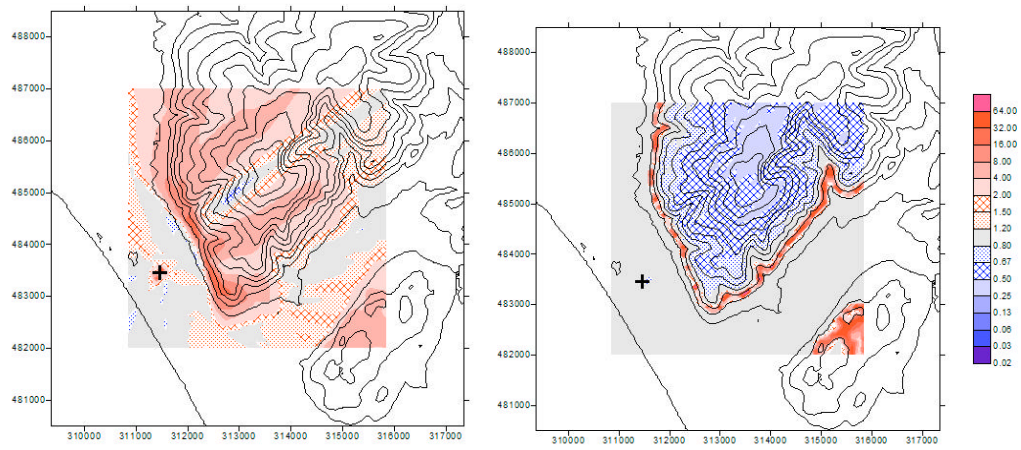

Figure 43 Amplification factors predicted by ADMS (left) and AERMOD (right) for complex terrain (coastal). Data shown as the 99.8th percentile of hourly averaged concentrations. Contour intervals = 50 m.

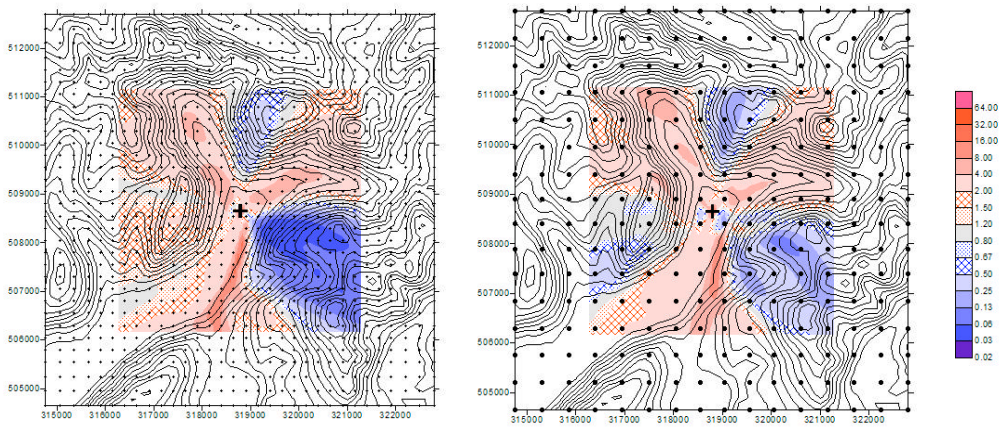

Figure 44 Amplification factors predicted by ADMS for a 32 ´ 32 cell terrain file (left) and a 16 ´ 16 terrain file (right) for complex terrain at an inland location. Annual averaged concentrations. Contour intervals = 50 m. Terrain nodes shown.

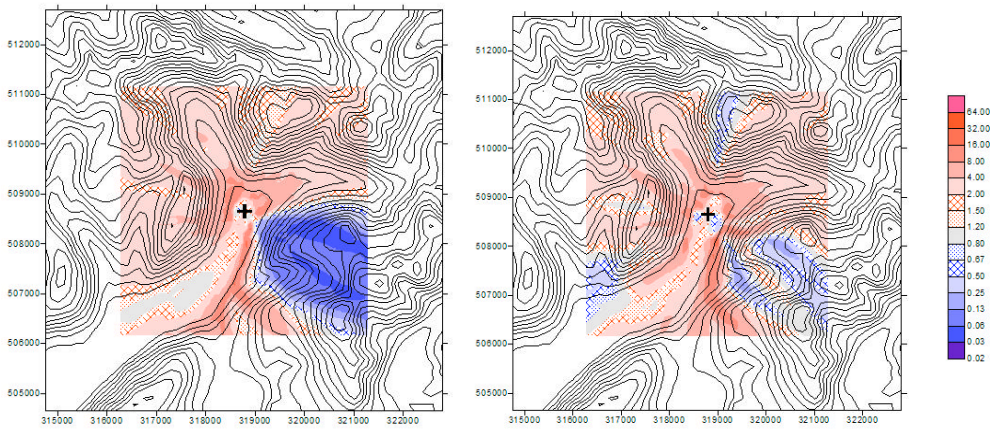

Figure 45 Amplification factors predicted by ADMS for a 32 ´ 32 cell terrain file (left) and a 16 ´ 16 cell terrain file (right) for complex terrain at an inland site. Data shown as the 99.8th percentile of hourly averaged concentrations. Contour intervals = 50 m.

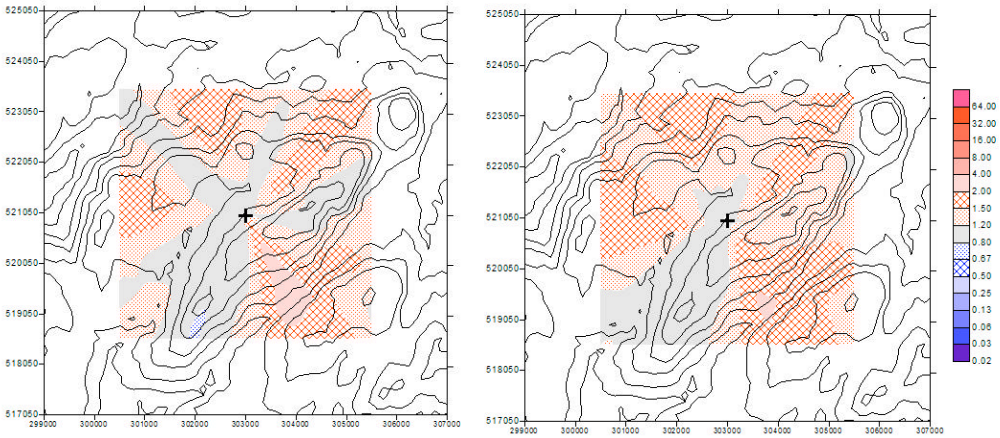

Figure 46 Amplification factors predicted by ADMS for a 32 ´ 32 cell terrain file (left) and a 16 ´ 16 cell terrain file (right) for moderate terrain at an inland site. Annual averaged concentrations. Contour intervals = 50 m.

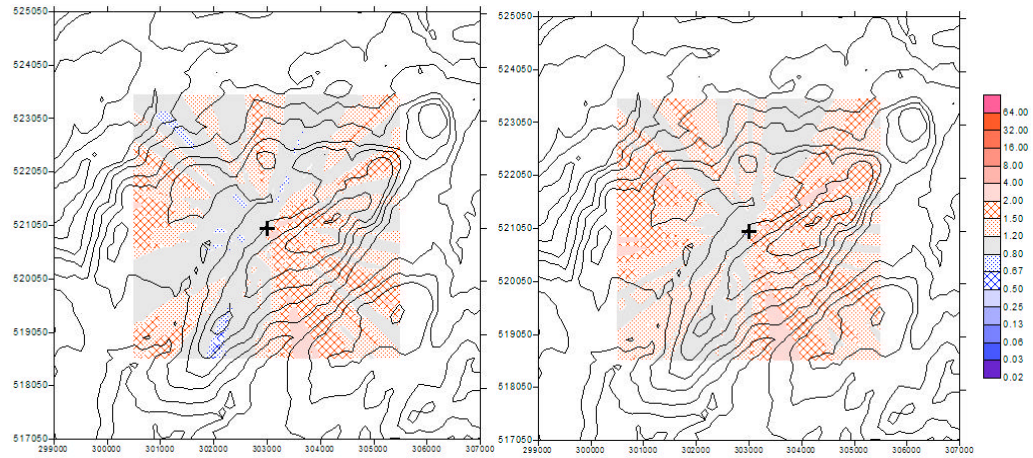

Figure 47 Amplification factors predicted by ADMS for a 32 ´ 32 cell terrain file (left) and a 16 ´ 16 cell terrain file (right) for moderate terrain at an inland site. Data shown as the 99.8th percentile of hourly averaged concentrations. Contour intervals = 50 m.

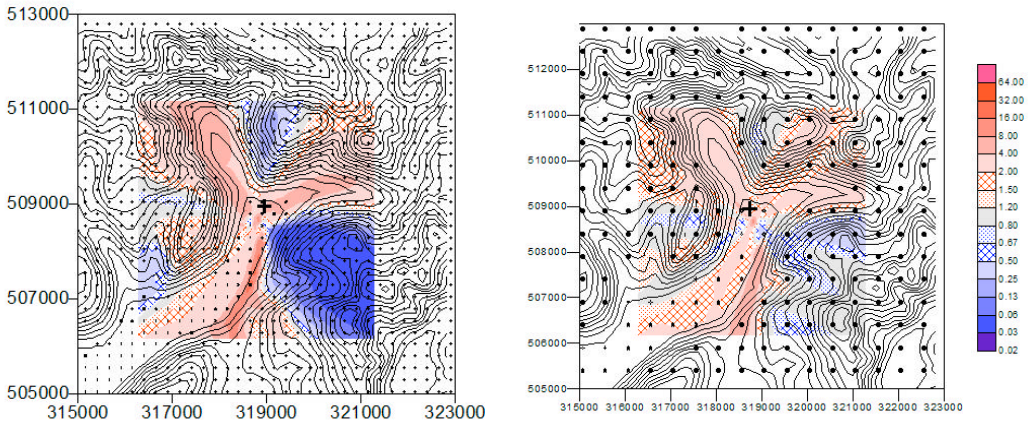

Figure 48 Amplification factors predicted by ADMS for a 16 km ´ 16 km terrain file (left) and a 32 km ´ 32 km terrain file (right) for complex terrain at an inland location. Annual averaged concentrations. Contour intervals = 50 m. Terrain nodes are shown within the area of the standard (8 km ´ 8km) domain for comparison with Figures 40 and 44.

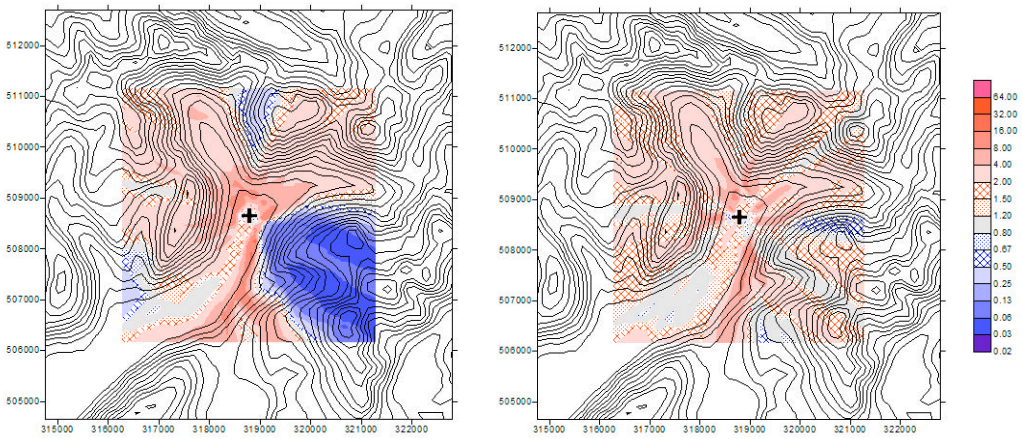

Figure 49 Amplification factors predicted by ADMS for a 16 km ´ 16 km terrain file (left) and a 32 km ´ 32 km terrain file (right) for complex terrain at an inland location. Data shown as the 99.8th percentile of hourly averaged concentrations. Contour intervals = 50 m.

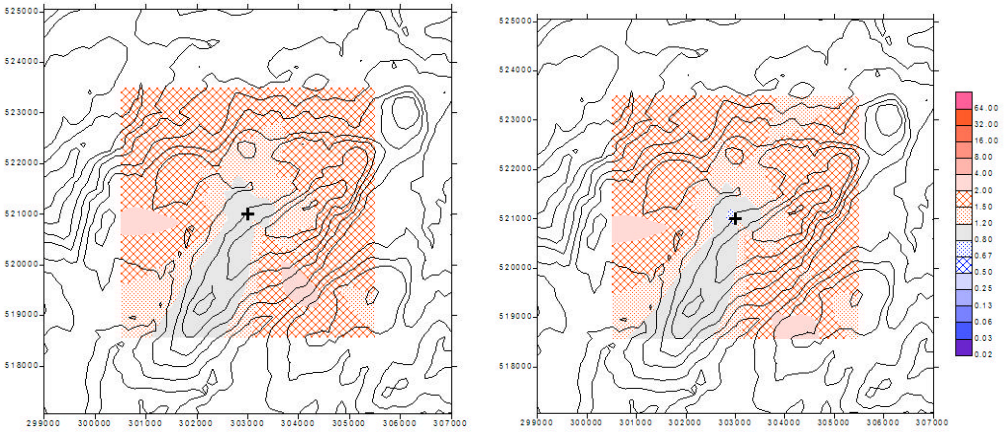

Figure 50 Amplification factors predicted by ADMS for a 16 km ´ 16 km terrain file (left) and a 32 km ´ 32 km terrain file (right) for moderate terrain at an inland location. Annual averaged concentrations. Contour intervals = 20 m.

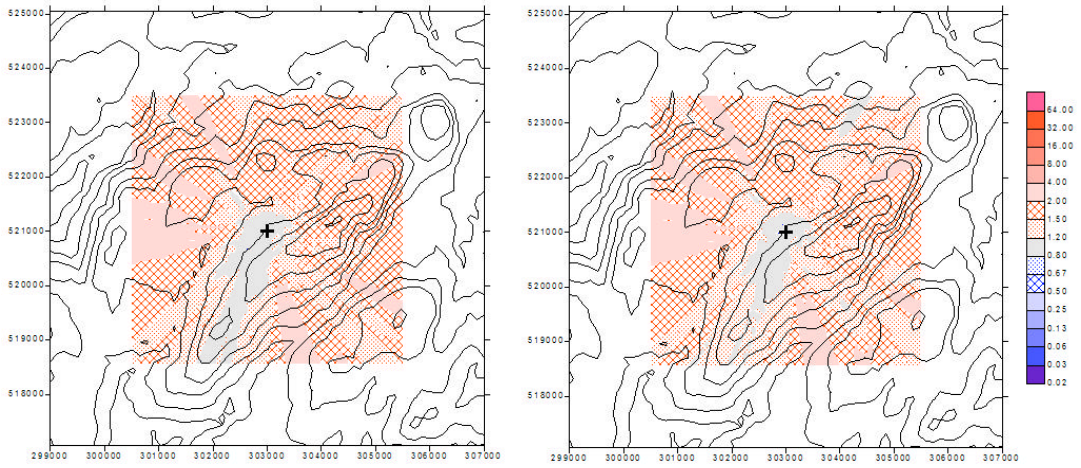

Figure 51 Amplification factors predicted by ADMS for a 16 km ´ 16 km terrain file (left) and a 32 km ´ 32 km terrain file (right) for moderate terrain at an inland location. Data shown as the 99.8th percentile of hourly averaged concentrations. Contour intervals = 20 m.

APPENDIX A : SUPPLEMENTARY AIR CONCENTRATION CONTOUR PLOTS

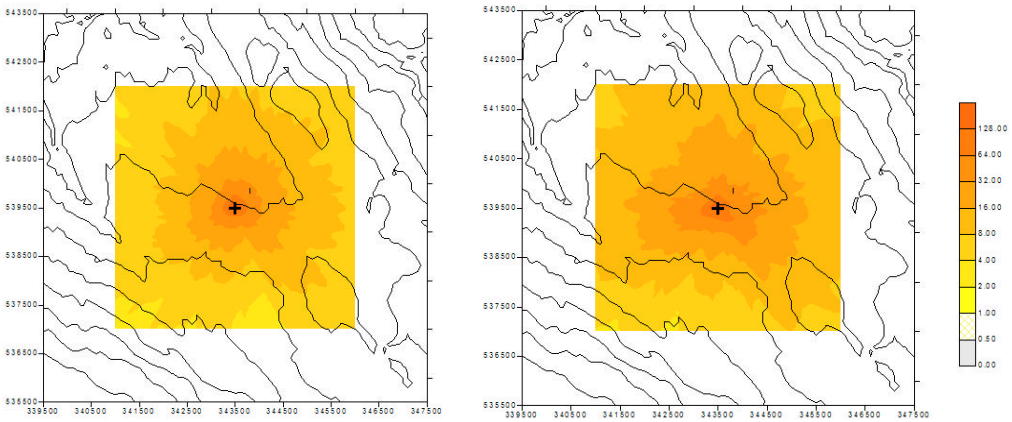

Figure A1 Air concentrations (mg m^{-3}) predicted by ADMS at the simple terrain (inland) location excluding any terrain effects (left) and including terrain effects (right). Concentrations determined as the 99.8th percentile of hourly averaged values. Contour intervals = 20 m.

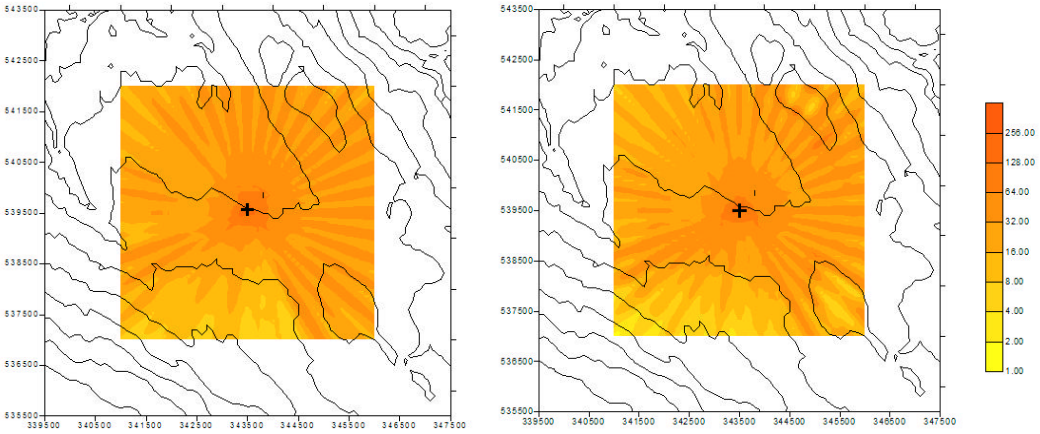

Figure A2 Air concentrations (mg m^{-3}) predicted by AERMOD at the simple terrain (inland) location excluding any terrain effects (left) and including terrain effects (right). Concentrations determined as the 99.8th percentile of hourly averaged values. Contour intervals = 20 m.

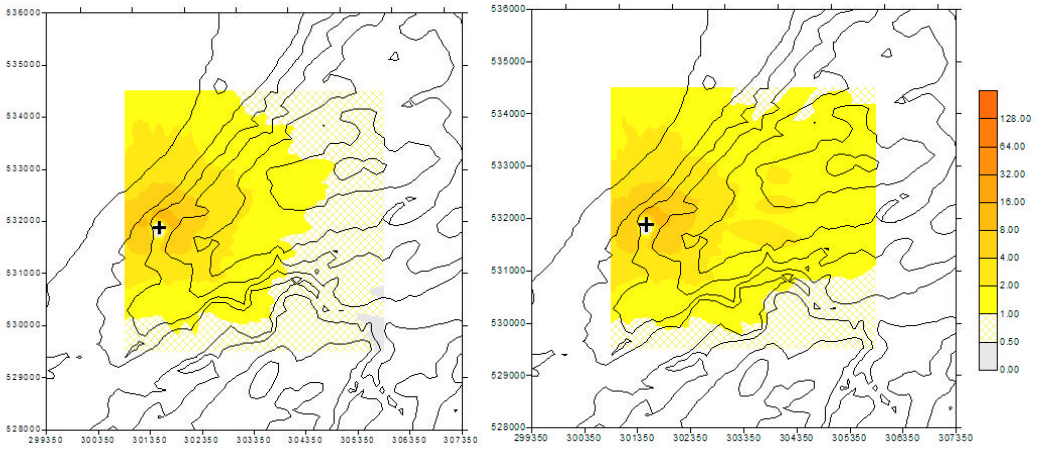

Figure A3 Air concentrations (mg m^{-3}) predicted by ADMS at the simple terrain (coastal) location excluding any terrain effects (left) and including terrain effects (right). Concentrations determined as the 99.8th percentile of hourly averaged values. Contour intervals = 20 m.

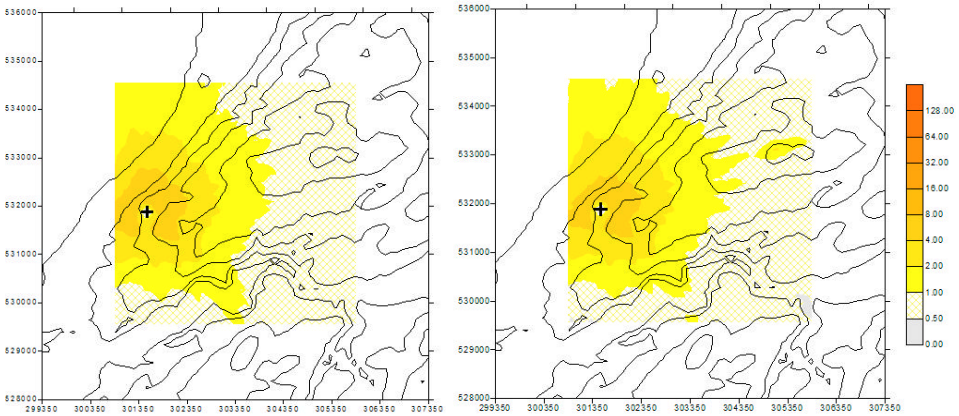

Figure A4 Air concentrations (mg m^{-3}) predicted by AERMOD at the simple terrain (coastal) location excluding any terrain effects (left) and including terrain effects (right). Concentrations determined as the 99.8th percentile of hourly averaged values. Contour intervals = 20 m.

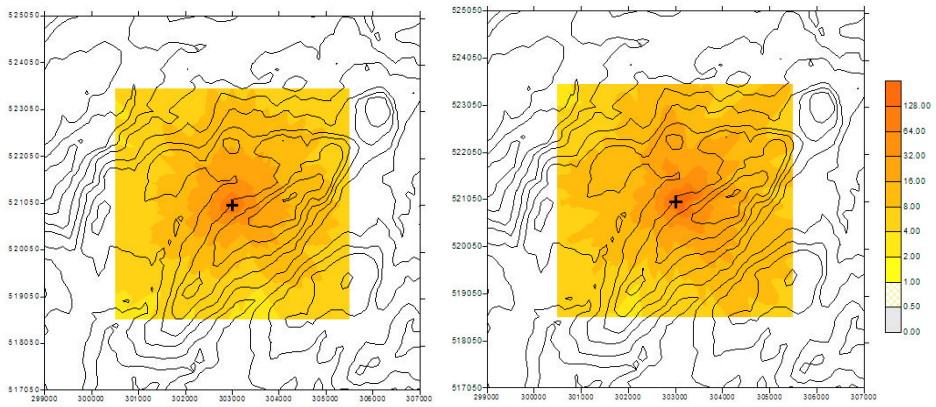

Figure A5 Air concentrations (mg m^{-3}) predicted by ADMS at the moderate terrain (inland) location excluding any terrain effects (left) and including terrain effects (right). Concentrations determined as the 99.8th percentile of hourly averaged values. Contour intervals = 20 m.

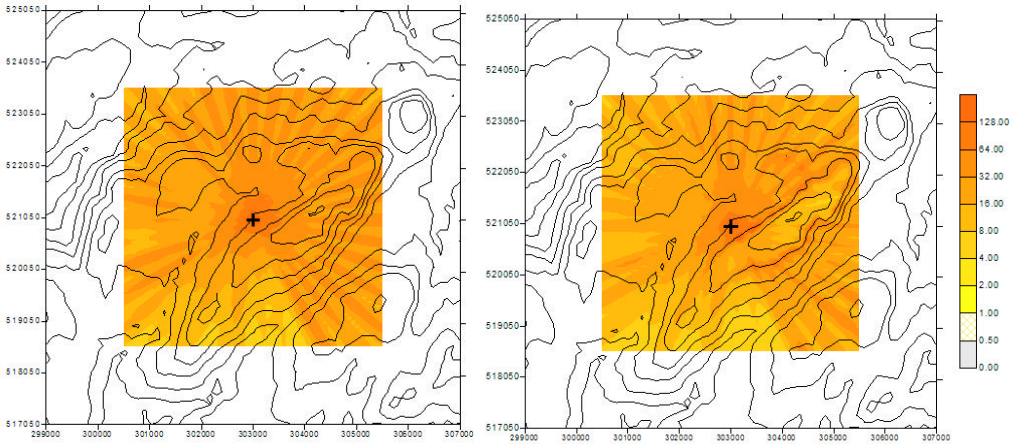

Figure A6 Air concentrations (mg m^{-3}) predicted by AERMOD at the moderate terrain (inland) location excluding any terrain effects (left) and including terrain effects (right). Concentrations determined as the 99.8th percentile of hourly averaged values. Contour intervals = 20 m.

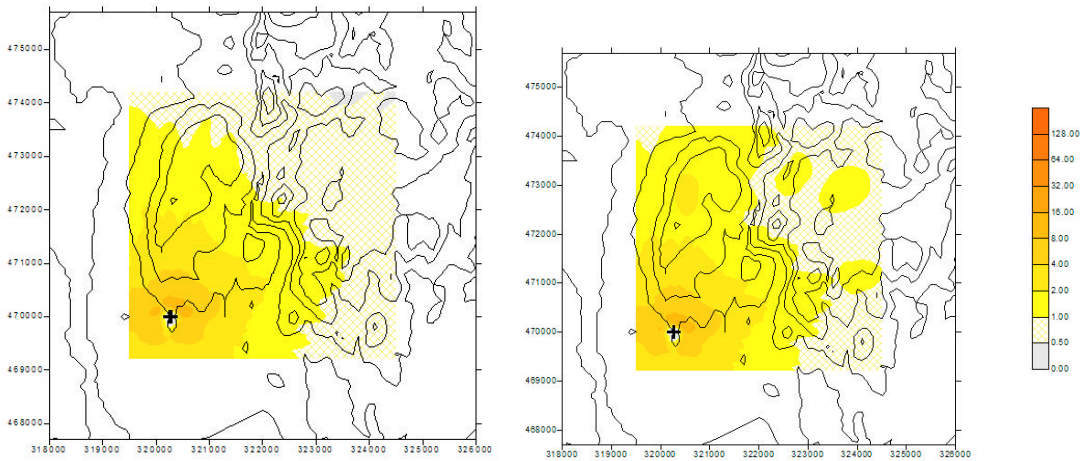

Figure A7 Air concentrations (mg m^{-3}) predicted by ADMS at the moderate terrain (coastal) location excluding any terrain effects (left) and including terrain effects (right). Concentrations determined as the 99.8th percentile of hourly averaged values. Contour intervals = 20 m.

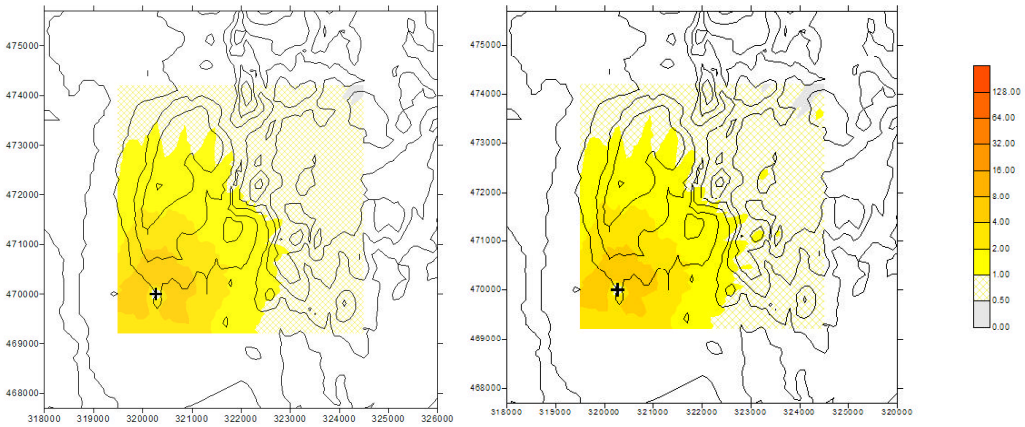

Figure A8 Air concentrations (mg m^{-3}) predicted by AERMOD at the moderate terrain (coastal) location excluding any terrain effects (left) and including terrain effects (right). Concentrations determined as the 99.8th percentile of hourly averaged values. Contour intervals = 20 m.

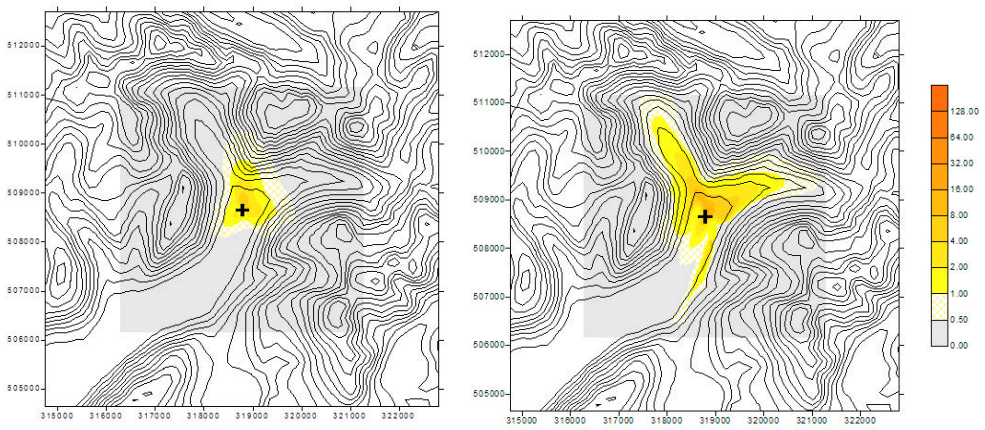

Figure A9 Air concentrations (mg m^{-3}) predicted by ADMS at the complex terrain (inland) location excluding any terrain effects (left) and including terrain effects (right). Concentrations determined as annual averaged values. Contour intervals = 50 m.

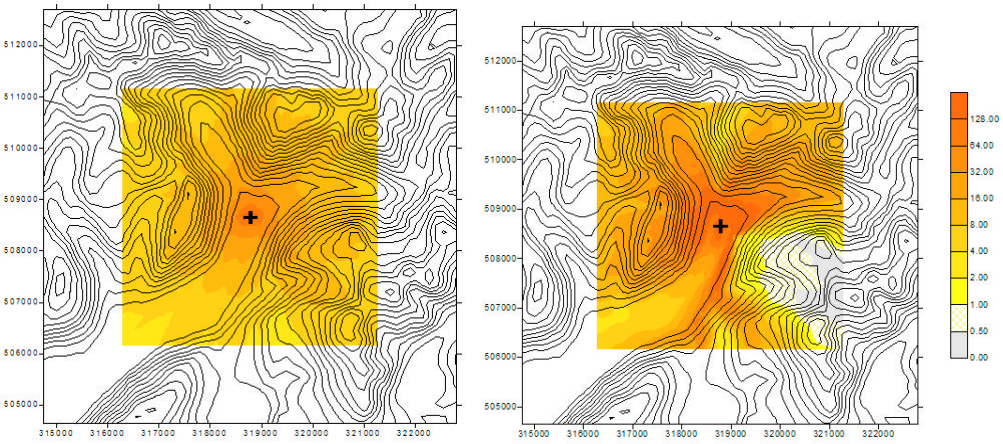

Figure A10 Air concentrations (mg m^{-3}) predicted by ADMS at the complex terrain (inland) location excluding any terrain effects (left) and including terrain effects (right). Concentrations determined as the 99.8th percentile of hourly averaged values. Contour intervals = 50 m.

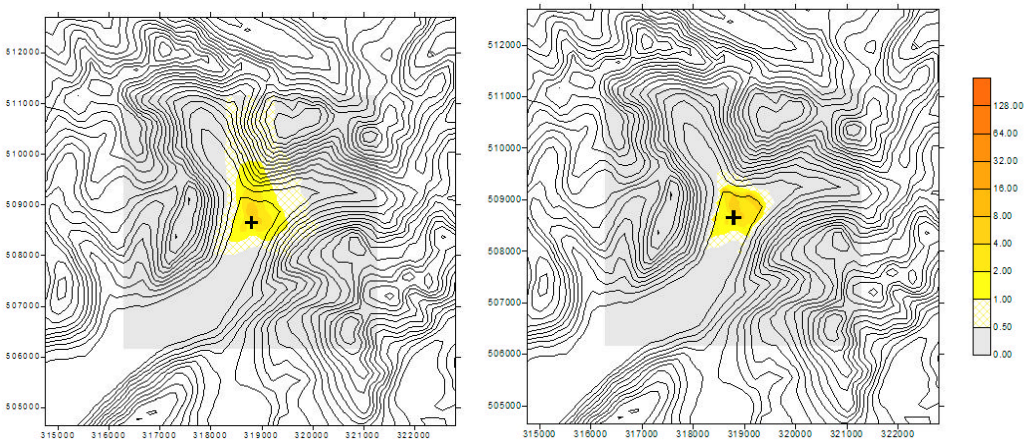

Figure A11 Air concentrations (μg m^{-3}) predicted by AERMOD at the complex terrain (inland) location excluding any terrain effects (left) and including terrain effects (right). Concentrations determined as annual averaged values. Contour intervals = 50 m.

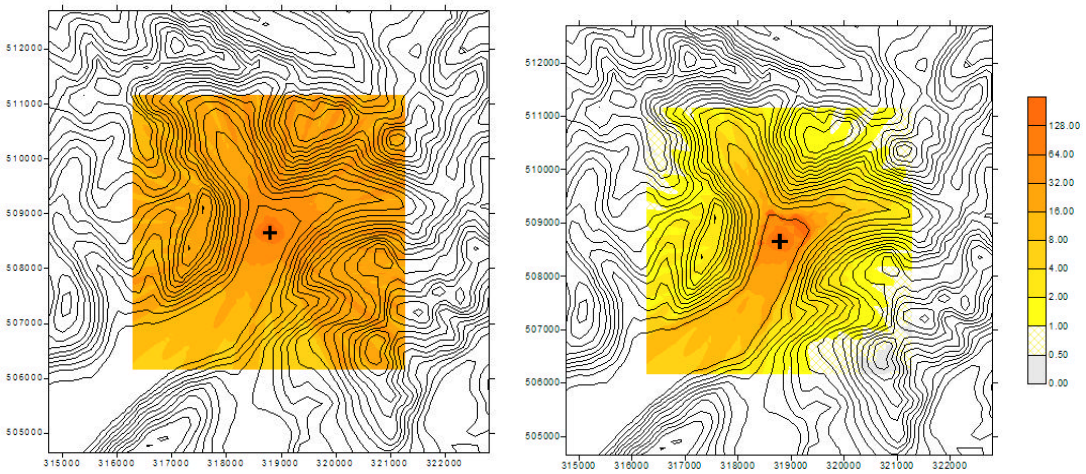

Figure A12 Air concentrations (μg m^{-3}) predicted by AERMOD at the complex terrain (inland) location excluding any terrain effects (left) and including terrain effects (right). Concentrations determined as the 99.8th percentile of hourly averaged values. Contour intervals = 50 m.

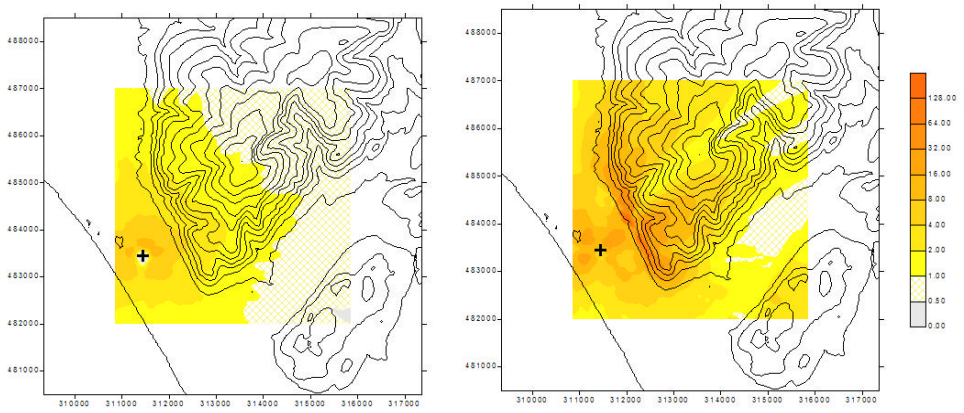

Figure A13 Air concentrations (mg m^{-3}) predicted by ADMS at the complex terrain (coastal) location excluding any terrain effects (left) and including terrain effects (right). Concentrations determined as the 99.8th percentile of hourly averaged values. Contour intervals = 50 m.

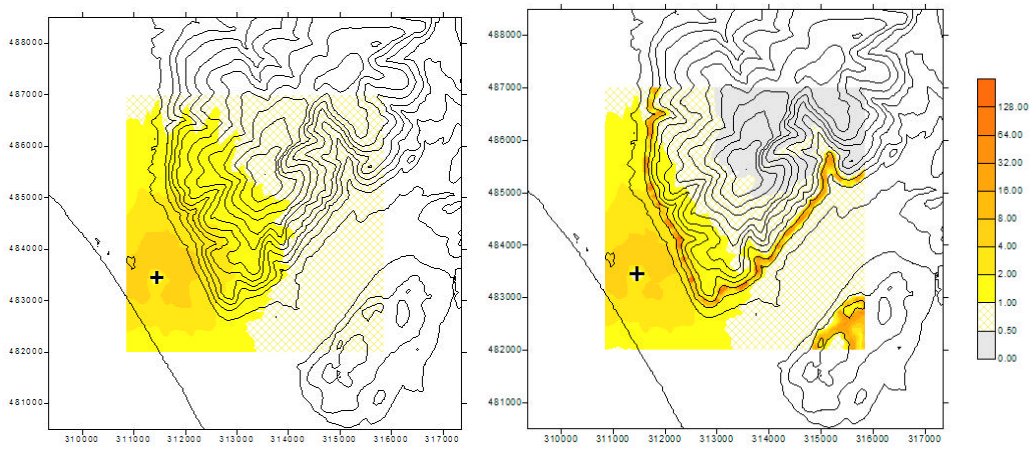

Figure A14 Air concentrations (mg m^{-3}) predicted by AERMOD at the complex terrain (coastal) location excluding any terrain effects (left) and including terrain effects (right). Concentrations determined as the 99.8th percentile of hourly averaged values. Contour intervals = 50 m.